SLAC-PUB-5082
June 1989
(M)

COLOR TRANSPARENCY AND THE STRUCTURE OF THE PROTON IN QUANTUM CHROMODYNAMICS*

STANLEY J. BRODSKY*
Stanford *Linear Accelerator Center*
Stanford University, Stanford, California 94305

Presented at the *Distinguished-Speaker Colloquium Series*
University of Minnesota, Minneapolis, Minnesota, February 2, 1989.
To be published by Addison Wesley in the book
"Trends in Theoretical Physics, Volume 1," edited by P. J. Ellis and Y. C. Tang.

* WORK SUPPORTED BY THE DEPARTMENT OF ENERGY, CONTRACT DE-AC03-76SF00515.

1. INTRODUCTION

One of the most remarkable claims of theoretical physics, is that the Lagrangian density of Quantum Chromodynamics (QCD),

$$\mathcal{L}_{QCD} = -\tfrac{1}{2}\,\mathrm{Tr}\,[F^{\mu\nu}F_{\mu\nu}] + \bar{\psi}(i\not{D} - m)\psi$$

$$F^{\mu\nu} = \partial^{\mu}A^{\nu} - \partial^{\nu}A^{\mu} + ig[A^{\mu}, A^{\nu}]$$

$$D^{\mu} = \partial^{\mu} + ig\,A^{\mu}$$

describes all aspects of the hadron and nuclear physics. This elegant expression compactly describes a renormalizable theory of color-triplet spin-a quark fields ψ and color-octet spin-l gluon fields A^{μ} with an exact symmetry under SU(3)-color local gauge transformations. According to QCD, the elementary degrees of freedom of hadrons and nuclei and their strong interactions are the quark and gluon quanta of these fields. The theory is, in fact, consistent with a vast array of experiments, particularly high momentum transfer phenomena, where because of the smallness of the effective coupling constant and factorization theorems for both inclusive and exclusive processes, the theory has high predictability.[1] (The term "exclusive" refers to reactions in which all particles are measured in the final state.)

The general structure of QCD indeed meshes remarkably well with the facts of the hadronic world, especially quark-based spectroscopy, current algebra, the approximate point-like structure of large momentum transfer inclusive reactions, and the logarithmic violation of scale invariance in deep inelastic lepton-hadron reactions. QCD has been successful in predicting the features of electron-positron and photon-photon annihilation into hadrons, including the magnitude and scaling of the cross sections, the complete form of the photon structure function, the production of hadronic jets with patterns conforming to elementary quark and gluon subprocesses. Recent Monte Carlo studies incorporating coherence (angle-ordering) have been successful in reproducing the detailed features of the two-jet $(q\bar{q})$ and three-jet $(q\bar{q}g)$ reactions. The experimental measurements appear to be consistent with the basic postulates of QCD, that the charge and weak currents within hadrons are carried by fractionally-charged quarks, and that the strength of the interactions between the quarks and gluons becomes weak at short distances, consistent with asymptotic freedom.

Nevertheless in some very striking cases, the predictions of QCD appear to be in dramatic conflict with experiment:

1. The spin dependence of large angle pp elastic scattering has an extraordinarily rich structure- particularly at center of mass energies $E_{CM} \simeq 5\ GeV$.

The observed behavior is quite different than the structureless predictions of the perturbative QCD theory of exclusive processes.

2. QCD predicts a rather novel feature: instead of the traditional Glauber theory of initial and final state interactions, QCD predicts negligible absorptive corrections, i.e., the "color transparency" of high momentum transfer quasi-elastic processes in nuclei. A recent experiment at Brookhaven National laboratory seems to confirm this prediction, at least at low energies, but the data show, that at the same energy where the anomalous spin correlations are observed in pp elastic scattering, the color transparency prediction unexpectedly fails.

3. Recent measurements by the European Muon Collaboration of the deep inelastic structure functions on a polarized proton show a number of unexpected features; a strong positive correlation of the up quark spin with the proton, a strong negative polarization of the down quark, and a significant strange quark content of the proton. The EMC data indicate that the net spin of the proton is carried by gluons and orbital angular momentum, rather than the quarks themselves.

4. The J/ψ and ψ' are supposed to be simple S-wave n=l and n=2 QCD bound states of the charm and anti-charm quarks. Yet these two states have anomalously different two-body decays into vector and pseudo-scalarhadrons.

5. The hadroproduction of charm states and charmonium is supposed to be predictable from the simple fusion subprocess $gg \rightarrow c\bar{c}$. However, recent measurements indicate that charm particles are produced at higher momentum fractions than allowed by the fusion mechanism, and they show a much more complex nuclear dependence than simple additivity in nucleon number predicted by the model.

All of these anomalies suggest that the proton itself is a much more complex object than suggested by simple non-relativistic quark models. Recent analyses of the proton distribution amplitude using QCD sum rules points to highly-nontrivial proton structure. Solutions to QCD in one-space and one-time dimension suggest that the momentum distributions of non-valence quarks in the hadrons have a non-trivial oscillatory structure. The data seems also to be suggesting that the "intrinsic" bound state structure of the proton has a non-negligible strange and charm quark content, in addition to the. "extrinsic" sources of heavy quarks created in the collision itself. As we shall see in this lecture, the apparent discrepancies with experiment are not so much a failure of QCD, but rather symptoms of the complexity and richness of the theory. An important tool for analyzing this complexity is the light-cone Fock state representation of hadron wavefunctions, which

provides a consistent but convenient framework for encoding the features of relativistic many-body systems in quantum field theory.

General Features of QCD

The quark fields of QCD carry flavor quantum numbers as well as the electromagnetic and weak currents. The charge and other quantum numbers of the hadrons thus reflect the quantum numbers of their quark constituents. However, the proton in QCD is only to first approximation a bound state of two u and one d quark. Because of quantum fluctuations, one expect that a highly relativistic bound state contains admixtures of $|uudg>$, $|uuds\bar{s}>$ and other higher particle number Fock components which match the proton' global quantum numbers. There is some evidence that the proton wavefunction even contains $|uudc\bar{c}>$ Fock states at the half-percent level:

The exchange of the spin-one color-octet gluons between the quarks and other gluons leads to strong confining forces at large distances, but progressively weaker forces at short distances. This is the "asymptotic freedom" property of QCD which allows perturbative calculations of large momentum transfer processes. The gluons are neutral with respect to the flavor and electroweak charges. In principle, QCD should give just as accurate a description of hadronic phenomena as quantum electrodynamics provides for the interactions of leptons. However, because of its. non-Abelian structure, calculations in QCD are much more complex. The central feature of the theory is, in fact, its non-perturbative nature which evidently leads to the confinement of quarks and gluons in color-singlet bound states. Rigorous proofs of confinement, however, have not been given. Because of the postulated confinement of the colored quanta, observables always involve the dynamics of bound systems; hadron-hadron interactions are thus as complicated as the Van der Waals and covalent exchange forces of neutral atoms.

Unlike atomic physics, the constituents of light hadrons in QCD are highly relativistic; because the forces are non-static, a hadron cannot be represented as a state of fixed number of quanta at a fixed time. The vacuum structure of the QCD Hamiltonian quantized at fixed time relative to the perturbative basis is also complex; it is believed that virtually every local color-singlet operator constructed from the product of quark and gluon fields may have a non-zero vacuum condensate expectation value. In the light-cone framework, the vacuum itself is trivial since it is an eigenstate of the bare Hamiltonian; the complexity of the vacuum at equal time gets shifted to the complexity of the Fock representation when one quantizes the theory on the light cone.

Despite the complexity of the theory, QCD has several key properties which make calculations tractable and systematic, at least in the short-distance, high

momentum-transfer domain. The critical feature is asymptotic freedom: the effective coupling constant $\alpha_s(Q^2)$ which controls the interactions of quarks and gluons at momentum transfer Q^2 vanishes logarithmically at high Q^2:

$$\alpha_s(Q^2) = \frac{4\pi}{\beta \log(Q^2/\Lambda^2_{\rm QCD})} \qquad (Q^2 \gg \Lambda^2_{\rm QCD}) . \tag{1}$$

[Here $\beta = 11 - \frac{2}{3} n_f$ is derived from the gluonic and quark loop corrections to the effective coupling constant; n_f is the number of quark contributions to the vacuum polarization with $m_f^2 \lesssim Q^2$.] The parameter $\Lambda_{\rm QCD}$ normalizes the value of $\alpha_s(Q_0^2)$ at a given momentum transfer Q_0^2, given a specific renormalization or cutoff scheme. The value of α_s can be determined fairly unambiguously using the measured branching ratio for upsilon radiative decay $\Upsilon(b\bar{b}) \to \gamma X$:[2]

$$\alpha_s(0.157\, M_\Upsilon) = \alpha_s(1.5\ {\rm GeV}) = 0.23 \pm 0.03 . \tag{2}$$

Taking the standard MS dimensional regularization scheme, this gives $\Lambda_{\overline{MS}} = 119^{+\,52}_{-\,34}$ MeV. A recent analysis of logarithmic scale-breaking of the isoscalar nucleon structure functions $F_2(x, Q^2)$ and $xF_3(x, Q^2)$ from deep inelastic neutrino and anti-neutrino interactions in neon by the BEBC WA59 collaboration[3] gives values for $\Lambda_{\overline{MS}}$ in the neighborhood of 100 MeV. The observed multijet distributions[6] in e^+e^- annihilation also suggest that $\Lambda_{\overline{MS}}$ is below 200 MeV and is perhaps as small as 100 MeV. In order to determine the absolute value of $\Lambda_{\overline{MS}}$ one must know the correct argument Q* of the running coupling constant appropriate to the measurement. The above determinations of $\Lambda_{\overline{MS}}$ use the method of Ref. 4 in which this scale is determined "automatically" by requiring that light fermion pairs contributions are summed by the running coupling constant, just as is done in Abelian QED.

In more physical terms, the effective potential between infinitely heavy quarks has the form [$C_F = 4/3$ for $n_c = 3$],[4]

$$\begin{aligned} V(Q^2) &= -C_F\, \frac{4\pi \alpha_V(Q^2)}{Q^2} \\ \alpha_V(Q^2) &= \frac{4\pi}{\beta \log(Q^2/\Lambda_V^2)} \qquad (Q^2 \gg \Lambda_V^2) \end{aligned} \tag{3}$$

where $\Lambda_V = \Lambda_{\overline{MS}}\, e^{5/6} \simeq 270 \pm 100$ MeV. Thus the effective physical scale of QCD is $\sim 1\ f_m^{-1}$. At momentum transfers beyond this scale, α_s becomes small, QCD perturbation theory should begin to become applicable, and a microscopic description of short-distance hadronic and nuclear phenomena in terms of quark and gluon subprocesses is expected to become viable.

The above argument is the main basis for the reliability of perturbative calculations for processes in which all of the interacting particles are forced to exchange large momentum transfer (a few GeV). Complimentary to asymptotic freedom is the existence of factorization theorems for both exclusive and inclusive processes at large momentum transfer which are valid for all gauge theories. In the case of exclusive processes (in which the kinematics of all the final state hadrons are fixed), any hadronic scattering amplitude can be represented as the product of a hard-scattering amplitude for the constituent quarks, convoluted with a distribution amplitude for each in-going or out-going hadron. The distribution amplitude contains all of the bound-state dynamics and specifies the momentum distribution of the quarks in each hadron independent of the process. The hard scattering amplitude can be calculated perturbatively in powers of $\alpha_s(Q^2)$. The predictions can be applied to form factors, exclusive photon-photon reactions, photoproduction, fixed-angle scattering, etc.

In the case of high momentum transfer inclusive reactions (in which final state hadrons are summed over), the hadronic cross section can be computed from the product of a perturbatively-calculable hard-scattering subprocess cross section involving quarks and gluons convoluted with the appropriate quark and gluon structure functions which incorporate all of bound-state dynamics. Since the distribution amplitudes and structure functions only depend on the composition of the respective hadron, but not the nature of the high momentum transfer reaction, the complicated non-perturbative QCD dynamics is factorized out as universal quantities. Recently there has been encouraging progress in actually calculating these fundamental quantities, which I shall briefly review here. Eventually these calculations can be compared with the phenomenological parameterization extracted from inclusive and exclusive experiments.

Hadronic Structure in QCD

The central unknown in the QCD predictions is the composition of the hadrons in terms of their quark and gluon quanta. Recently several important tools have been developed which allow specific predictions for the hadronic wave functions directly from the theory. A primary tool is the use of light-cone quantization to construct a consistent relativistic Fock state basis for the hadrons in terms of quark and gluon quanta. The distribution amplitude and the structure functions are defined directly in terms of these light-cone wave functions. The form factor of a hadron can be computed exactly in terms of a convolution of initial and final light-cone Fock state wave functions.

A second important tool is the use of QCD sum rules to constrain moments of the hadron distribution amplitudes.[5] This method, developed by Chernyak and Zhitnitskii, has yielded important information on the possible momentum space

structure of hadrons. A particularly important advance is the construction of nucleon distribution amplitudes, which together with the QCD factorization formulae, predicts the correct sign and magnitude as well as scaling behavior of the proton and neutron form factors. A recent analysis by King and Sachrajda[7] has confirmed these results.

Another recent advance has been the development of a formalism to calculate the moments of the meson distribution amplitude using lattice gauge theory. The most recent analysis, by Martinelli and Sachrajda,[8] gives moments for the pion distribution amplitude in good agreement with the QCD sum rule calculation. The results from both the lattice calculations and QCD sum rules also demonstrate that the-light quarks are highly relativistic in the bound state wave functions. This gives further indication that while potential models are useful for enumerating the spectrum of hadrons (because they express the relevant degrees of freedom), they are not reliable predicting wave function structure. However, in the case of the proton, the lattice calculation[8] of the lowest moments suggests equal partition of momentum among the three valence quarks.

Fock State Expansion on the Light Cone

A key problem in the application of QCD to hadron and nuclear physics is how to determine the wave function of a relativistic multi-particle composite system. It is not possible to represent a relativistic field-theoretic bound system limited to a fixed number of constituents at a given time since the interactions create new quanta from the vacuum. Although relativistic wave functions can be represented formally in terms of the covariant Bethe-Salpeter formalism, calculations beyond ladder approximation appear intractable. Unfortunately, the Bethe-Salpeter ladder approximation is often inadequate. For example, in order to derive the Dirac equation for the electron in a static Coulomb field from the Bethe-Salpeter equation for muonium with $m_\mu/m_e \to \infty$ one requires an infinite number of irreducible kernel contributions to the QED potential. Matrix elements of currents and the wave function normalization also require, at least formally, the consideration of an infinite sum of irreducible kernels. The relative-time dependence of the Bethe Salpeter amplitudes for states with three or more constituent fields adds severe complexities.

A different and more intuitive procedure would be to extend the Schrödinger wave function description of bound states to the relativistic domain by developing a relativistic many-body Fock expansion for the hadronic state. Formally this can be done by quantizing QCD at equal time, and calculating matrix elements from the time-ordered expansion of the S-matrix. However, the calculation of each covariant Feynman diagram with n-vertices requires the calculation of n! frame-dependent time-ordered amplitudes. Even worse, the calculation of the normalization of a

bound state wave function (or the matrix element of a charge or current operator) requires the computation of contributions from all amplitudes involving particle production from the vacuum. (Note that even after normal-ordering, the interaction Hamiltonian density for QED, H_I = e : $\bar{\psi}\gamma_\mu\psi A^\mu$:, contains contributions $b^\dagger d^\dagger a^\dagger$ which create particles from the perturbative vacuum.)

Fortunately, there is a natural and consistent covariant framework, originally due to Dirac,[10] (quantization on the "light front ") for describing bound states in gauge theory analogous to the Fock state in non-relativistic physics. This framework is the light-cone quantization formalism in which

$$|\pi\rangle = |q\bar{q}\rangle\,\psi^{\pi}_{q\bar{q}} + |q\bar{q}g\rangle\,\psi^{\pi}_{q\bar{q}g} + \cdots$$
$$|p\rangle = |qqq\rangle\,\psi^{p}_{qqq} + |qqqg\rangle\,\psi^{p}_{qqqg} + \cdots \qquad (4)$$

Each wave function component ψ_n, etc. describes a state of fixed number of quark and gluon quanta evaluated in the interaction picture at equal light-cone "time" τ = t + z/c. Given the $\{\psi_n\}$, virtually any hadronic property can be computed, including anomalous moments, form factors, structure functions for inclusive processes, distribution amplitudes for exclusive processes, etc.

The use of light-cone quantization and equal τ wave functions, rather than equal t wave functions, is necessary for a sensible Fock state expansion. It is also convenient to use r-ordered light-cone perturbation theory (LCPTh) in place of covariant perturbation theory for much of the analysis of light-cone dominated processes such as deep inelastic scattering, or large-$p_\perp$ exclusive reactions.

The use of quark and gluon degrees of freedom to represent hadron dynamics seems paradoxical since free quark and gluon quanta have not been observed. Nevertheless, we can use a complete orthonormal Fock basis of free quarks and gluons, color-singlet eigenstates of the free part H_0^{QCD} of the QCD Hamiltonian to expand any hadronic state at a given time t. It is particularly advantageous to quantize the theory at a fixed light-cone time $\tau = t + z/c$ and choose the light-cone $A^+ = A^0 + A^z = 0$ gauge since the formulation has simple properties under Lorentz transformations, there are no ghost (negative metric) gluonic degrees of freedom, and complications due to vacuum fluctuations are minimized. Thus in e^+e^- annihilation into hadrons at high energies it is vastly simpler to use the quark and gluon Fock basis rather than the set of J = 1, J_z = 1, Q = 0 multi-particle hadronic basis to represent the final state. Notice that the complete hadronic basis must include gluonium and other hadronic states with exotic quantum numbers. Empirically, the perturbative QCD calculations of the final state based on jets or clusters of quarks and gluons, have been shown to give a very successful representation of the observed energy and momentum distributions.

Since both the hadronic and quark-gluon bases are complete, either can be used to represent the evolution of a QCD system. For example, the proton QCD eigenstate can be defined in terms of its projections on the free quark and gluon momentum space basis to define Fock wavefunctions; the sum of squares of these quantities then defines the structure functions measured in deep inelastic scattering.

In the case of large momentum transfer exclusive reactions such as the elastic proton form factor, the state formed immediately after the hard collision is most simply described as a valence Fock state with the quarks at small relative impact parameter $b_\perp \sim 1/Q$, where $Q = p_T$ is the momentum transfer scale. Such a state has a small color-dipole moment and thus can penetrate a nuclear medium with minimal interaction. The small impact parameter state eventually evolves to the final recoil hadron, but at high energies this occurs outside the nuclear volume. Thus quasi-elastic hard exclusive reactions are predicted to have cross sections which are additive in the number of nucleons in the nucleus. This is the phenomenon of "color transparency." which is in striking contrast to Glauber and other calculations based on strong initial and final state absorption corrections. Alternatively, the small impact state can be represented as a coherent sum of all hadrons with the same conserved quantum numbers. At high energies, the phase coherence of the state can be maintained through the nucleus, and the coherent state can penetrate the nucleus without interaction. This is the dual representation of color transparency.

In the following sections I will discuss recent developments in hadron and nuclear physics which make use of the quark/gluon light-cone Fock representation of hadronic systems. The method of discretized light-cone quantization (DLCQ) provides a numerical method for solving gauge theories in the light-cone Fock basis. Recent results for QCD in one space and one time are presented in section 12. The most important tool for examining the structure of hadrons is deep inelastic and elastic lepton scattering. I give a survey of tests of QCD in exclusive and inclusive electroproduction in section 3, especially experiments which use a nuclear target to filter or modify the hadronic state. I also give a brief review of what is known about proton structure in QCD. A new approach to shadowing and anti-shadowing of nuclear structure functions is also presented. The distinction between intrinsic and extrinsic contributions to the nucleon structure function is emphasized,

One of the most important challenges to the validity of the QCD description of proton interactions is the extraordinary sensitivity of high energy large angle proton-proton scattering to the spin correlations of the incident protons. A solution to this problem based on heavy quark thresholds is described in section 11. A prediction for a new form of quasi-stable nuclear matter is also briefly discussed.

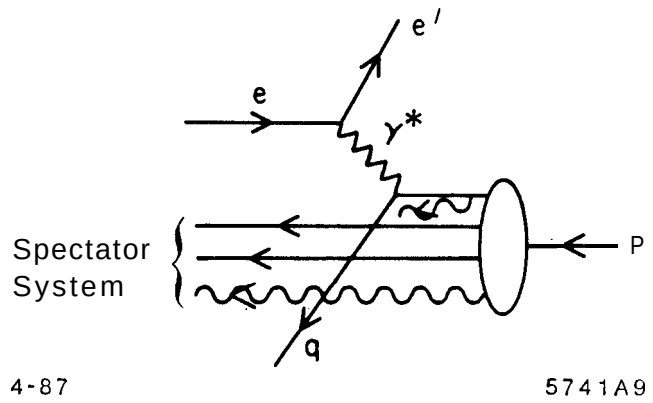

Figure 1. Struck quark and spectator systems in electroproduction.

A scanning transmission electron microscope[11] provides an image of a specimen by combining information from both the-elastically and inelastically scattered-electrons that emerge after passing through the target. A high energy electroproduction experiment which measures both exclusive and inclusive reactions is a close analog of an electron microscope, providing images of the nucleon and nucleus at a resolution scale $\lambda \sim 1/Q$ where $Q^2 = -(p_e - p'_e)^2$ is the momentum transfer squared. At the most basic level, Bjorken scaling of deep inelastic structure functions implies the production of a single quark jet, recoiling against the scattered lepton. The spectator system- the remnant of the target remaining after the scattered quark is removed-is a colored $\bar{3}$ system. (See fig. 1.) According to QCD factorization, the recoiling quark jet, together with the gluonic radiation produced in the scattering process, produces hadrons in a universal way, independent of the target or particular hard scattering reaction. This jet should be identical to the light quark jets produced in e^+e^- annihilation. A very close analogy can be made between soft radiation from colored quark and gluon quanta, and soft photon radiation from charged particles in QED. In contrast, the hadronization of the spectator system depends in detail on the target properties. Unlike the quark jet, the leading particles of the target spectator system do not evolve and thus should not depend on the momentum transfer Q^2 [at fixed $W^2 = (q + p)^2$]. Measurements of the final state radiation pattern in ep collisions at HERA should be able to discriminate between these different types of QCD radiators.

Measurements of the nucleon and nuclear structure functions have not only tested the short-distance properties of the theory, (such as the scaling properties of structure functions and their logarithmic evolution with momentum transfer), but they have also illuminated the nonperturbative bound state structure of the nucleon and nuclei in terms of their quark and gluon degrees of freedom. For the most part, this information has been obtained from single-arm inclusive experiments where only the recoil lepton was detected.

In the future we can expect to see much more extensive measurements of the structure of the nucleon and nucleus by utilizing an internal target facility in an electron storage ring, such as PEP, Tristan, HERA, or LEP. The entire final state of electroproduction can be measured in coincidence with the scattered electron with close to 4π acceptance. In the case of the planned gas jet PEGASYS experiment at PEP $(E(e^{\pm}) \sim 15\ \mathrm{GeV})$, measurements can be performed well above the onset of Bjorken scaling. Both polarized and unpolarized hydrogen and nuclear targets may be feasible, and eventually even polarized electron beams may be available. High precision comparisons between electron and positron scattering would allow the study of higher order QED and electroweak interference effects. The asymmetry in the cross sections for $e^{\pm}p \to e^{\pm}\gamma X$ can be sizeable,[12] providing a sum rule for the cube of the charges of the quarks in the target. The PEGASYS kinematic range interpolates between the lower energy CEBAF domain where quark degrees of freedom begin to become manifest, and the much higher energies of HERA, which is far into the perturbative QCD regime of logarithmic evolution and multi-jet structure.

Since the intrinsic mass scales of QCD $\Lambda_{\overline{MS}}$, $\langle k_{\perp}^2 \rangle^{\frac{1}{2}}$, and $m_q (q = u, d, s)$ are less than a few hundred MeV, quark and gluon degrees of freedom should become evident at momentum transfers as low as a few GeV. The observation of Bjorken scaling at Q^2 as low as 1 GeV^2 supports this argument. At larger momentum transfer, one studies logarithmic structure function evolution, the onset of new quark flavors, and multi-jet production. However, the dynamics of hadrons and nuclei in terms of their light quark and gluon degrees of freedom can be studied at moderate energies. At a more detailed level, the features of the standard leading twist description are modified by coherent or non-perturbative effects. For example, higher twist-power-law suppressed contributions arise when two or more quarks recoil against the scattered lepton.

The study of QCD phenomena in the intermediate energy range can also be carried out at $\bar{p}p$ facilities such as LEAR and the proposed AMPLE facility at Fermilab, designed to measure $p\bar{p}$ annihilation at anti-proton laboratory energies up to 10 GeV. The $\gamma\gamma$ reactions (for real and virtual photons from tagged e*) provide some of the cleanest tests of QCD. Presently these reactions can be studied

at the PEP, Cornell, and Tristan e^+e^- storage rings. One can test the scaling laws of QCD in exclusive reactions involving two large momentum scales, the virtual photon mass and the p_T of the reaction. An interesting feature of QCD is that at large p_T^2, the Q^2 dependence of each exclusive virtual photoproduction amplitude becomes minimal for $Q^2 \ll p_T^2$. This can be contrasted with the vector meson dominance model which predicts a universal fall-off in Q^2 at any p_T. This feature is due to the photon's point-like direct local coupling to the quark current in QCD. I will discuss QCD tests in photon-photon reactions in section 8.

2. Nuclear Effects in QCD

The study of electroproduction in nuclear targets gives the experimentalist the extraordinary ability to modify the environment in which hadronization occurs. The essential question is how the nucleus changes or influences the mechanism in which the struck quark and the spectator system of the target nucleon form final state hadrons. The nucleus acts as a background field modifying the dynamics in interesting, though possibly subtle, ways. In particular, the observation of non-additivity of the nuclear structure functions as measured by the EMC and SLAC/American University collaborations have opened up a whole range of new physics questions:

1. What is the effect of simple potential-model nuclear binding, as predicted, for example, by the shell model? What is the associated modification of meson distributions required by momentum sum rules?
2. Is there a physical change in the nucleon size, and hence the shape of quark momentum distributions?
3. Are there nuclear modifications of the nucleonic and mesonic degrees of freedom, such as induced mesonic currents, isobars, six-quark states, or even "hidden color" degrees of freedom?
4. Does the nuclear environment modify the starting momentum scale evolution scale for gluonic radiative corrections?
5. What are the effects of diffractive contributions to deep inelastic structure functions which leave the nucleon or nuclear target intact?
6. Are there shadowing and possibly anti-shadowing coherence effects influencing the propagation of virtual photons or redistributing the nuclear constituents? Do these appear at leading twist?
7. How important are interference effects between quark currents in different nucleons?[13]

It seems likely that all of these non-additive effects occur at some level in the nuclear environment. In particular it will be important to examine the A-dependence of each reaction channel by channel.

The use of nuclear targets in electroproduction allows one to probe effects specific to the physics of the nucleus itself such as the short-distance structure of the deuteron, high momentum nucleon-nucleon components, and coherent effects such as shadowing, anti-shadowing, and $x > 1$ behavior. However, perhaps the most interesting aspect for high energy physics is the use of the nucleus to modify the environment in which quark hadronization and particle formation occurs.

The Target Length Condition

There are several general properties of the effect of the nuclear environment which follow from quantum mechanics and the structure of gauge theory. The first effect is the "formation zone" which reflects the principle that a quark or hadron can change state only after a finite intrinsic time in its rest system. This implies that the scattered quark in electroproduction cannot suffer an inelastic reaction with mass squared change ΔM^2 while propagating a distance L if its laboratory energy is greater than $\Delta M^2 L$. Thus a high energies, the quark jet does not change its state or hadronize over a distance scale proportional to its energy; inelastic or absorptive processes cannot occur inside a nucleus-at least for the very fast hadronic fragments. The energy condition is called the-target length condition[16,17] However the outgoing quark can still scatter elastically as it traverses the nuclear volume, thus spreading its transverse momentum due to multiple scattering. Recently Bodwin and Lepage and I have explained the quantum mechanical origin of formation zone physics in terms of the destructive interference of inelastic amplitudes that occur on two different scattering centers in the nuclear target.[19] The discussion in that paper for the suppression of inelastic interactions of the incoming anti-quark in Drell-Yan massive lepton pair reactions can be carried over directly to the suppression of final state interactions of the struck quark in electroproduction.

Color Transparency

One can also use a nuclear target to test an important principle of gauge theory controlling quark hadronization into exclusive channels inside nuclei: "color transparency".[14] Suppose that a hadronic state has a small transverse size $b_\perp$. Because of the cancellation of gluonic interactions with wavelength smaller than $b_\perp$, such a small color-singlet hadronic state will propagate through the nucleus with a small cross section for interacting in either elastically or inelastically. In particular, the recoil proton in large momentum transfer electron-proton scattering is produced initially as a small color singlet three-quark state of transverse size $b_\perp \sim 1/Q$. If the electron-proton scattering occurs inside a nuclear target (quasi-

elastic scattering) then the recoil nucleon can propagate through the nuclear volume without significant final-state interactions. This perturbative QCD prediction is in striking contrast to standard treatments of quasi-elastic scattering which predict significant final state scattering and absorption in the nucleus due to large elastic and inelastic nucleon-nucleon cross sections. The theoretical calculations of the color transparency effect must also take into account the expansion of the state as it evolves to a normal proton of normal transverse size while it traverses the nucleus. I will discuss color transparency further in Section 10.

Shadowing and Anti-Shadowing

One of the most striking nuclear effects seen in the deep inelastic structure functions is the depletion of the effective number of nucleons F_2^A/F_2^N in the region of low $x = x_{bj}$. The results from the EMC collaboration indicate that the effect is roughly Q^2-independent; i.e. shadowing is a leading twist in the operator product analysis. In contrast, the shadowing of the real photo-absorption cross section due to p-dominance falls away as an inverse power of Q^2.

Shadowing is a destructive interference effect which causes a diminished flux and interactions in the interior and back face of the nucleus. The Glauber analysis of hadron-nucleus scattering corresponds to the following: the incident hadron scatters elastically on a nucleon N_1 on the front face of the nucleus. At high energies the phase of the amplitude is imaginary. The hadron then propagates through the nucleus to nucleon N_2 where it interacts inelastically. The accumulated phase of the propagator is also i so that this multi-scattering amplitude is coherent and opposite in phase to the amplitude where the beam hadron interacts directly on N_2 without initial-state interactions. Thus the target nucleon N_2 sees less incoming flux; it is shadowed by elastic interactions on the front face of the nucleus. If the hadron-nucleon cross section is large, then the effective number of nucleons participating in the inelastic interactions is reduced to $\sim A^{2/3}$, the number of surface nucleons.

In the case of virtual photo-absorption, the photon converts to a $q\bar{q}$ pair at a distance proportional to $\omega = x^{-1} = 2p \cdot q/Q^2$ laboratory frame. The nuclear structure function F_2^A can then be written as an integral over the inelastic cross section $\sigma_{\bar{q}A}(s')$ where s' grows as 1/x for fixed space-like $\bar{q}$ mass. Thus the A-dependence of the cross section is equivalent to the shadowing of the $\bar{q}$ interactions in the nucleus. Recently Hung Lu and I have applied the standard Glauber multi-scattering theory, assuming that formalism can be taken over to off-shell $\bar{q}$ interactions!" Our results show that for reasonable values of the 'if-nucleon cross section, one can easily understand the magnitude of the shadowing effect at small x. Moreover, if one introduces a $\alpha_R \simeq \frac{1}{2}$ Reggeon contribution to the $\bar{q}N$ amplitude, the real part of the phase introduced by such a contribution automatically leads to "anti-shadowing" at x $\sim$ 0.1 (effective number of nucleons $F_2^A(x,Q)/F_2^N(x,Q) > A$) of

the few percent magnitude seen by the SLAC and EMC experiments. Since the Reggeon term is non-singlet, anti-shadowing is associated with a redistribution of the valence quarks in the nucleus.

Our analysis provides the input or starting point for the log Q^2 evolution of the deep inelastic structure functions. The parameters for the effective quark-nucleon cross section required to understand shadowing phenomena provide important information on the interactions of quarks and gluons in nuclear matter.

The above analysis also has implications for the nature of particle production for virtual photo-absorption in nuclei. At high Q^2 and x > 0.3, hadron production should be uniform throughout the nucleus. At low x or at low Q^2, where shadowing occurs the inelastic reaction occurs mainly at the front surface. These features can be examined in detail by studying non-additive multiparticle correlations in both the target and current fragmentation regions.

3. Proton Structure and Electroproduction

Spin Effects in Deep Inelastic Scattering

The EMC and SLAC data on polarized structure functions imply significant correlations between the spin of the target proton with the spin of the gluons and strange quarks. Thus there should be significant correlations between the target spin and spin observables in the electroproduction final state, both in the current: and target fragmentation region. It thus would be interesting to measure the spin of specific hadrons which are helicity self-analyzing through their decay products such as the ρ and the A.

It is useful to keep in mind the following simple model for the helicity parallel and helicity anti-parallel gluon distributions in the nucleon: $G^{+}_{g/N}$ (x) = $\frac{3}{2}(1-x)^4/x$ and $G^{-}_{g/N}$ (x) = $\frac{3}{2}(1-x)^6/$x, respectively. This model is consistent with the momentum fraction carried by gluons in the proton, correct crossing behavior, dimensional counting rules at x $\rightarrow 1$, and Regge behavior at small x. Integrating over x, one finds that the gluon carries, on the average, $11/24$ of the total nucleon J_z. It is thus consistent with experiment and the Skryme model prediction that more of the nucleon spin is carried by gluons rather than quarks.[21]

The analyses of the EMC and SLAC spin-dependent structure functions as well as elastic neutrino-proton scattering imply substantial strange and anti-strange quarks in the proton, highly spin-correlated with the proton spin. The usual description of the strange sea assumes that $s\bar{s}$ is strictly due to the simple gluon splitting process. The spin correlation of the strange quarks then requires a very large gluon spin correlation, much stronger than the simple mode1 given above. Alternatively the strange sea may be "intrinsic" to the bound state equation of

motion of the nucleon and thus the strong strange spin correlation may be a non-perturbative phenomena. One expects contributions at order $1/m_s^2$ to the strange sea from cuts of strange loops quark loops in the wavefunction with 2, 3, and 4 gluons connecting to the other quark and gluon constituents of the nucleon. Alternatively, one can regard the strange sea as a manifestation of intermediate $K - \Lambda$ and other virtual meson-baryon pair states in the fluctuations of the proton ground state.

Experiments which examine the entire final state in electroproduction can discriminate between these extrinsic and intrinsic components to the strange sea. For example, consider events in which a strange hadron is observed at large z in the fragmentation region of the recoil jet, signifying the production and tagging of a strange quark. In the case of intrinsic strangeness, the associated $\bar{s}$ will be in the target fragmentation region. In the case that the strange quark is created extrinsically via $\gamma^* g \rightarrow s\bar{s}$, both the tagged s quark and the $\bar{s}$ hadrons will be found predominantly in the current fragmentation region.

"Extrinsic" versus "Intrinsic" Contributions to the Proton Structure Functions

The central focus of inelastic electroproduction is the electron-quark interaction, which at large momentum transfer can be calculated as an incoherent sum of individual quark contributions. The deep inelastic electron-proton cross section is thus given by the convolution of the electron-quark cross section times the structure functions, or equivalently the probability distributions $G_{q/p}(x, Q^2)$. In the "infinite momentum frame" where the proton has large momentum P^μ and the virtual photon momentum is in the transverse direction, $G_{q/p}(x, Q^2)$ is the probability of finding a quark q with momentum fraction x = $Q^2/2p \cdot q$ in the proton. However in the rest frame of the target, many different physical processes occur: the photon can scatter out a quark as in the atomic physics photoelectric effect, it can hit a quark which created from a vacuum fluctuation near the proton, or the photon can first make a $q\bar{q}$ pair, either of which can interact in the target. Thus the electron interacts with quarks which are both *intrinsic* to the proton's structure itself, or quarks which are *extrinsic;* i.e. created in the electron-proton collision itself. Much of the phenomena at small values of x such as Regge behavior, sea distributions associated with photon-gluon fusion processes, and shadowing in nuclear structure functions can be identified with the extrinsic interactions, rather than processes directly connected with the proton's intrinsic structure.

There is an amusing, though *gedanken* way to (in principle) separate the extrinsic and intrinsic contributions to the proton's structure functions. For example, suppose that one wishes to isolate the intrinsic contribution $G^I_{d/p}(x, Q)$ to the d-quark distribution in the proton. Let us imagine that there exists another set of quarks $\{q_o\} = u_o, d_o, s_o, c_o, \ldots$ identical in all respects to the usual set of quarks but

carrying zero electromagnetic and weak charges. The experimentalist could then measure the difference in scattering of electrons on protons versus electrons scattering on a new baryon with valence quarks $|uud_o>$. This is analogous to an "empty target" subtraction. Contributions from $q\bar{q}$ pair production in the gluonic field of the target (photon-gluon fusion) effectively cancel, so that one can then identify the difference in scattering with the intrinsic d-quark distribution of the nucleon. Because of the Pauli exclusion principle, $d\bar{d}$ production on the proton where the d is produced in the same quantum state as the d in the nucleon is absent, but the corresponding contribution is allowed in the case of the $|uud_o>$ target. Because of this extra subtraction, the contributions associated with Reggeon exchange also cancel in the difference, and thus the intrinsic structure function $G^J(x, Q)$ vanishes at $x \to 0$. The intrinsic contribution gives finite expectation values for the light-cone kinetic energy operator, "sigma" terms, and the $J = 0$ fixed poles associated with $< 1/x >$.[22]

Higher Twist and other QCD Contributions to Electroproduction

Although there have been extensive measurements of the deep inelastic structure functions, some aspects remain to be verified, and will require data over a large range of Q^2. For example, how much of-the scale violation is due to power-law (higher twist) contributions[23] versus logarithmic PQCD evolution? Does the Bjorken-scaling non-isosinglet structure function $F_2(x, Q)$ behave as $Cx^{1-\alpha_\rho}$ as $x \to 0$ as dictated by Regge exchange and duality or is this a manifestation of higher twist contributions to the virtual photo-absorption cross section which falls as $1/Q^2$? Are the non-additive shadowing and anti-shadowing nuclear effects really leading twist or are they Q^2 dependent?

Electron-proton scattering also involves additional processes such as photoproduction, Compton processes, QED radiative corrections, etc. Electroproduction reactions in which large transverse momentum photons appear are particularly interesting. In the exclusive process $e^{\pm}p \to e^{\pm}\gamma p$ one can isolate the virtual Compton cross section as well as the real part of the Compton amplitude. In the inclusive reaction $e^{\pm}p \to e^{\pm}\gamma X$ one can determine reactions and sum rules proportional to the quark charge cubed.

It is thus interesting to consider inclusive electron-proton collisions from a general point of view. As long as there is at least one particle detected at large transverse momentum, whether it is a scattered electron, or a produced hard photon, or a hadron at large P_T, one can use the factorization formula[24]

$$\frac{d\sigma(AB \to CX)}{d^3p_c/E_c} \cong \sum_{ab,cd} \int_0^1 dx_a \int_0^1 dx_b \int_0^1 \frac{dx_c}{x_c^2}$$

$$\times G_{a/A}(x_a, Q) G_{b/B}(x_b, Q) \tilde{G}_{C/c}(x_c, Q)$$

$$\times \delta(s' + t' + u') \frac{s'}{\pi} \frac{d\sigma}{dt'}(ab \to cd)$$

which- has general validity in gauge theory. The systems A, B, C can be leptons, photons, hadrons, or nuclei. The primary subprocess in electroproduction is $eq \to eq$. The electron structure function $G_{e/e}(x, Q)$ automatically provides the (leading logarithmic) QED radiative corrections. The spectrum of the electron beam plays the role of the non-perturbative or initial structure function. (See Fig. 2(b).) The subprocess $\gamma^* q \to gq$ corresponds to photon-induced two-jet production. (See Fig. 2(a).) This subprocess dominates reactions in which the large transverse momentum trigger is a hadron rather than the scattered lepton. Thus one sees that conventional deep inelastic $eq \to eq$ scattering subprocess is just one of the several modes of electroproduction.

The dominant contribution to the meson semi-inclusive cross section is predicted by QCD factorization to be due to jet fragmentation from the recoil quark and spectator diquark jets.

When the momentum transfer is in the intermediate range $1 \lesssim Q^2 \lesssim 10$ GeV^2, several other contributions for meson production are expected to become important in $eN \to e'MX$. These include:

1. Higher twist contributions to jet fragmentation:

$$\frac{dN_\pi}{dz} = D_{\pi/q}(z, Q^2) \cong A(1-z)^2 + \frac{C}{Q^2} \quad (z \to 1).$$

The scaling term reflects the behavior of the pion fragmentation function at large fractional momentum ($z \to 1$) as predicted by perturbative QCD (one-gluon exchange). (See Fig. 3(a).) The C/Q^2 term[25] is computed from the same perturbative diagrams. For large z where this term dominates, we predict that the deep inelastic cross section will be dominantly longitudinal rather than transverse $R = \sigma_L/\sigma_T > 1$.

2. "Direct" meson production. Isolated pions may also be created by elastic

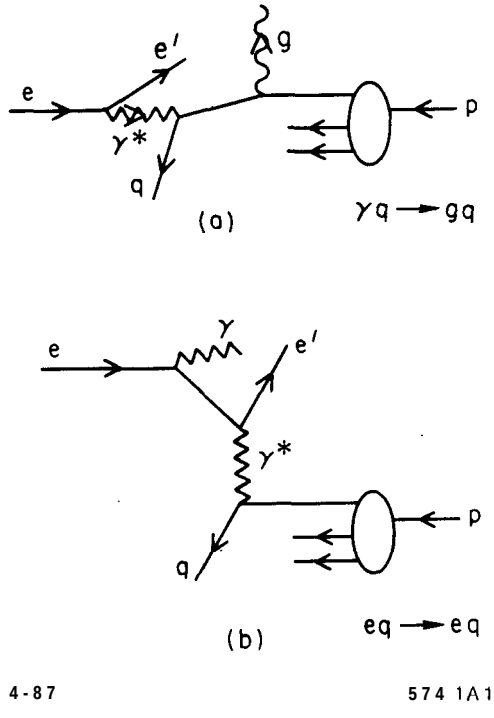

Figure 2. Applicationof gauge theory factorization to electroproduction. (a) The $\gamma q \rightarrow$ **gq** subprocess produces hadron jets at high p_T. (b) The **eq** $\rightarrow$ **eq** produces one quark jet and one recoil electron jet at high p_T. The QED radiative corrections are incorporated into the electron and photon QED structure functions.

scattering off of an effective pion current: (See Fig. 3(b).)

$$\frac{d\sigma}{dQ^2 dx_\pi} = G_{\pi/p}(x_\pi) \left.\frac{d\sigma}{dQ^2}\right|_{e\pi \rightarrow e\pi}$$

$$\left.\frac{d\sigma}{dy dQ^2}\right|_{e\pi \rightarrow e\pi} = \frac{4\pi\alpha^2}{(Q^2)^2} |F_\pi(Q^2)|^2 (1 - y) \ .$$

Here $y = q \cdot p/p_e \ . \ p$. In the case of a nuclear target, one can test for non-additivity of virtual pions due to nuclear effects, as predicted in models[26] for the EMC effect[27] at small x_{Bj}. Jaffe and Hoodbhoy[13] have shown that the existence of quark exchange diagrams involving quarks of different nucleons in the nucleus invalidates general applicability of the simplest convolution formulae conventionally used in such analyses. The $G_{\pi/p}(x, Q)$ structure function is predicted to behave roughly as $(1 - x)^5$ at large x, as predicted from spectator quark counting rules.[29,24] Applications of these rules to other off-shell nucleon processes are discussed in Refs. 30 and 28.

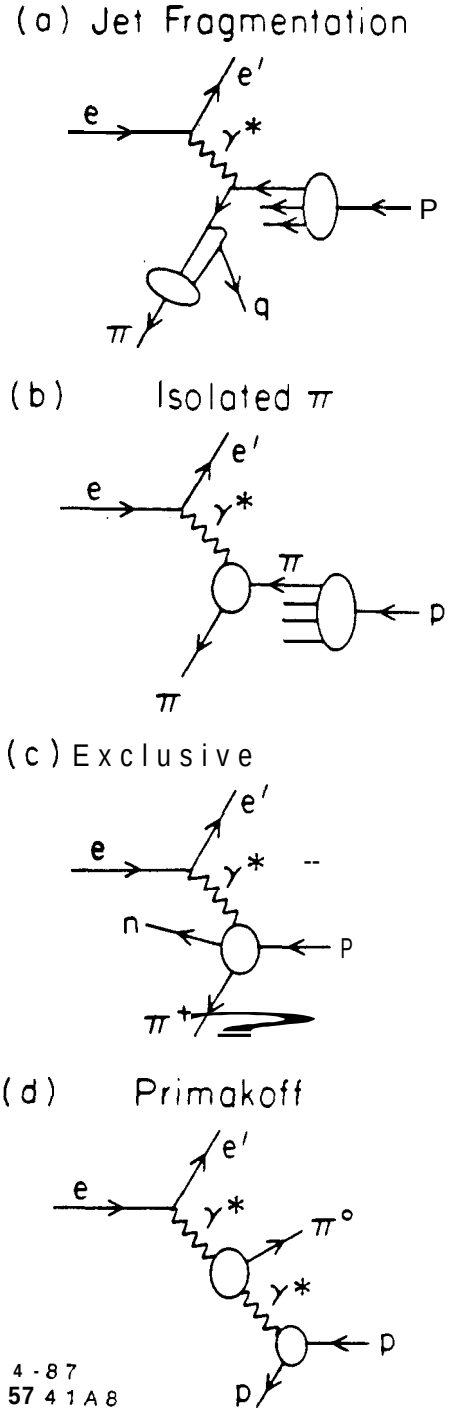

Figure 3. QCD contributions to pion electroproduction. (a) Jet fragmentation, including leading and $1/Q^2$ higher twist contributions. (b) Isolated pion contributions at order $1/Q^4$. (c) Exclusive production. (d) Primakoff contribution.

3. Exclusive Channels. (See, Fig. 3(c).) The mesons can of course be produced

in exclusive channels; e.g. $\gamma^* p \rightarrow \pi^+ n$, $\gamma^* p \rightarrow \rho^0 p$. Pion electroproduction extrapolated to $t = m_\pi^2$ provides the basic knowledge of the pion form factor at spacelike Q^2. With the advent of the perturbative QCD analyses of large momentum transfer exclusive reactions, predictions can be given over the whole range of large t and Q^2. Exclusive processes are discussed in more detail in Section 5-8.

4. Another meson production channel is the Primakoff reaction $\gamma^* \gamma \rightarrow \pi^0$, etc., which dominates over other events at very low target recoil momentum. (See Fig. 3(d).) Such measurements would allow the determination of the $\gamma \rightarrow \pi^0$ transition form factor. This quantity, combined with the QCD analysis of the pion form factor leads to a method to determine the QCD running coupling constant $\alpha_s(Q^2)$ solely from exclusive measurements.[31]

Hadronization of the Quark and Spectator Systems

At the most basic level, Bjorken scaling of deep inelastic structure functions implies the production of a single quark jet, recoiling against the scattered lepton. The spectator system-the remnant of the target remaining after the scattered quark is removed-is a color-3 system. The struck quark is sensitive to the magnitude of the momentum transfer Q and logarithmically evolves by radiated gluons with relative transverse momentum controlled by Q^2 and the available phase-space. According to QCD factorization, the recoiling-quark jet, together with the gluonic radiation produced in the scattering process, produces hadrons in a universal way, independent of the target or particular hard scattering reaction. This jet should be identical to the light quark jets produced in e^+e^- annihilation. In contrast, the hadronization of the spectator system depends in detail on the target properties. Unlike the quark jet, the leading particles of the target spectator system do not evolve and thus should not depend on the momentum transfer Q^2 [at fixed $W^2 = (q + p)^2$]. At present we do not have a basic understanding of the physics of hadronization, although phenomenological approaches, such as the Lund string model, have been successful in parameterizing many features of the data.

Analogs between QCD and QED

Many of the novel features expected in QCD are also apparent in Quantum Electrodynamics (QED). It is thus often useful to keep a QED analog in mind, replacing the target by a neutral atom such as positronium. Even in QED where there is no confinement, one expects in certain kinematic regions significant corrections to the Bjorken scaling associated with positron or electron knockout, in addition to the logarithmic evolution of the QED structure functions associated with induced photon radiation. For example, at low Q^2, the interference between amplitudes where different constituents are struck become important. Near threshold, where

charged particles emerge at low relative velocities, there are strong Coulomb distortions, as summarized by the Sommerfeld[18] factor. In QCD these have their analog in a phenomena called "jet coalescence"[32]. The Coulomb distortion factor must be included if one wants to maintain duality between the inelastic. continuum and a summation over exclusive channels in electroproduction.[33]

4. Applications of QCD to the Phenomenology of Exclusive Reactions

In this section I will discuss the application of QCD to exclusive reactions at large momentum transfer. The primary processes of interest are those in which one learns new information on the structure of the proton and other hadrons. The wavefunctions involved in such reactions are also relevant to the understanding of jet hadronization and the computation of hadron matrix elements for weak decays, etc. This includes form factors at large momentum transfer Q and large angle scattering reactions. Specific examples are reactions such as $e^-p \to e^-p$, $e^+e^- \to p\bar{p}$, elastic scattering reactions at large angles and energies such as $\pi^+p \to \pi^+p$ and $pp \to pp$, two-photon annihilation processes such as $\gamma\gamma \to K^+K^-$ or $\bar{p}p \to \gamma\gamma$, exclusive nuclear processes such as deuteron photo-disintegration $\gamma d \to np$, and exclusive decays such as $\pi^+ \to \mu^+\nu$ or $J/\psi \to \pi^+\pi^-\pi^0$.

As discussed in the introduction, QCD has two essential properties which make calculations of processes at short distance or--high-momentum transfer tractable and systematic. The critical feature is asymptotic freedom: the effective coupling constant $\alpha_s(Q^2)$ which controls the interactions of quarks and gluons at momentum transfer Q^2 vanishes logarithmically at large Q^2 since it allows perturbative expansions in $\alpha_s(Q^2)$. Complementary to asymptotic freedom is the existence of *factorization* theorems for both exclusive and inclusive processes at large momentum transfer. In the case of "hard" exclusive processes (in which the kinematics of all the final state hadrons are fixed at large invariant mass), the hadronic amplitude can be represented as the product of a process-dependent hard-scattering amplitude $T_H(x_i, Q)$ for the scattering of the constituent quarks convoluted with a process-independent *distribution amplitude* $\phi(x, Q)$ for each incoming or outgoing hadron.[34] When Q^2 is large, T_H is computable in perturbation theory as is the Q-dependence of $\phi(x, \mathrm{Q})$.

In Table I we give a summary of the main scaling laws and properties of large momentum transfer exclusive and inclusive cross sections which are derivable starting from the light-cone Fock space basis and the perturbative expansion for QCD.

As emphasized in Section 1, a convenient relativistic description of hadron wavefunctions is given by the set, of n-body momentum space amplitudes, $\psi_n(x_i, k_{\perp_i}, \lambda_i), i =$

Table I Comparison of Exclusive and Inclusive Cross Sections

Exclusive Amplitudes	Inclusive Cross Sections
$\mathcal{M} \sim \Pi\, \phi(x_i, Q) \otimes T_H(x_i, Q)$	$d\sigma \sim \Pi\, G(x_a, Q) \otimes d\hat{\sigma}(x_a, Q)$
$\phi(x, Q) = \int^{Q} [d^2 k_\perp]\, \psi^{Q}_{\text{val}}(x, k_\perp)$	$G(x, Q) = \sum_n \int^{Q} [d^2 k_\perp]\, [dx]'\, \lvert\psi^{Q}_{n}(x, k_\perp)\rvert^2$
Measure ϕ in $\gamma \to M\overline{M}$	Measure G in $\ell p \to \ell X$
$\sum_{i \in H} \lambda_i = \lambda_H$	$\sum_{i \in H} \lambda_i \neq \lambda_H$
Evolution	
$\frac{\partial \phi(x, Q)}{\partial \log Q^2} = \alpha_s \int [dy]\, V(x, y)\, \phi(y)$	$\frac{\partial G(x, Q)}{\partial \log Q^2} = \alpha_s \int dy\, P(x/y)\, G(y)$
$\lim_{Q \to \infty} \phi(x, Q) = \prod_i x_i \cdot C_{\text{flavor}}$	$\lim_{Q \to \infty} G(x, Q) = \delta(x)\, C$
Power Law Behavior	
$\frac{d\sigma}{dx}(A + B \to C + D) \cong \frac{1}{s^{n-2}} f(\theta_{c.m.})$	$\frac{d\sigma}{d^2p/E}(AB \to CX) \cong \sum \frac{(1 - x_T)^{2n_s - 1}}{(Q^2)^{n_{act} - 2}} f(\theta_{c.m.})$
$n = n_A + n_B + n_C + n_D$	$n_{act} = n_a + n_b + n_c + n_d$
T_H : expansion in $\alpha_s(Q^2)$	$d\hat{\sigma}$: expansion in $\alpha_s(Q^2)$
Complications	
End point singularities	Multiple scales
Pinch singularities	Phase-space limits on evolution
High Fock states	Heavy quark thresholds
	Higher twist multiparticle processes
	Initial and final state interactions

1, 2, . . .n, defined on the free quark and gluon Fock basis at equal "light-cone time" $\tau = t+z/c$ in the physical "light-cone" gauge $A^+ \equiv A^0+A^3 = 0$. (Here $x_i = k_i^+/p^+$, $\sum_i x_i = 1$, is the light-cone momentum fraction of quark or gluon i in the n — particle Fock state; $k_{\perp i}$, with $\sum_i k_{\perp i} = 0$, is its transverse momentum relative to the total momentum p^μ; and λ_i is its helicity.) The quark and gluon structure functions $G_{q/H}$ (x, Q) and $G_{g/H}(x, Q)$ whichcontrol hard inclusive reactions and the hadron distribution amplitudes $\phi_H(x, Q)$ whichcontrol hard exclusive reactions are simply related to these wavefunctions:

$$G_{q/H}(x,Q) \propto \sum_n^Q \int \Pi d^2k_{\perp i} \int \Pi dx_i \, |\psi_n(x_i, k_{\perp i})|^2 \delta(x_q - x) \quad ,$$

and

$$\phi_H(x_i, Q) \propto \int^Q \Pi d^2k_{\perp i} \, \psi_{\text{valence}}(x_i, k_{\perp i}) \quad .$$

In the case of inclusive reactions, such as deep inelastic lepton scattering, two basic aspects of QCD are relevant: (1) the scale invariance of the underlying lepton-quark subprocess cross section, and (2) the form and evolution of the structure functions. A structure function is a sum of squares of the light-cone wavefunctions. The logarithmic evolution of $G_q(x, Q^2)$ is controlled by the wavefunctions which fall off as $|\psi(x, \vec{k}_\perp)|^2 \sim$ a,($k_\perp^2$)/ $k_\perp^2$ at large $k_\perp^2$. This form is a consequence of the pointlike $q \to gq$, $g \to$ gg, and g $\to q\bar{q}$ splitting. By taking the logarithmic derivative of G with respect to Q one derives the evolution equations of the structure function. All of the hadron's Fock states generally participate; the necessity for taking into account the (non-valence) higher-particle Fock states in the proton is apparent from two facts: (1) the proton's large gluon momentum fraction and (2) the recent results from the EMC collaboration[35] suggesting that, on the average, little of the proton's helicity is carried by the light quarks.[21]

In the case of exclusive electroproduction reactions such as the baryon form factor, again two basic aspects of QCD are relevant: (1) the scaling of the underlying hard scattering amplitude (such as $l + qqq \to l + qqq$), and (2) the form and evolution of the hadron distribution amplitudes. The distribution amplitude is defined as an integral over the lowest (valence) light-cone Fock state. The logarithmic variation of $\phi(x, Q^2)$is derived from the integration at large $k_\perp$, *i.e.* wavefunctions which behave as $\psi(x, \vec{k}_\perp) \sim \alpha_s(k_\perp^2)/k_\perp^2$ at large $k_\perp^2$ This behavior follows from the simple one-gluon exchange contribution to the tail of the valence wavefunction. By taking the logarithmic derivative, one then obtains the evolution equation for the hadron distribution amplitude.

The form factor of a hadron at any momentum transfer can be computed exactly in terms of a convolution of initial and final light-cone Fock state wavefunctions.[36] In general, all of the Fock states contribute. In contrast, exclusive reactions with high momentum transfer Q, perturbative QCD predicts that only the lowest particle number (valence) Fock state is required to compute the contribution to the amplitude to leading order in 1/Q. For example, in the light-cone Fock expansion the proton is represented as a column vector of states ψ_{qqq}, ψ_{qqqg}, $\psi_{qqq\bar{q}q}$ .... In the light-cone gauge, $A^+ = A^0 + A^3 = 0$, only the minimal "valence" three-quark Fock state needs to be considered at large momentum transfer since any-additional quark or gluon forced to absorb large momentum transfer yields a power-law suppressed contribution to the hadronic amplitude. Thus at large Q^2, the baryon form factor can be systematically computed by iterating the equation of motion for its valence Fock state wherever large relative momentum occurs. To leading order the kernel is effectively one-gluon exchange. The sum of the hard gluon exchange contributions can be arranged as the gauge invariant amplitude T_H, the final form factor having the form

$$F_B(Q^2) = \int [dy] \int [dx]\, \phi_B^\dagger(y_j, Q) T_H(x_i, y_j, Q) \phi_B(x_i, Q) .$$

The essential gauge-invariant input for hard exclusive processes is the distribution amplitude $\phi_H(x, Q)$. For example $\phi_\pi(x, Q)$ is the amplitude for finding a quark and antiquark in the pion carrying momentum fractions x and $1 - x$ at impact (transverse space) separations less than $b_\perp < 1/Q$. The distribution amplitude thus plays the role of the "wavefunction at the origin" in analogous non-relativistic calculations of form factors. In the relativistic theory, its dependence on log Q is controlled by evolution equations derivable from perturbation theory or the operator product expansion. A complete discussion may be found in the papers by Lepage and myself,[38] and our recent review in ref.1. A discussion of the light-cone Fock state wavefunctions and their relation to observables is given in Ref. 37.

The distribution amplitude contains all of the bound-state dynamics and specifies the momentum distribution of the quarks in the hadron. The hard-scattering amplitude for a given exclusive process can be calculated perturbatively as a function of $\alpha_s(Q^2)$. Similar analyses can be applied to form factors, exclusive photon-photon reactions, and with increasing degrees of complication, to photoproduction, fixed-angle scattering, etc. In the case of the simplest processes, $\gamma\gamma \to M\overline{M}$ and the meson form factors, the leading order analysis can be readily extended to all-orders in perturbation theory.

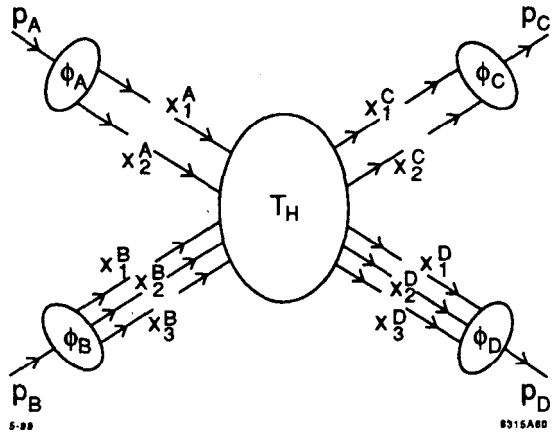

Figure 4. QCD factorization for two-body amplitudes at large momentum transfer.

In the case of exclusive processes such as photo-production, Compton scattering, meson-baryon scattering, etc., the leading hard scattering QCD contribution at large momentum transfer $Q^2 = tu/s$ has the form (helicity labels and suppressed) (see Fig. 4)

$$\mathcal{M}_{A+B\to C+D}(Q^2, \theta_{\text{c.m.}}) = \int [dx] \phi_C(x_c, \tilde{Q})\, \phi_D(x_d, \tilde{Q})\, T_H(x_i; Q^2, \theta_{\text{c.m.}}) \times \phi_A(x_a, \tilde{Q})\, \phi_B(x_b, \tilde{Q})$$

In general the distribution amplitude is evaluated at the characteristic scale $\tilde{Q}$ set by the effective virtuality of the quark propagators.

By definition, the hard scattering amplitude T_H for a given exclusive process is constructed by replacing each external hadron with its massless, collinear valence partons, each carrying a finite fraction x_i of the hadron's momentum. Thus T_H is the scattering amplitude for the constituents. The essential behavior of the amplitude is determined by T_H, computed where each hadron is replaced by its (collinear) quark constituents. We note that T_H is "collinear irreducible," i.e. the transverse momentum integrations of all reducible loop integration are restricted to $k_\perp^2 > \mathcal{O}(Q^2)$ since the small $k_\perp$ region is already contained in ϕ. If the internal propagators in T_H are all far-off-shell $\mathcal{O}(Q^2)$, then a perturbative expansion in $\alpha_s(Q^2)$ can be carried out.

Higher twist corrections to the quark and gluon propagator due to mass terms and intrinsic transverse momenta of a few hundred MeV give nominal corrections of higher order in $1/Q^2$. These finite mass corrections combine with the leading twist results to give a smooth. approach to small Q^2. It is thus reasonable that

PQCD scaling laws become valid at relatively low momentum transfer of order of a few GeV.

General Features of Exclusive Processes in QCD

The factorization theorem for large-momentum-transfer exclusive reactions separates the dynamics of hard-scattering quark and gluon amplitudes T_H from process-independent distribution amplitudes $\phi_H(x, Q)$ whichisolates all of the bound state dynamics. However, as seen from Table I, even without complete information on the hadronic wave functions, it is still possible to make predictions at large momentum transfer directly from QCD.

Although detailed calculations of the hard-scattering amplitude have not been carried out in all of the hadron-hadron scattering cases, one can abstract some general features of QCD common to all exclusive processes at large momentum transfer:

1. Since the distribution amplitude ϕ_H is the L_z = 0 orbital-angular-momentum projection of the hadron wave function, the sum of the interacting constituents' spin along the hadron's momentum equals the hadron spin:[39]

$$\sum_{i \in H} s_i^z = s_H^z.$$

In contrast, there are any number of non-interacting spectator constituents in inclusive reactions, and the spin of the active quarks or gluons is only statistically related to the hadron spin (except at the edge of phase space x $\rightarrow$ 1).

2. Since all loop integrations in T_H are of order $\tilde{Q}$, the quark and hadron masses can be neglected at large Q^2 up to corrections of order $\sim m/\tilde{Q}$. The vector-gluon coupling conserves quark helicity when all masses are neglected-i.e. $\bar{u}_\downarrow \gamma^\mu u_\uparrow$ = 0. Thus total quark helicity is conserved in T_H. In addition, because of (2), each hadron's helicity is the sum of the helicities of its valence quarks in T_H. We thus have the selection rule

$$\sum_{\text{initial}} \lambda_H - \sum_{\text{final}} \lambda_H = 0,$$

i.e. total hadronic helicity is conserved up to corrections of order m/Q or higher. Only (flavor-singlet) mesons in the 0^{-+} nonet can have a two-gluon valence component and thus even for these states the quark helicity equals the hadronic helicity. Consequently hadronic-helicity conservation applies for all amplitudes involving light meson and baryons.[40] Exclusive reactions

which involve hadrons with quarks or gluons in higher orbital angular states are suppressed by powers.

3. The nominal power-law behavior of an exclusive amplitude at fixed $\theta_{c.m.}$ is $(1/Q)^{n-4}$, where n is the number of external elementary particles (quarks, gluons, leptons, photons, . ..) in T_H. This dimensional-counting rule[41] is modified by the Q^2 dependence of the factors of $\alpha_s(Q^2)$ in T_H, by the Q^2 evolution of the distribution amplitudes, and possibly by a small power correction associated with the Sudakov suppression of pinch singularities in hadron-hadron scattering.

The dimensional-counting rules for the power-law falloff appear to be experimentally well established for a wide variety of processes.[24,42] The helicity-conservation rule is also one of the most characteristic features of QCD, being a direct consequence of the gluon's spin. A scalar-or tensor-gluon-quark coupling flips the quark's helicity. Thus, for such theories, helicity may or may not be conserved in any given diagram contribution to T_H depending upon the number of interactions involved. Only for a vector theory, such as QCD, can one have a helicity selection rule valid to all orders in perturbation theory.

5. Electromagnetic Form Factors

Any helicity conserving baryon form factor at large Q^2 has the form: [see Fig. 5(a)]

$$F_B(Q^2) = \int_0^1 [dy] \int_0^1 [dx]\, \phi_B^\dagger(y_j, Q) T_H(x_i, y_j, Q) \phi_B(x_i, Q) ,$$

where to leading order in $\alpha_s(Q^2)$, T_H is computed from $3q + \gamma^* \to 3q$ tree graph amplitudes: [Fig. 5(b).]

$$T_H = \left[\frac{\alpha_s(Q^2)}{Q^2}\right]^2 f(x_i, y_j)$$

and

$$\phi_B(x_i, Q) = \int [d^2 k_\perp]\, \psi_V(x_i, \vec{k}_{\perp i}) \theta(k_{\perp i}^2 < Q^2)$$

is the valence three-quark wavefunction [Fig. 5(c)] evaluated at quark impact separation $b_\perp \sim \mathcal{O}(Q^{-1})$. Since ϕ_B only depends logarithmically on Q^2 in QCD, the main dynamical dependence of $F_B(Q^2)$ is the power behavior $(Q^2)^{-2}$ derived from scaling of the elementary. propagators in T_H. More explicitly, the proton's

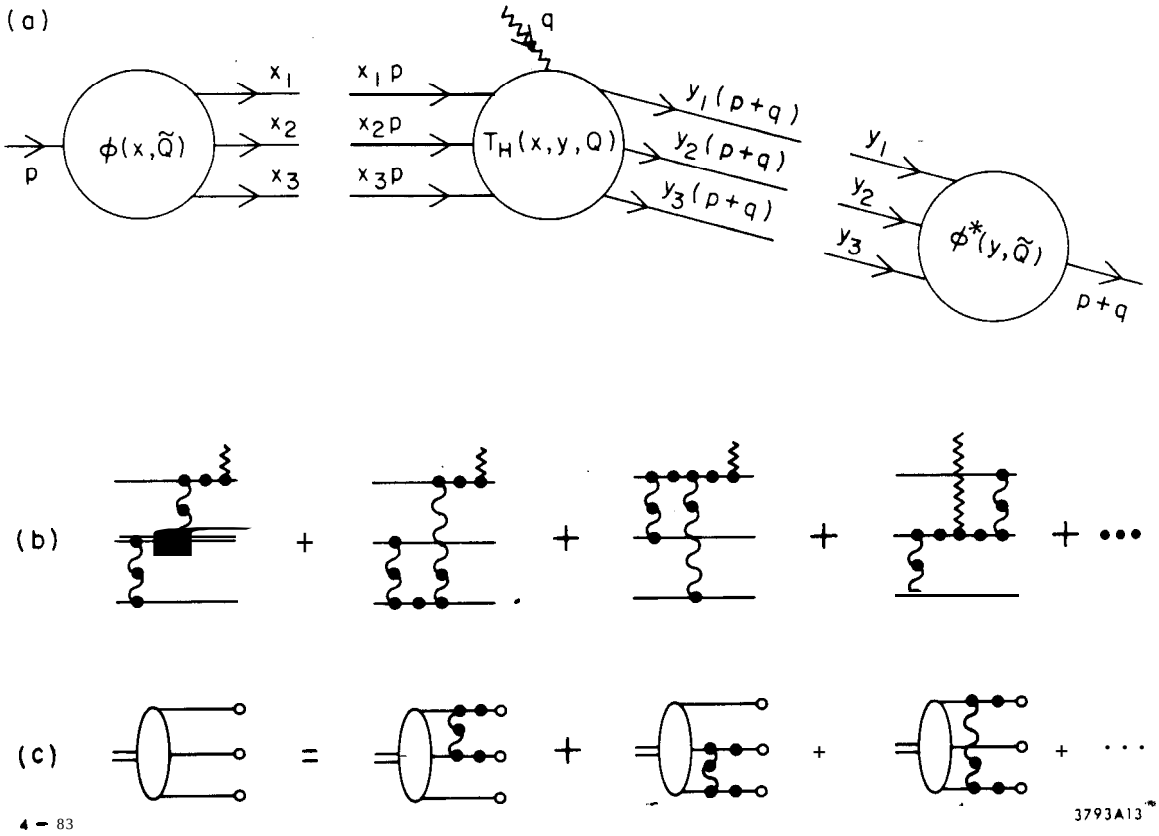

Figure 5. (a) Factorization of the nucleon form factor at large Q^2 in QCD. (b) The leading order diagrams for the hard scattering amplitude T_H. The dots indicate insertions which enter the renormalization of the coupling constant. (c) The leading order diagrams which determine the Q^2 dependence of the distribution amplitude $\phi(x, Q)$.

magnetic form factor has the form:[38]

$$G_M(Q^2) = \left[\frac{\alpha_s(Q^2)}{Q^2}\right]^2 \sum_{n,m} a_{nm} \left(\log \frac{Q^2}{\Lambda^2}\right)^{-\gamma_n-\gamma_m} \times \left[1 + \mathcal{O}(\alpha_s(Q)) + \mathcal{O}\left(\frac{1}{Q}\right)\right].$$

The first factor, in agreement with the quark counting rule, is due to the hard scattering of the three valence quarks from the initial to final nucleon direction. Higher Fock states lead to form factor contributions of successively higher order in $1/Q^2$. The logarithmic corrections derive from an evolution equation for the nucleon distribution amplitude. The γ_n are the computed anomalous dimensions,

reflecting the short distance scaling of three-quark composite operators.[44] The results hold for any baryon to baryon vector or axial vector transition amplitude that conserves the baryon helicity. Helicity non-conserving form factors should fall as an additional power of $1/Q^2$.[39] Measurements[43] of the transition form factor to the $J = 3/2$ N(1520) nucleon resonance are consistent with $J_z = \pm 1/2$ dominance, as predicted by the helicity conservation rule.[39] A review of the data on spin effects in electron nucleon scattering in the resonance region is given in Ref. 43. It is important to explicitly verify that $F_2(Q^2)/F_1(Q^2)$ decreases at large Q^2. The angular distribution decay of the $J/\psi \to p\bar{p}$ is consistent with the QCD prediction $\lambda_p + \lambda_{\bar{p}} = 0$.

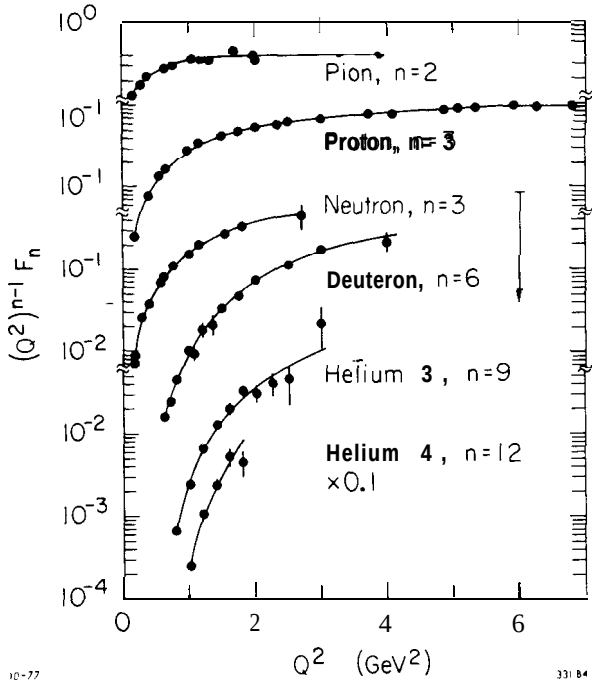

Figure 6. Comparison of experiment [45] with the QCD dimensional counting rule $(Q^2)^{n-1}F(Q^2) \sim const$ for form factors. The proton data extends beyond 30 GeV^2.

Thus, modulo logarithmic factors, one obtains a dimensional counting rule for any hadronic or nuclear form factor at large Q^2 ($\lambda = \lambda' = 0$ or $1/2$)

$$F(Q^2) \sim \left(\frac{1}{Q^2}\right)^{n-1},$$

$$F_1^N \sim \frac{1}{Q^4}, \quad F_\pi \sim \frac{1}{Q^2}, \quad F_d \sim \frac{1}{Q^{10}},$$

where n is the minimum number of fields in the hadron. Since quark helicity is conserved in T_H and $\phi(x_i, Q)$ is the $L_z = 0$ projection of the wavefunction, total hadronic helicity is conserved at large momentum transfer for any QCD exclusive reaction. The dominant nucleon form factor thus corresponds to $F_1(Q^2)$ or $G_M(Q^2)$; the Pauli form factor $F_2(Q^2)$ is suppressed by an extra power of Q^2. Similarly, in the case of the deuteron, the dominant form factor has helicity $\lambda = \lambda' = 0$, corresponding to $\sqrt{A(Q^2)}$.

The comparison of experimental form factors with the predicted nominal power-law behavior is shown in Fig. 6. The general form of the logarithmic corrections to the leading power contributions form factors can be derived from the operator product expansion at short distance[46,44] or by solving an evolution equation[38] for the distribution amplitude computed from gluon exchange [Fig. 5(c)], the only QCD contribution which falls sufficiently small at large transverse momentum to effect the large Q^2 dependence.

The comparison of the proton form factor data with the QCD prediction arbitrarily normalized is shown in Fig. 7. The fall-off of $(Q^2)^2 G_M(Q^2)$ with Q^2 is consistent with the logarithmic fall-off of the square of QCD running coupling constant. As we shall discuss below, the QCD sum rule[5] model form for the nucleon distribution amplitude together with the QCD factorization formulae, predicts the correct sign and magnitude as well as scaling-behavior of the proton and neutron form factors.[47]

Comparison of QCD Scaling for Exclusive Processes with Experiment

Phenomenologically the dimensional counting power laws appear consistent with measurements of form factors, photon-induced amplitudes, and elastic hadron-hadron scattering at large angles and momentum transfer.[42] The successes of the quark counting rules can be taken as strong evidence for QCD since the derivation of the counting rules require scale invariant tree graphs, soft corrections from higher loop corrections to the hard scattering amplitude, and strong suppression of pinch singularities. QCD is the only field theory of spin $\frac{1}{2}$ fields that has all of these properties.

As shown in Fig. 8, the data for $\gamma p \to \pi^+ n$ cross section at $\theta_{CM} = \pi/2$ are consistent with the normalization and scaling $d\sigma/dt\,(\gamma p \to \pi^+ n) \simeq [1\text{ nb}/(s/10\text{ GeV})^7]\, f(t/s)$.

The check of fixed angle scaling in proton-proton elastic scattering is shown in Figs. 9. Extensive measurements of the $pp \to pp$ cross section have been made at ANL, BNL and other laboratories. The scaling law $s^{10} d\sigma/dt(pp \to pp) \simeq const.$ predicted by QCD seems to work quite well over a large range of energy and angle. The best fit gives the power $N = 9.7 \pm 0.5$ compared to the dimensional counting

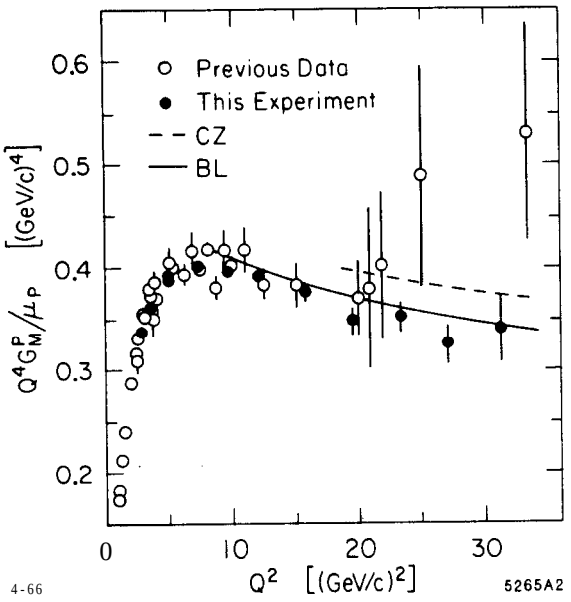

Figure 7. Comparison of the scaling behavior of the proton magnetic form factor with the theoretical predictions of Refs. 38 and 5. The CZ predictions[55] are normalized in sign and magnitude. The data are from Ref. 47.

prediction N=10. There are, however, measurable deviations from fixed power dependence which are not readily apparent on the log-log plot. As emphasized by Hendry[49] the $s^{10}d\sigma/dt$ cross section exhibits oscillatory behavior with p_T (see Section 11). Even more serious is the fact that polarization measurements[51] show significant spin-spin correlations (A_{NN}), and the single spin asymmetry (A_N) is not consistent with predictions based on hadron helicity conservation which is expected to be valid for the leading power behavior.[39] Recent discussions of these effects have been given by Farrar[52] and Lipkin.[53] We discuss a new explanation of all of these effects in Section 11.

As emphasized by Landshoff, the ISR data for high energy elastic pp scattering at small $|t|/s$ can be parameterized in the form $d\sigma/dt \sim const/t^8$ for 2 $GeV^2 <$ $|t| <$ 10 GeV^2. This suggests a role for triple gluon exchange pinch contributions at large energies where multiple vector exchange diagrams could dominate. However, from Mueller's analysis[54] one expects stronger fall-off in t due to the Sudakov form factor suppression. This paradox implies that the role of the pinch singularity in large momentum transfer exclusive reactions is not well understood and deserve further attention. Pinch singularities are also expected to modify the dimensional counting scaling laws for wide-angle scattering, but the change in the exponent of s is small and hard to detect experimentally. However, Ralston and Pire[15] have suggested that the oscillatory behavior in the wide-angle pp scattering amplitude

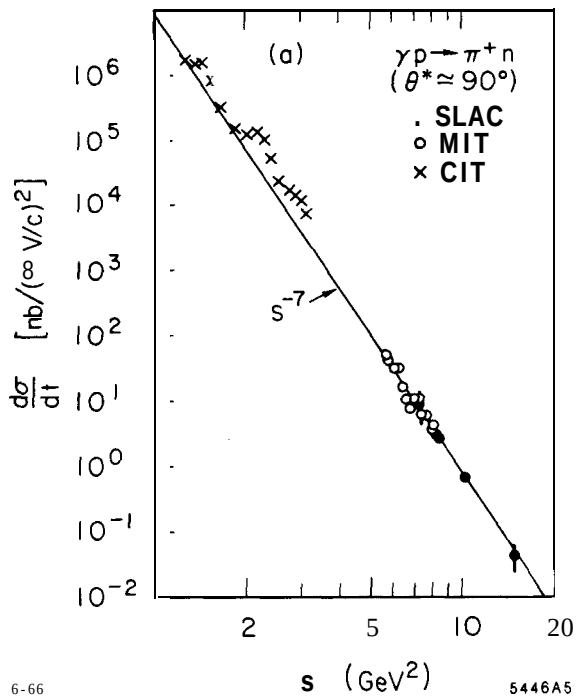

Figure 8. Comparison of photoproduction data with the dimensional counting power-law prediction. The data are summarized in Ref. 48.

results from interference between the pinch contributions and the ordinary hard-scattering contributions to the pp amplitude. Pinch singularities do not arise in form factors, or such photon-induced processes as $\gamma\gamma \to M\overline{M}$,[5] $\gamma^* + \gamma \to M$,[38] $\gamma^* \to M_1 \ldots M_N$ at fixed angle,[55] $\gamma\gamma \to B\overline{B}, \gamma\, B \to \gamma\, B$, etc.[56,57]

The role of pinch contributions in large momentum transfer exclusive reactions has recently been clarified by Botts and Sterman.[58] In agreement with Mueller they show that the Sudakov vertex corrections suppress large impact separation contributions from multi-scattering diagrams, reducing the net power to a value very close to the dimensional counting prediction, e.g $d\sigma/dt(pp \to pp) = f(\theta_{cm})/s^{9.66}$ rather than $1/s^{10}$. The pinch contributions are thus asymptotically dominant over hard scattering diagrams which carry five powers of the running coupling constant. Furthermore the effective quark separation is of order $b_\perp \sim 1/Q$ so that the predictions for color transparency in quasi-elastic scattering in nuclei will hold for pinch contributions as well as the usual hard-scattering diagrams. The contributions to the pinch amplitude coming from regions of integration where one or more of the exchanged gluons carries soft momentum, is suppressed because of the presence of four powers of the hadron distribution amplitude, so the region of validity of the QCD scaling is, extended to quite low momentum transfer. Botts

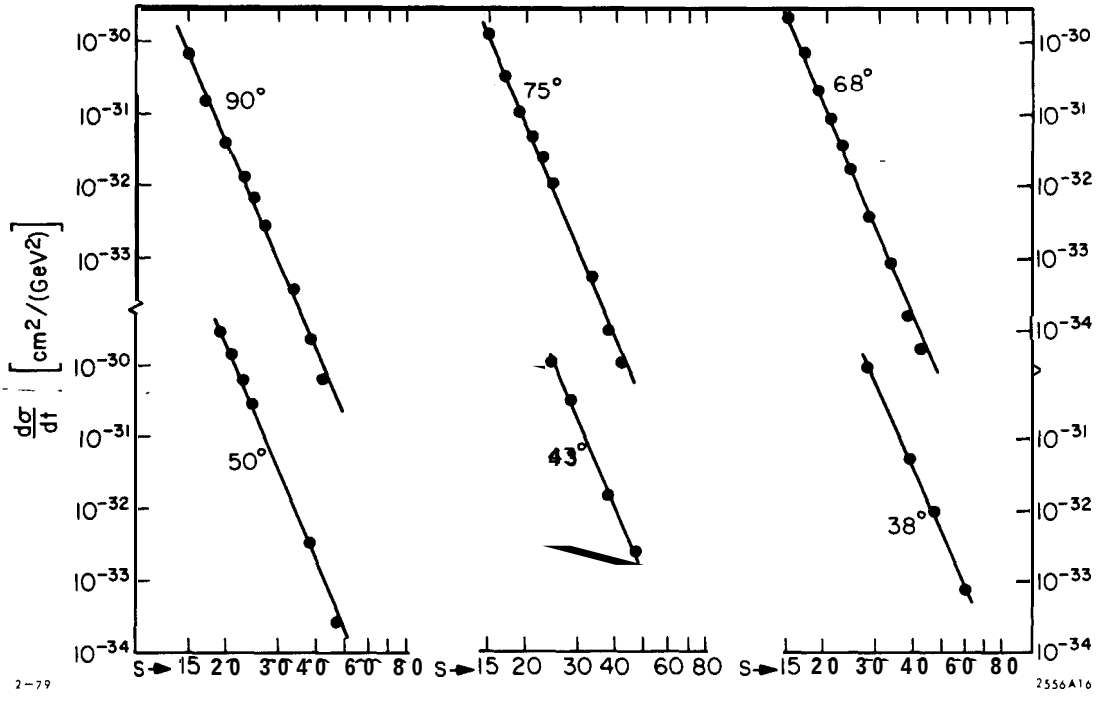

Figure 9. Test of fixed-8_{CM} scaling for elastic **pp** scattering. The data compilation is from Landshoff and Polkinghorne.

and Sterman do not find an energy-dependent structure in the pinch analysis of the type required to account for the observed "oscillations" about $1/s^{10}$ behavior seen in the pp scattering data. It is also apparent from the structure of the pinch contributions that they do not have large spin-spin correlations of the type observed in the data of Krisch et al. (See section 11.)

6. Hadronic Wavefunction Phenomenology

Let us now return to the question of the normalization of exclusive amplitudes in QCD. It should be emphasized that because of the uncertain magnitude of corrections of higher order in $\alpha_s(Q^2)$, comparisons with the normalization of experiment with model predictions could be misleading. Nevertheless, in this section it shall be assumed that the leading order normalization is at least approximately accurate. If the higher order corrections are indeed small, then the normalization of the proton form factor at large Q^2 is a non-trivial test of the distribution amplitude shape; for example, if the proton wave function has a non-relativistic shape peaked at $x_i \sim 1/3$ then one obtains the wrong sign for the nucleon form factor. Furthermore symmetrical distribution amplitudes predict a very small magnitude for $Q^4 G_M^p(Q^2)$ at large Q^2.

The phenomenology of hadron wavefunctions in QCD is now just beginning. Constraints on the baryon and meson distribution amplitudes have been recently obtained using QCD sum rules and lattice gauge theory. The results are expressed in terms of gauge-invariant moments $< x_j^m >= \int \Pi dx_i\, x_j^m\, \phi(x_i, \mu)$ of the hadron's distribution amplitude. A particularly important challenge is the construction of the baryon distribution amplitude.In the case of the proton form factor, the constants a_{nm} in the QCD prediction for G_M must be computed from moments of the nucleon's distribution amplitude $\phi(x_i, Q)$. There are now extensive theoretical efforts to compute this nonperturbative input directly from QCD. The QCD sum rule analysis of Chernyak et *al.*[5,59] provides constraints on the first 12 moments of $\phi(x, Q)$. Using as a basis the polynomials which are eigenstates of the nucleon evolution equation, one gets a model representation of the nucleon distribution amplitude, as well as its evolution with the momentum transfer scale. The moments of the proton distribution amplitude computed by Chernyak et al., have now been confirmed in an independent analysis by Sachrajda and King.[60]

A three-dimensional "snapshot" of the proton's uud wavefunction at equal light-cone time as deduced from QCD sum rules at $\mu \sim 1$ GeV by Chernyak et *al.*[59] and King and Sachrajda[60] is shown in Fig. 10. The QCD sum rule analysis predicts a surprising feature: strong flavor asymmetry in the nucleon's momentum distribution. The computed moments of the distribution amplitude imply that 65% of the proton's momentum in its S-quark valence state is carried by the u-quark* which has the same helicity as the parent hadron.

Dziembowski and Mankiewicz[64] have recently shown that the asymmetric form of the CZ distribution amplitude can result from a rotationally-invariant CM wave function transformed to the light cone using free quark dynamics. They find that one can simultaneously fit low energy phenomena (charge radii, magnetic moments, etc.), the measured high momentum transfer hadron form factors, and the CZ distribution amplitudes with a self-consistent ansatz for the quark wave functions. Thus for the first time one has a somewhat complete model for the relativistic three-quark structure of the hadrons. In the model the transverse size of the valence wave function is not found to be significantly smaller than the mean radius of the proton-averaged over all Fock states as argued in Ref. 61. Dziembowski et al. also find that the perturbative QCD contribution to the form factors in their model dominates over the soft contribution (obtained by convoluting the non-perturbative wave functions) at a scale $Q/N \approx 1$ GeV, where N is the number of valence constituents. (This criterion was also derived in Ref. 30.)

Gari and Stefanis[62] have developed a model for the nucleon form factors which incorporates the CZ distribution amplitude predictions at high Q^2 together with VMD constraints at low Q^2. Their analysis predicts sizeable values for the neutron

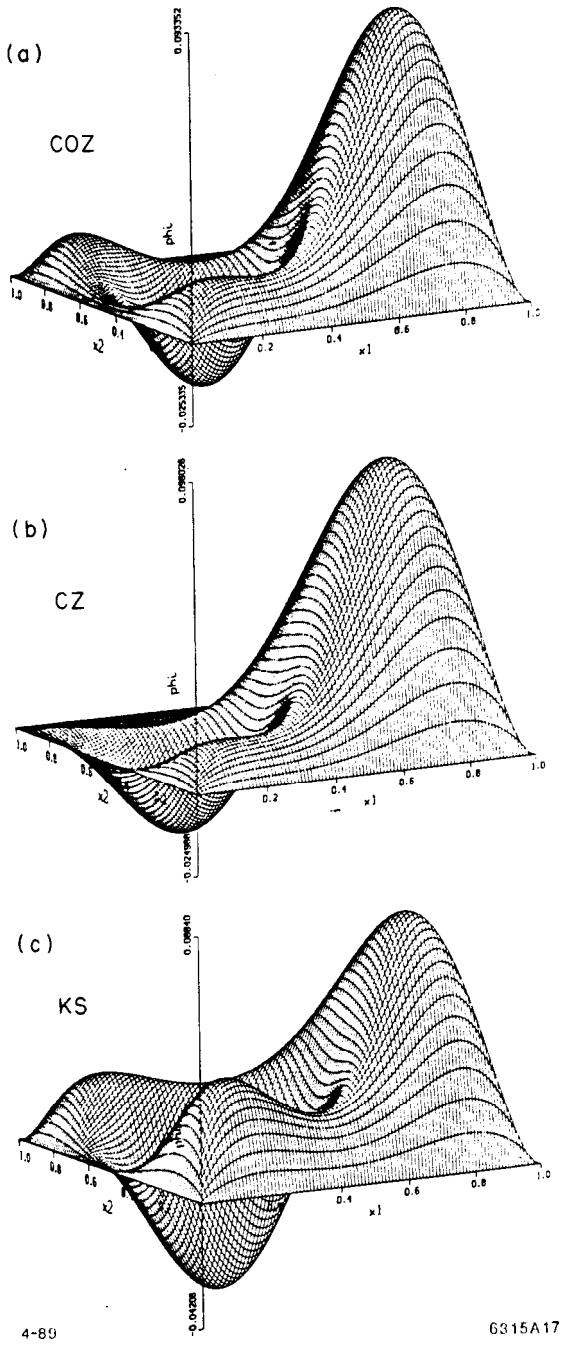

Figure 10. The proton distribution amplitude $\phi_p(x_i, \mu)$ determined at the scale $\mu \sim 1$ GeV from QCD sum rules.

electric form factor at intermediate values of Q^2.

A detailed phenomenological analysis of the nucleon form factors for different shapes of the distribution amplitudes has been given by Ji, Sill, and Lombard-

Nelsen.[63] Their results show that the CZ wave function is consistent with the sign and magnitude of the proton form factor at large Q^2 as recently measured by the American University/SLAC collaboration[47] (see Fig. 11).

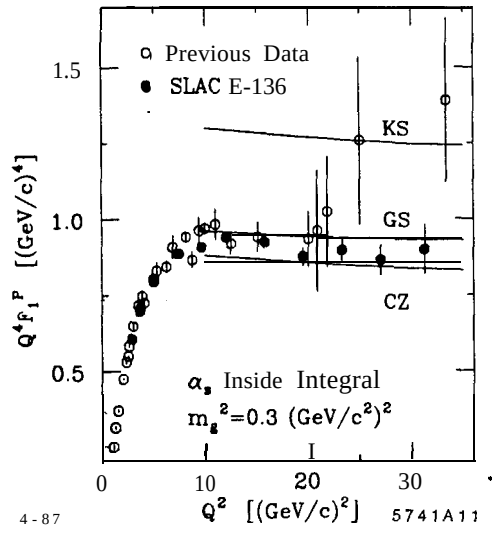

Figure 11. Predictions for the normalization and sign of the proton form factor at high Q^2 using perturbative QCD factorization and QCD sum rule predictions for the proton distribution amplitude (from Ref. 63.) The predictions use forms given by Chernyak and Zhitnitsky, King and Sachrajda,[60] and Gari and Stefanis.[62]

It should be stressed that the magnitude of the proton form factor is sensitive to the x $\sim$ 1 dependence of the proton distribution amplitude, where non-perturbative effects could be important.[65] The asymmetry of the distribution amplitude emphasizes contributions from the large x region. Since non-leading corrections are expected when the quark propagator scale $Q^2(1-x)$ is small, in principle relatively large momentum transfer is required to clearly test the perturbative QCD predictions. Chernyak et *al.*[59] have studied this effect in some detail and claim that their QCD sum rule predictions are not significantly changed when higher moments of the distribution amplitude are included.

It is important to notice that the perturbative scaling regime of the meson form factor is controlled by the virtuality of the quark propagator. When the quark is far off-shell, multiple gluon exchange contributions involving soft gluon insertions are suppressed by inverse powers of the quark propagator; there is not sufficient time to exchange soft gluons or gluonium. Thus the perturbative analysis is valid as long as the single gluon exchange propagator has inverse power behavior. There is thus no reason to require that the gluon be far off-shell, as in the analysis of ref. 66.

The moments of distribution amplitudes can also be computed using lattice gauge theory.[67] In the case of the pion distribution amplitudes, there is good agreement of the lattice gauge theory computations of Martinelli and Sachrajda[68] with the QCD sum rule results. This check has strengthened confidence in the reliability of the QCD sum rule method, although the shape of the meson distribution amplitudes are unexpectedly structured: the pion distribution amplitude is broad and has a dip at x = 1/2. The QCD sum rule meson distributions, combined with the perturbative QCD factorization predictions, account well for the scaling, normalization of the pion form factor and $\gamma\gamma \to M^+M^-$ cross sections.

In the case of the baryon, the asymmetric three-quark distributions are consistent with the normalization of the baryon form factor at large Q^2 and also the branching ratio for $J/\psi \to p\bar{p}$. The data for large angle Compton scattering $\gamma p \to \gamma p$ are also well described.[69] However, a very recent lattice calculation of the lowest two moments by Martinelli and Sachrajda[68] does not show skewing of the average fraction of momentum of the valence quarks in the proton. This lattice result is in contradiction to the predictions of the QCD sum rules and does cast some doubt on the validity of the model of the proton distribution proposed by Chernyak *et al.*[59] The lattice calculation is performed in the quenched approximation with Wilson fermions and requires an extrapolation to the chiral limit.

The contribution of soft momentum exchange to the hadron form factors is a potentially serious complication when one uses the QCD sum rule model distribution amplitudes. In the analysis of Ref. 66 it was argued that only about 1% of the proton form factor comes from regions of integration in which all the propagators are hard. A new analysis by Dziembowski *et al.*[70] shows that the QCD sum rule[5] distribution amplitudes of Chernyak *et al.*[5] together with the perturbative QCD prediction gives contributions to the form factors which agree with the measured normalization of the pion form factor at $Q^2 > 4\ GeV^2$ and proton form factor $Q^2 > 20\ GeV^2$ to within a factor of two. In the calculation the virtuality of the exchanged gluon is restricted to $|k^2| > 0.25\ GeV^2$. The authors assume $\alpha_s = 0.3$ and that the underlying wavefunctions fall off exponentially at the $x \simeq 1$ endpoints. Another model of the proton distribution amplitude with diquark clustering[71] chosen to satisfy the QCD sum rule moments come even closer. Considering the uncertainty in the magnitude of the higher order corrections, one really cannot expect better agreement between the QCD predictions and experiment.

The relative importance of non-perturbative contributions to form factors is also an issue. Unfortunately, there is little that can be said until we have a deeper understanding of the end-point behavior of hadronic wavefunctions, and of the role played by Sudakov form factors in the end-point region. Models have been constructed in which non-perturbative effects persist to high Q.[66] Other models

have been constructed in which such effects vanish rapidly as Q increases.[72,73,64]

If the QCD sum rule results are correct then, the light hadrons are highly structured oscillating momentum-space valence wavefunctions. In the case of mesons, the results from both the lattice calculations and QCD sum rules show that the light quarks are highly relativistic. This gives further indication that while non-relativistic potential models are useful for enumerating the spectrum of hadrons (because they express the relevant degrees of freedom), they may not be reliable in predicting wavefunction structure.

7. The Pre-QCD Development of Exclusive Reactions

The study of exclusive processes in terms of underlying quark subprocesses in fact began before the discovery of QCD. The advent of the parton model and Bjorken scaling for deep inelastic structure functions in the late 1960's brought a new focus to the structure of form factors and exclusive processes at large momentum transfer. The underlying theme of the parton model was the concept that quarks carried the electromagnetic current within hadrons. The use of time-ordered perturbation theory in an "infinite momentum frame", or equivalently, quantization on the light cone, provided a natural language for hadrons as composites of relativistic partons, i.e. point-like constituents.[74] Drell and Yan[36] showed how to compute current matrix elements in terms of a Fock state expansion at infinite momentum. (Later their result was shown to be exact in the light-cone quantization scheme.)

Drell and Yan suggested that hadron form factors are dominated by the endpoint region $x \approx 1$. Then it is clear from the Drell-Yan formula that the form factor fall-off at large Q^2 is closely related to the $x \to 1$ behavior of the hadron structure function. The relation found by Drell and Yan was

$$F(Q^2) \sim \frac{1}{(Q^2)^n} \quad \text{if} \quad F_2(x, Q^2) \sim (1-x)^{2n-1}.$$

Gribov and Lipatov[75] extended this relationship to fragmentation functions $D(z, Q^2)$ at $z \to 1$, taking into account cancellations due to quark spin. Feynman[76] noted that the Drell-Yan relationship was also true in gauge theory models in which the endpoint behavior of structure functions is suppressed due to the emission of soft or "wee" partons by charged lines. The endpoint region is thus suppressed in QCD relative to the leading perturbative contributions.

The parton model was extended to exclusive processes such as hadron-hadron scattering and photoproduction by Blankenbecler, Brodsky, and Gunion[24] and by Landshoff and Polkinghorne.[77] It was recognized that independent of specific

dynamics, hadrons could interact and scatter simply by exchanging their common constituents. These authors showed that the amplitude due to quark interchange (or rearrangement) could be written in closed form as an overlap of the light-cone wavefunctions of the incident and final hadrons. In order to make definite predictions, model wavefunctions were chosen to reproduce the fall-off of the form factors obtained from the Drell-Yan formula. Two-body exclusive amplitudes in the "constituent interchange model" then take the form of "fixed-angle" scaling laws

$$\frac{d\sigma}{dt}(AB \to CD) \sim \frac{f(\theta_{cm})}{s^N}$$

where the power N reflects the power-law fall-off of the elastic form factors of the scattered hadrons. The form of the angular dependence $f(\theta_{cm})$ reflects the number of interchanged quarks.

Even though the constituent interchange is model was motivated in part by the Drell-Yan endpoint analysis of form factors, many of the predictions and systematics of quark interchange remain applicable in the QCD analysis.[24] A comprehensive series of measurements of elastic meson nucleon scattering reactions has recently been carried out by Baller *et al.*[78] at BNL. Empirically, the quark interchange. amplitudes gives a reasonable account of the scaling, angular dependence, and relative magnitudes of the various channels. For example, the strong differences between K^+p and K^-p scattering is accounted for by u quark interchange in the K^+p amplitude. It is inconsistent with gluon exchange as the dominant amplitude since this produces equal scattering for the two channels. The dominance of quark interchange over gluon exchange is a surprising result which eventually needs to be understood in the context of QCD.

The prediction of fixed angle scaling laws laid the groundwork for the derivation of the "dimensional counting rules." As discussed by Farrar and myself in Ref. 41, it is natural to assume that at large momentum transfer, an exclusive amplitude factorize as a convolution of hadron wavefunctions which couple the hadrons to their quark constituents with a hard scattering amplitude T_H which scatters the quarks from the initial to final direction. Since the hadron wavefunction is maximal when the quarks are nearly collinear with each parent hadron, the large momentum transfer occurs in T_H. The pre-QCD argument went as follows: the dimension of T_H is $[L^{n-4}]$ where n = $n_A + n_B + n_C + n_D$ is the total number of fields entering T_H. In a renormalizable theory where the coupling constant is dimensionless and masses can be neglected at large momentum transfer, all connected tree-graphs for T_H then scale as $[1/\sqrt{s}]^{n-4}$ at fixed t/s. This immediately gives the dimensional

counting law[41]

$$\frac{d\sigma}{dt}(AB \to CD) \sim \frac{f(\theta_{cm})}{s^{n_A+n_B+n_C+n_D-2}}.$$

In the case of incident or final photons or leptons n = 1. Specializing to elastic lepton-hadron scattering, this also implies $F(Q^2) \sim 1/(Q^2)^{n_H-1}$ for the spin averaged form factor, where n_H is the number of constituents in hadron H. These results were obtained independently by Matveev et *al.*[41] on the basis of an "automodality" principle, that the underlying constituent interactions are scale free.

-As we have seen, the dimensional counting scaling laws will generally be modified by the accumulation of logarithms from higher loop corrections to the hard scattering amplitude T_H; the .phenomenological success of the counting rules in their simplest form thus implies that the loop corrections be somewhat mild. As we have seen, it is the asymptotic freedom property of QCD which in fact makes higher order corrections an exponentiation of a log log Q^2 series, thus preserving the form of the dimensional counting rules modulo only logarithmic corrections.

8. Exclusive $\gamma\gamma$ Reactions

Two-photon reactions have a number of unique features which are especially* important for testing QCD, especially in exclusive channels:"]

1. Any even charge conjugation hadronic state can be created in the annihilation of two photons-an initial state of minimum complexity. Because $\gamma\gamma$ annihilation is complete, there are no spectator hadrons to confuse resonance analyses. Thus, one. has a clean environment for identifying the exotic color-singlet even C composites of quarks and gluons $|q\bar{q}>$, $|gg>$, $|ggg>$, $|q\bar{q}g>$, $|qq\bar{q}\bar{q}>$, ... which are expected to be present in the few GeV mass range. (Because of mixing, the actual mass eigenstates of QCD may be complicated admixtures of the various Fock components.)

2. The mass and polarization of each of the incident virtual photons can be continuously varied, allowing highly detailed tests of theory. Because a spin-one state cannot couple to two on-shell photons, a J = 1 resonance can be uniquely identified by the onset of its production with increasing photon mass.[80]

3. Two-photon physics plays an especially important role in probing dynamical mechanisms. In the low momentum transfer domain, $\gamma\gamma$ reactions such as the total annihilation cross section and exclusive vector meson pair production can give important insights into the nature of diffractive reactions in

QCD. Photons in QCD couple directly to the quark currents at any resolution scale (see Fig. 12). Predictions for high momentum transfer $\gamma\gamma$ reactions, including the photon structure functions, $F_2^\gamma(x, Q^2)$ and $F_L^\gamma(x, Q^2)$, high p_T jet production, and exclusive channels are thus much more specific than corresponding hadron-induced reactions. The pointlike coupling of the annihilating photons leads to a host of special features which differ markedly with predictions based on vector meson dominance models.

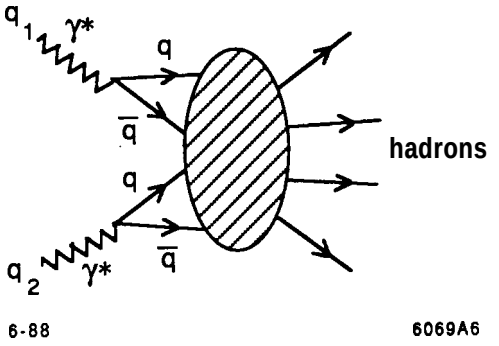

Figure 12. Photon-photon annihilation in QCD. The photons couple directly to one or two quark currents.

4. Exclusive $\gamma\gamma$ processes provide a window for viewing the wavefunctions of hadrons in terms of their quark and gluon degrees of freedom. In the case of $\gamma\gamma$ annihilation into hadron pairs, the angular distribution of the production cross section directly reflects the shape of the distribution amplitude (valence wavefunction) of each hadron.

Thus far experiment has not been sufficiently precise to measure the logarithmic modification of dimensional counting rules predicted by QCD. Perturbative QCD predictions for $\gamma\gamma$ exclusive processes at high momentum transfer and high invariant pair mass provide some of the most severe tests of the theory.[31] A simple, but still very important example[38] is the Q^2-dependence of the reaction $\gamma^*\gamma \to M$ where M is a pseudoscalar meson such as the η. The invariant amplitude contains only one form factor:

$$M_{\mu\nu} = \epsilon_{\mu\nu\sigma\tau} p_\eta^\sigma q^\tau F_{\gamma\eta}(Q^2) \, .$$

It is easy to see from power counting at large Q^2 that the dominant amplitude (in light-cone gauge) gives $F_{\gamma\eta}(Q^2) \sim 1/Q^2$ and arises from diagrams (see Fig. 13) which have the minimum path carrying Q^2: i.e. diagrams in which there is only a single quark propagator between the two photons. The coefficient of $1/Q^2$ involves only the two-particle $q\bar{q}$ distribution amplitude $\phi(x, Q)$, which evolves

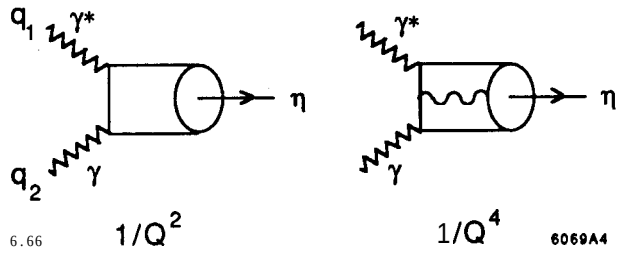

Figure 13. Calculation of the $\gamma - \eta$ transition form factor in QCD from the valence $q\bar{q}$ and $q\bar{q}g$ Fock states.

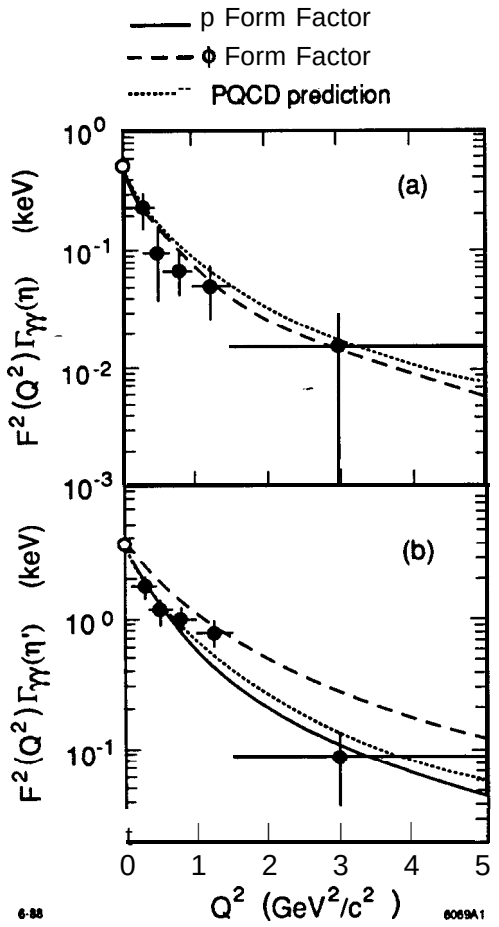

Figure 14. Comparison of TPC/$\gamma\gamma$ data[61] for the $7 - \eta$ and $7 - \eta'$ transition form factors with the QCD leading twist prediction of Ref. 31. The VMD predictions are also shown. See S. Yellin, this meeting.

logarithmically on Q. Higher particle number Fock states give higher power-law falloff contributions to the exclusive amplitude.

The TPC/$\gamma\gamma$ data[81] shown in Fig. 14 are in striking agreement with the predicted QCD power: a fit to the data gives $F_{\gamma\eta}(Q^2) \sim (1/Q^2)^n$ with n = 1.05 $\pm$ 0.15. Data for the η' from Pluto and the TPC/$\gamma\gamma$ experiments give similar results, consistent with scale-free behavior of the QCD quark propagator and the point coupling to the quark current for both the real and virtual photons. In the case of deep inelastic lepton scattering, the observation of Bjorken scaling tests these properties when both photons are virtual.

The QCD power law prediction, $F_{\gamma\eta}(Q^2) \sim 1/Q^2$, is consistent with dimensional- counting[41] and also emerges from current algebra arguments (when both photons are very virtual).[82] On the other hand, the $1/Q^2$ falloff is also expected in vector meson dominance models. The QCD and VDM predictions can be readily discriminated by studying $\gamma^*\gamma^* \to \eta$. In VMD one expects a product of form factors; in QCD the falloff of the amplitude is still $1/Q^2$ where Q^2 is a linear combination of Q_1^2 and Q_2^2. It is clearly very important to test this essential feature of QCD.

Exclusive two-body processes $\gamma\gamma \to H\overline{H}$ at large $s = W_{\gamma\gamma}^2 = (q_1 + q_2)^2$ and fixed $\theta_{\rm cm}^{\gamma\gamma}$ provide a particularly important laboratory for testing QCD, since the large momentum-transfer behavior, helicity structure, and often even the absolute normalization can be rigorously predicted.[31,69] The angular dependence of some of the $\gamma\gamma \to H\overline{H}$ cross sections reflects the shape of the hadron distribution amplitudes $\phi_H(x_i, Q)$. The $\gamma_\lambda\gamma_{\lambda'} \to H\overline{H}$ amplitude can be written as a factorized form

$$\mathcal{M}_{\lambda\lambda'}(W_{\gamma\gamma}, \theta_{\rm cm}) = \int_0^1 [dy_i]\, \phi_H^*(x_i, Q)\, \phi_{\overline{H}}^*(y_i, Q)\, T_{\lambda\lambda'}(x, y; W_{\gamma\gamma}, \theta_{\rm cm})$$

where $T_{\lambda\lambda'}$ is the hard scattering helicity amplitude. To leading order $T \propto \alpha(\alpha_s/W_{\gamma\gamma}^2)^n$ and $d\sigma/dt \sim W_{\gamma\gamma}^{-(2n+2)} f(\theta_{\rm cm})$ where n = 1 for meson and n = 2 for baryon pairs.

Lowest order predictions for pseudo-scalar and vector-meson pairs for each helicity amplitude are given in Ref. 31. In each case the helicities of the hadron pairs are equal and opposite to leading order in $1/W^2$. The normalization and angular dependence of the leading order predictions for $\gamma\gamma$ annihilation into charged meson pairs are almost model independent; i.e. they are insensitive to the precise form of the meson distribution.amplitude. If the meson distribution amplitudes is

symmetric in x and $(1 - x)$, then the same quantity

$$\int_0^1 dx \, \frac{\phi_\pi(x, Q)}{(1-x)}$$

controls the x-integration for both $F_\pi(Q^2)$ and to high accuracy $M(\gamma\gamma \to \pi^+\pi^-)$. Thus for charged pion pairs one obtains the relation:

$$\frac{\frac{d\sigma}{dt}(\gamma\gamma \to \pi^+\pi^-)}{\frac{d\sigma}{dt}(\gamma\gamma \to \mu^+\mu^-)} \sim \frac{4|F_\pi(s)|^2}{1 - \cos^4 \theta_{\rm cm}} .$$

Note that in the case of charged kaon pairs, the asymmetry of the distribution amplitude may give a small correction to this relation.

The scaling behavior, angular behavior, and normalization of the $\gamma\gamma$ exclusive pair production reactions are nontrivial predictions of QCD. Recent Mark II meson pair data and PEP4/PEP9 data[83] for separated $\pi^+\pi^-$ and K^+K^- production in the range $1.6 < W_{\gamma\gamma} < 3.2$ GeV near 90" are in satisfactory agreement with the normalization and energy dependence predicted by QCD (see Fig. 15). In the case of $\pi^0\pi^0$ production, the cos $\theta_{\rm cm}$ dependence of the cross section can be inverted to determine the z-dependence of the pion distribution amplitude.

The wavefunction of hadrons containing light and heavy quarks such as the K, D-meson are likely to be asymmetric due to the disparity of the quark masses. In a gauge theory one expects that the wavefunction is maximum when the quarks have zero relative velocity; this corresponds to $x_i \propto m_{i\perp}$ where $m_\perp^2 = k_\perp^2 + m^2$. An explicit model for the skewing of the meson distribution amplitudes based on QCD sum rules is given by Benyayoun and Chernyak.[84] These authors also apply their model to two-photon exclusive processes such as $\gamma\gamma \to K^+K^-$ and obtain some modification compared to the strictly symmetric distribution amplitudes. If the same conventions are used to label the quark lines, the calculations of Benyayoun and Chernyak are in complete agreement with those of Ref. 31.

The one-loop corrections to the hard scattering amplitude for meson pairs have been calculated by Nizic.[85] The QCD predictions for mesons containing admixtures of the $|gg\rangle$ Fock state is given by Atkinson, Sucher, and Tsokos.[69]

The perturbative QCD analysis has been extended to baryon-pair production in comprehensive analyses by Farrar et *al.*[86,69] and by Gunion et *al.*[69] Predictions are given for the "sideways" Compton process $\gamma\gamma \to p\bar{p}$, $\Delta\bar{\Delta}$ pair production, and the entire decuplet set of baryon pair states. The arduous calculation of 280 $\gamma\gamma \to qqqqqq$ diagrams in T_H required for calculating $\gamma\gamma \to 25$ is greatly simplified

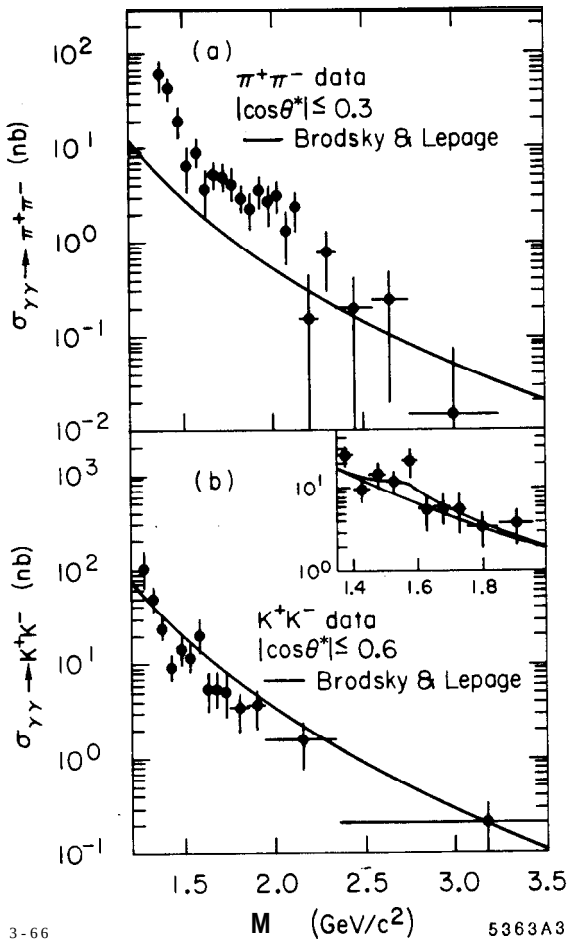

Figure 15. Comparison of $\gamma\gamma \to \pi^+\pi^-$ and $\gamma\gamma \to K^+K^-$ meson pair production data with the parameter-free perturbative QCD prediction of Ref. 31. The theory predicts the normalization and scaling of the cross sections. The data are from the TPC/$\gamma\gamma$ collaboration.[83]

by using two-component spinor techniques. The doubly charged A pair is predicted to have a fairly small normalization. Experimentally such resonance pairs may be difficult to identify under the continuum background.

The normalization and angular distribution of the QCD predictions for proton-antiproton production shown in Fig. **16** depend in detail on the form of the nucleon distribution amplitude, and thus provide severe tests of the model form derived by Chernyak, Ogloblin, and Zhitnitsky[59] from QCD sum rules.

An important check of the QCD predictions can be obtained by combining data from $\gamma\gamma \to p\bar{p}$ and the annihilation reaction, $p\bar{p} \to \gamma\gamma$, with large angle Compton scattering $\gamma p \to \gamma p$. The available data[87] for large angle Compton scattering (see

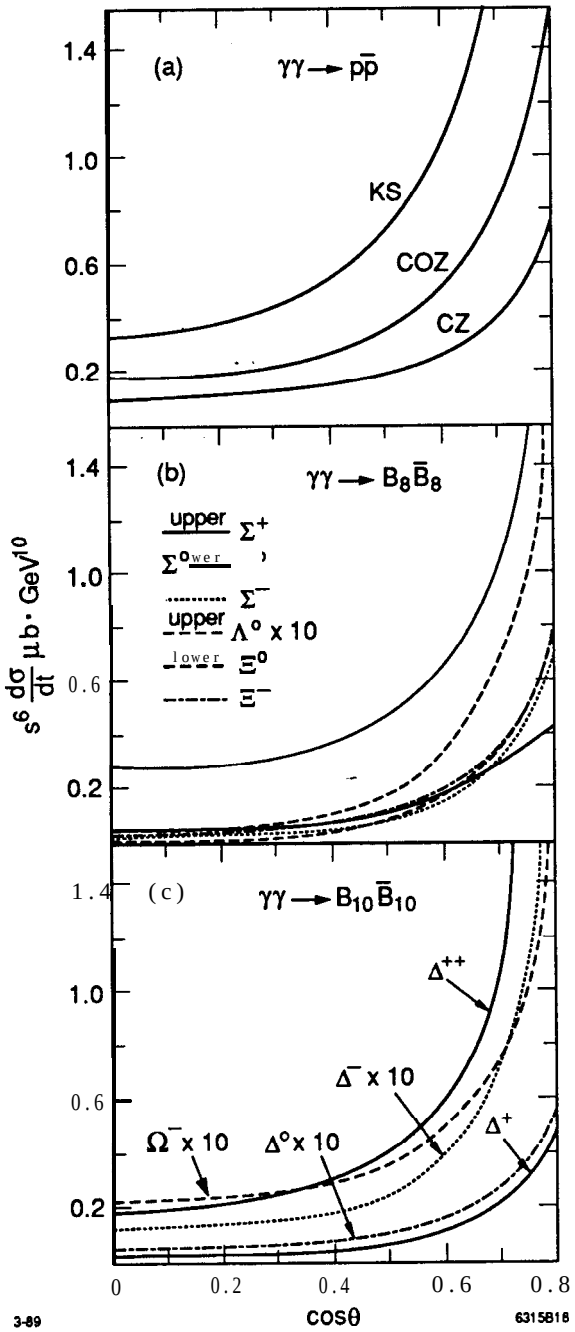

Figure 16. Perturbative QCD predictions by Farrar and Zhang for the $\cos(\theta_{cm})$ dependence of the $77 \rightarrow p\bar{p}$ cross section assuming the King-Sachrajda (KS), Chernyak, Ogloblin, and Zhitnitsky (COZ) [59], and original Chernyak and Zhitnitsky (CZ) [5] forms for the' proton distribution amplitude, $\phi_p(x_i, Q)$.

Fig. 17). for 5 GeV^2 < s < 10 GeV^2 are consistent with the dimensional counting scaling prediction, $s^6 d\sigma/dt = f(\theta_{cm})$. In general, comparisons between channels related by crossing of the Mandelstam variables place a severe constraint on the angular dependence and analytic form of the underlying QCD exclusive amplitude. Furthermore in $p\bar{p}$ collisions one can study timelike photon production into e^+e^- and examine the virtual photon mass dependence of the Compton amplitude. Predictions for the q^2 dependence of the $p\bar{p} \rightarrow \gamma\gamma^*$ amplitude can be obtained by crossing the results of Gunion and Millers.[69]

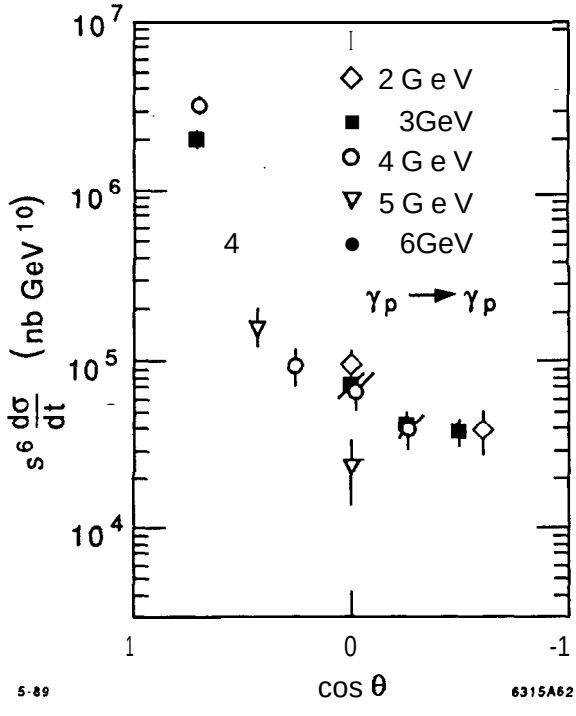

Figure 17. Test of dimensional counting for Compton scattering for 2 < E^{γ}_{lab} < 6 GeV.[87]

The region of applicability of the leading power-law predictions for $\gamma\gamma \rightarrow p\bar{p}$ requires that one be beyond resonance or threshold effects. It presumably is set by the scale where $Q^4 G_M(Q^2)$ is roughly constant, i.e. Q^2 > 3 GeV^2. Present measurements may thus be too close to threshold for meaningful tests.[88] It should be noted that unlike the case for charged meson pair production, the QCD predictions for baryons are sensitive to the form of the running coupling constant and the endpoint behavior of the wavefunctions.

The QCD predictions for $\gamma\gamma \rightarrow H\overline{H}$ can be extended to the case of one or two virtual photons, for measurements in which one or both electrons are tagged. Be-

cause of the direct coupling of the photons to the quarks, the Q_1^2 and Q_2^2 dependence of the $\gamma\gamma \to H\overline{H}$ amplitude for transversely polarized photons is minimal at W^2 large and fixed θ_{cm}, since the off-shell quark and gluon propagators in T_H already transfer hard momenta; i.e. the 2γ coupling is effectively local for $Q_1^2, Q_2^2 \ll p_T^2$. The $\gamma^*\gamma^* \to \overline{B}B$ and $M\overline{M}$ amplitudes for off-shell photons have been calculated by Millers and Gunion.[69] In each case, the predictions show strong sensitivity to the form of the respective baryon and meson distribution amplitudes.

We also note that photon-photon collisions provide a way to measure the running coupling constant in an exclusive channel, independent of the form of hadronic distribution amplitudes.[31] The photon-meson transition form factors $F_{\gamma \to M}(Q^2)$, A4 = π^0, η^0, f, etc., are measurable in tagged $e\gamma \to e'M$ reactions. QCD predicts

$$\alpha_s(Q^2) = \frac{1}{4\pi} \frac{F_\pi(Q^2)}{Q^2 |F_{\pi\gamma}(Q^2)|^2}$$

where to leading order the pion distribution amplitude enters both numerator and denominator in the same manner.

The complete calculations of the tree-graph structure (see Figs. **18,** 19, 20) of both $\gamma\gamma \to M\overline{M}$ and $\gamma\gamma \to B\overline{B}$ amplitudes has now been completed. One can use crossing to compute T_H for $p\overline{p} \to \gamma\gamma$ to leading order in $\alpha_s(p_T^2)$ from the calculations reported by Farrar, Maina and Neri[69] and Gunion and Millers.[69] Examples* of the predicted angular distributions are shown in Figs. 21 and 22.

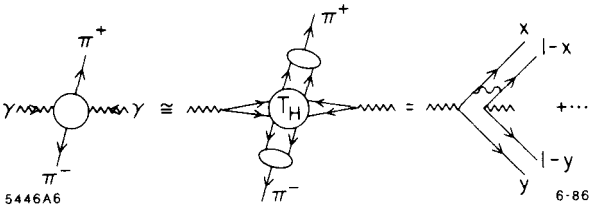

Figure 18. Application of QCD to two-photon production of meson pairs.[69]

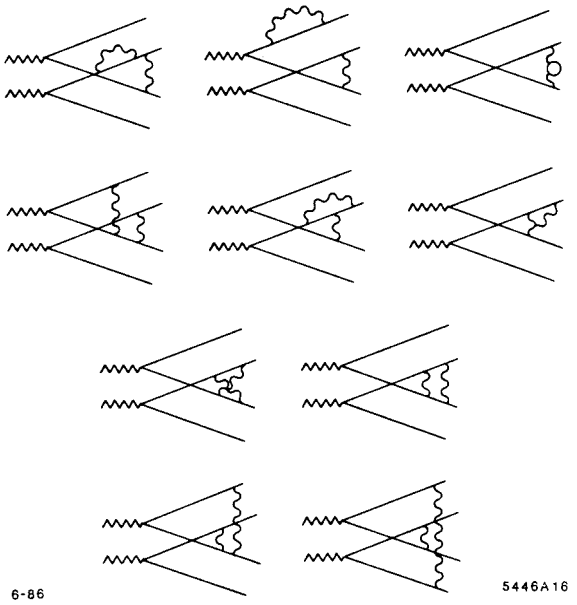

Figure 19. Next-to-leading perturbative contribution to T_H for the process $77 \rightarrow M\overline{M}$. The calculation has been done by Nizic.[89]

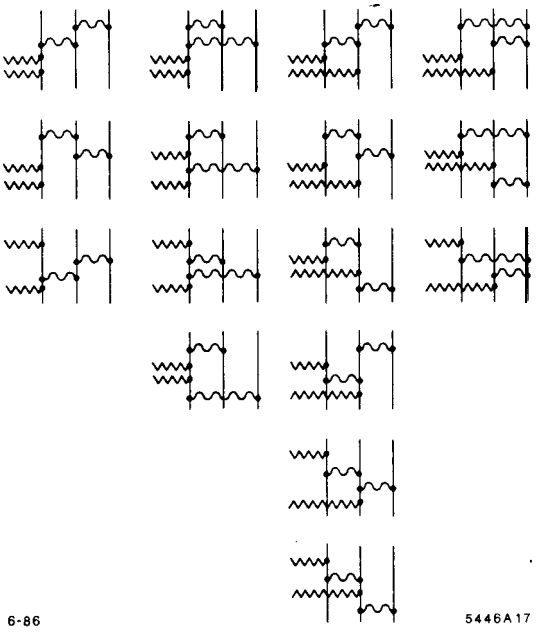

Figure 20. Leading diagrams for $7 + 7 \rightarrow \bar{p} + p$ calculated in Ref. 69.

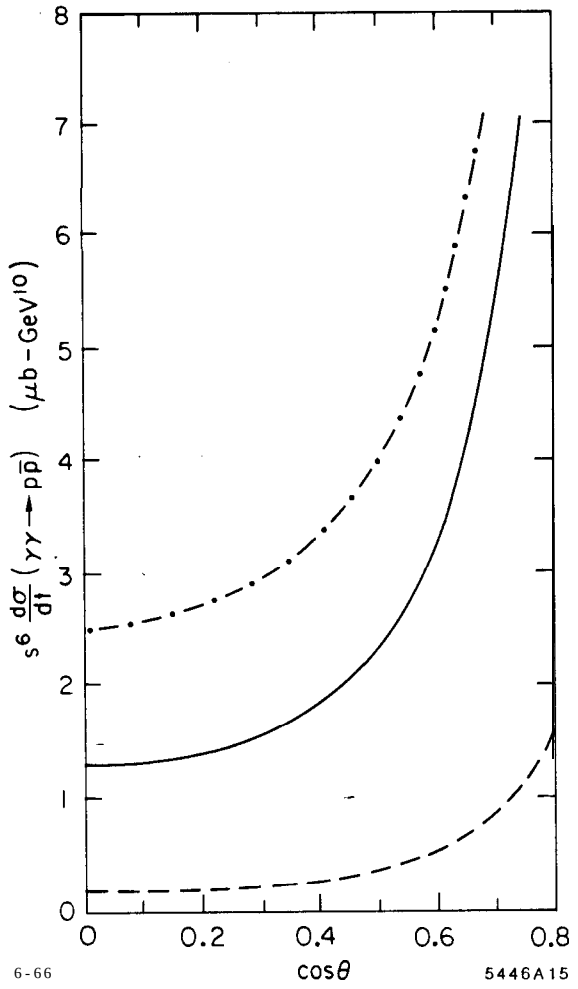

Figure 21. QCD prediction for the scaling and angular distribution for $\gamma+\gamma \to \bar{p}+p$ calculated by Farrar et *al.*[69] The dashed-dot curve corresponds to $4\Lambda^2/s = 0.0016$ and a maximum running coupling constant $\alpha_s^{max} = 0.8$. The solid curve corresponds to $4\Lambda^2/s = 0.016$ and a maximum running coupling constant $\alpha_s^{max} = 0.5$. The dashed. curve corresponds to a fixed $\alpha_s = 0.3$. The results are very sensitive to the endpoint behavior of the proton distribution amplitude. The CZ form is assumed.

9. Exclusive Nuclear Reactions — Reduced Amplitudes

The nucleus is itself an interesting QCD structure. At short distances nuclear wavefunctions and nuclear interactions necessarily involve *hidden color*, degrees of freedom orthogonal to the channels described by the usual nucleon or isobar degrees of freedom. At asymptotic momentum transfer, the deuteron form factor and distribution amplitude are rigorously calculable. One can also derive new types of testable scaling laws for exclusive nuclear amplitudes in terms of the reduced

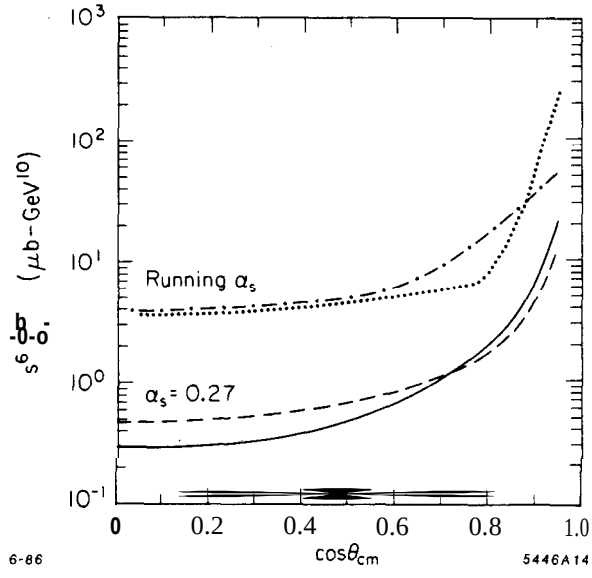

Figure 22. QCD prediction for the scaling and angular distribution for $\gamma+\gamma \rightarrow \bar{p}+p$ calculated by Gunion, Sparks and Millers.[69] CZ distribution amplitudes are assumed. The solid and running curves are for real photon annihilation. The dashed and dot-dashed curves correspond to one photon space-like, with Q_b^2/s = 0.1.

amplitude formalism.

An ultimate goal of QCD phenomenology is to describe the nuclear force and the structure of nuclei in terms of quark and gluon degrees of freedom. Explicit signals of QCD in nuclei have been elusive, in part because of the fact that an effective Lagrangian containing meson and nucleon degrees of freedom must be in some sense equivalent to QCD if one is limited to low-energy probes. On the other hand, an effective local field theory of nucleon and meson fields cannot correctly describe the observed off-shell falloff of form factors, vertex amplitudes, Z-graph diagrams, etc. because hadron compositeness is not taken into account.

We have already mentioned the prediction $F_d(Q^2) \sim 1/Q^{10}$ which comes from simple quark counting rules, as well as perturbative QCD. One cannot expect this asymptotic prediction to become accurate until very large Q^2 is reached since the momentum transfer has to be shared by at least six constituents. However there is a simple way to isolate the QCD physics due to the compositeness of the nucleus, not the nucleons. The deuteron form factor is the probability amplitude for the deuteron to scatter from p to $p + q$ but remain intact. Note that for vanishing nuclear binding energy $\epsilon_d \rightarrow 0$, the deuteron can be regarded as two nucleons sharing the deuteron four-momentum (see Fig. 23). The momentum ℓ is limited by the binding and can thus be neglected. To first approximation the proton and

neutron share the deuteron's momentum equally. Since the deuteron form factor contains the probability amplitudes for the proton and neutron to scatter from $p/2$ to $p/2 + q/2$; it is natural to define the reduced deuteron form factor[90,91]

$$f_d(Q^2) \equiv \frac{F_d(Q^2)}{F_{1N}\left(\frac{Q^2}{4}\right) F_{1N}\left(\frac{Q^2}{4}\right)}.$$

The effect of nucleon compositeness is removed from the reduced form factor. QCD then predicts the scaling

$$f_d(Q^2) \sim \frac{1}{Q^2}$$

i.e. the same scaling law as a meson form factor. Diagrammatically, the extra power of $1/Q^2$ comes from the propagator of the struck quark line, the one propagator not contained in the nucleon form factors. Because of hadron helicity conservation, the prediction is for the leading helicity-conserving deuteron form factor ($\lambda = \lambda' = 0$.) As shown in Fig. 24, this scaling is consistent with experiment for Q = $p_T \gtrsim 1$ GeV.[92]

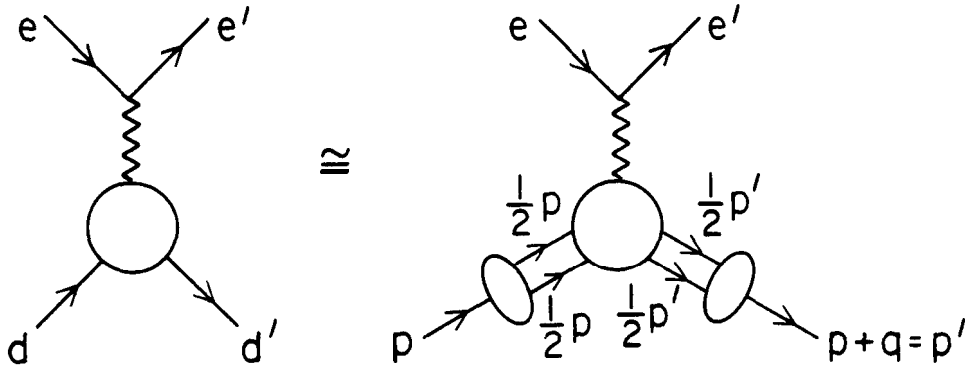

Figure 23. Application of the reduced amplitude formalism to the deuteron form factor at large momentum transfer.

The distinction between the QCD and other treatments of nuclear amplitudes is particularly clear in the reaction $\gamma d \to np$; *i.e.* photodisintegration of the deuteron at fixed center of mass angle. Using dimensional counting, the leading power-law prediction from QCD is simply $\frac{d\sigma}{dt}(\gamma d \to np) \sim \frac{1}{s^{11}} F(\theta_{\rm cm})$. Again we note that the virtual momenta are partitioned among many quarks and gluons, so that finite mass corrections will be significant at low to medium energies. Nevertheless, one can test the basic QCD dynamics in these reactions taking into account much of the finite-mass, higher-twist corrections by using the "reduced amplitude" formalism.[90,91] Thus the photodisintegration amplitude contains the probability amplitude (i.e. nucleon form factors) for the proton and neutron to each remain intact after absorbing momentum transfers $p_p - 1/2p_d$ and $p_n - 1/2p_d$, respectively (see Fig. 25). After the form factors are removed, the remaining "reduced" amplitude should scale as $F(\theta_{\rm cm})/p_T$. The single inverse power of transverse momentum p_T is the slowest conceivable in any theory, but it is the unique power predicted by PQCD.

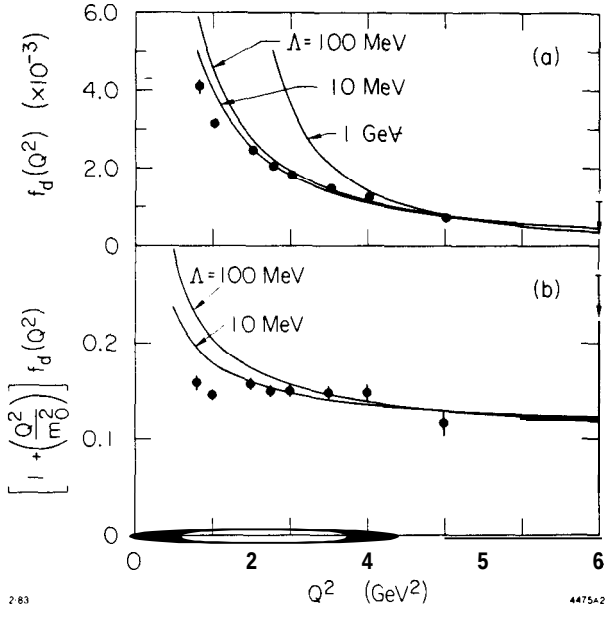

Figure 24. Scaling of the deuteron reduced form factor. The data are summarized in Ref. 90.

The prediction that $f(\theta_{\rm cm})$ is energy dependent at high-momentum transfer is compared with experiment in Fig. 26. It is particularly striking to see the QCD prediction verified at incident photon lab energies as low as 1 GeV. A comparison with a standard nuclear physics model with exchange currents is also shown for

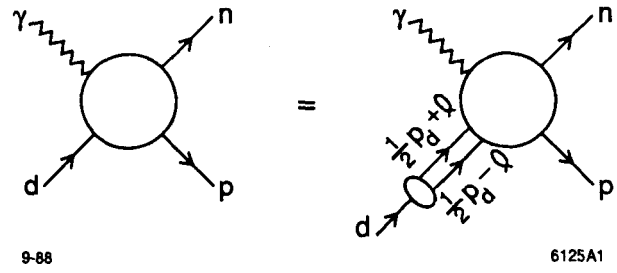

Figure 25. Construction of the reduced nuclear amplitude for two-body inelastic deuteron reactions!"

comparison as the solid curve in Fig. 26(a). The fact that this prediction falls less fast than the data suggests that meson and nucleon compositeness are not taken to into account correctly. An extension of these data to other angles and higher energy would clearly be very valuable.

An important question is whether the normalization of the $\gamma d \to pn$ amplitude is correctly predicted by perturbative QCD. A recent analysis by Fujita[96] shows that mass corrections to the leading QCD prediction are not significant in the region in which the data show scaling. However Fujita also finds that in a model based on simple one-gluon plus quark-interchange mechanism, normalized to the nucleon-nucleon scattering amplitude, gives a photo-disintegration amplitude with a normalization an order of magnitude below the data. However this model only allows for diagrams in which the photon insertion acts only on the quark lines which couple to the exchanged gluon. It is expected that including other diagrams in which the photon couples to the current of the other four quarks will increase the photo-disintegration amplitude by a large factor.

The derivation of the evolution equation for the deuteron and other multi-quark states is given in Refs. 97 and **91.** In the case of the deuteron, the evolution equation couples five different color singlet states composed of the six quarks. The leading anomalous dimension for the deuteron distribution amplitude and the helicity-conserving deuteron form factor at asymptotic Q^2 is given in Ref. 97.

There are a number of related tests of QCD and reduced amplitudes which require $\bar{p}$ beams[91] such as $\bar{p}d \to \gamma n$ and $\bar{p}d \to \pi^- p$ in the fixed $\theta_{\rm cm}$ region. These reactions are particularly interesting tests of QCD in nuclei. Dimensional counting rules predict the asymptotic behavior $\frac{d\sigma}{dt}(\bar{p}d \to \pi^- p) \sim \frac{1}{(p_T^2)^{12}} f(\theta_{\rm cm})$ since there are 14 initial and final quanta involved. Again one notes that the $\bar{p}d \to \pi^- p$ amplitude contains a factor representing the probability amplitude (i.e. form factor) for the proton to remain intact after absorbing momentum transfer squared $\hat{t} = (p - 1/2 p_d)^2$ and the $\overline{N}N$ time-like form factor at $\hat{s} = (\bar{p} + 1/2 p_d)^2$. Thus

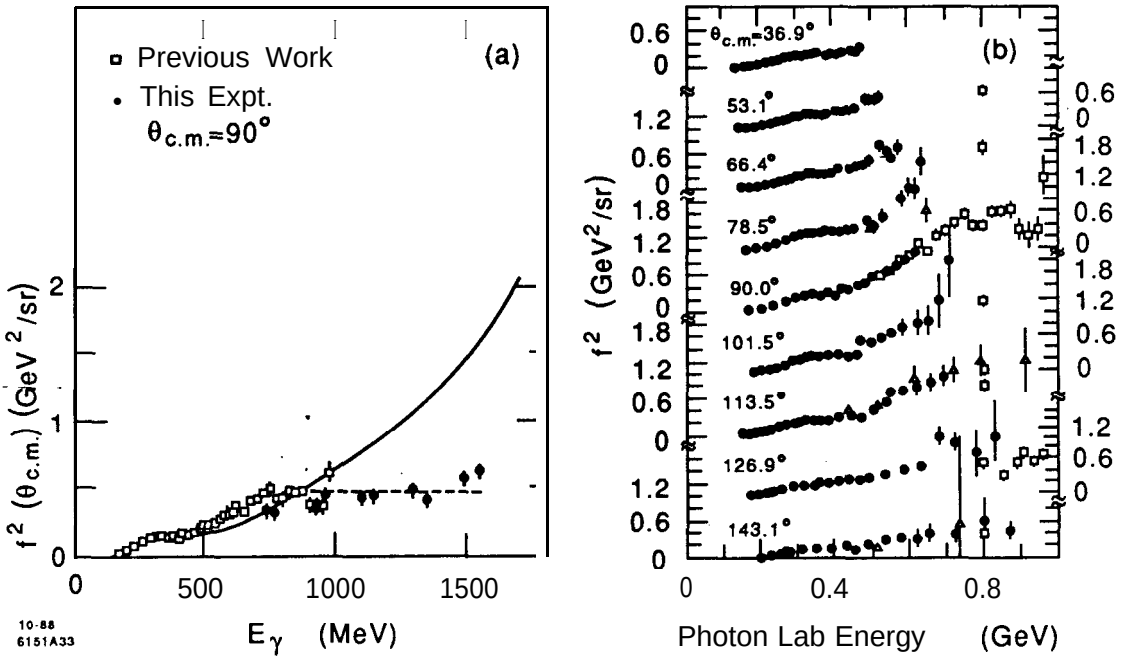

Figure 26. Comparison of deuteron photodisintegration data with the scaling prediction which requires $f^2(\theta_{cm})$ to be at most logarithmically dependent on energy at large momentum transfer. The data in (a) are from the recent experiment of Ref. 93. The nuclear physics prediction shown in (a) is from Ref. 94. The data in (b) are from Ref. 95.

$\mathcal{M}_{\bar{p}d\to\pi^- p} \sim F_{1N}(\hat{t})\, F_{1N}(\hat{s})\, \mathcal{M}_r$, where $\mathcal{M}_r$ has the same QCD scaling properties as quark meson scattering. One thus predicts

$$\frac{\frac{d\sigma}{d\Omega}\,(\bar{p}d \to \pi^- p)}{F_{1N}^2(\hat{t})\, F_{1N}^2(\hat{s})} \sim \frac{f(\Omega)}{p_T^2}\ .$$

The reduced amplitude scaling for $\gamma d \to pn$ at large angles and $p_T \gtrsim 1$ GeV (see Fig. 26). One thus expects similar precocious scaling behavior to hold for $\bar{p}d \to \pi^- p$ and other $\bar{p}d$ exclusive reduced amplitudes. Recent analyses by Kondratyuk and Sapozhnikov[98] show that standard nuclear physics wavefunctions and interactions cannot explain the magnitude of the data for two-body anti-proton annihilation reactions such as $\bar{p}d \to \pi^- p$.

10. A TEST OF COLOR TRANSPARENCY

A striking feature of the QCD description of exclusive processes is "color transparency:" The only part of the hadronic wavefunction that scatters at large momentum transfer is its valence Fock state where the quarks are at small relative impact separation. Such a fluctuation has a small color-dipole moment and thus has negligible interactions with other hadrons. Since such a state stays small over a distance proportional to its energy, this implies that quasi-elastic hadron-nucleon scattering at large momentum transfer as illustrated in Fig. 27 can occur additively on all of the nucleons in a nucleus with minimal attenuation due to elastic or inelastic final state interactions in the nucleus, i.e. the nucleus becomes "transparent." By contrast, in conventional Glauber scattering, one predicts strong, nearly energy-independent initial and final state attenuation. A detailed discussion of the time and energy scales required for the validity of the PQCD prediction is given in by Farrar et al. and Mueller in Ref. 14.

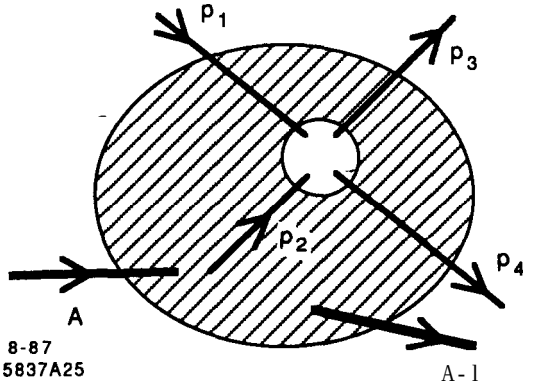

Figure 27. Quasi-elastic pp scattering inside a nuclear target. Normally one expects such processes to be attenuated by elastic and inelastic interactions of the incident proton and the final state interaction of the scattered proton. Perturbative QCD predicts minimal attenuation; i.e. "color transparency," at large momentum transfer.[14]

A recent experiment [99] at BNL measuring quasi-elastic $pp \to pp$ scattering at $\theta_{cm} = 90°$ in various nuclei appears to confirm the color transparency prediction—at least for p_{lab} up to 10 GeV/c (see Fig. 28). Descriptions of elastic scattering which involve soft hadronic wavefunctions cannot account for the data. However, at higher energies, $p_{lab} \sim 12$ GeV/c, normal attenuation is observed in the BNL experiment. This is the same kinematical region $E_{cm} \sim 5$ GeV where the large spin correlation in A_{NN} are observed.[100] I shall argue that both features may be signaling new s-channel physics associated with the onset of charmed hadron production.[101] Clearly, much more testing of the color transparency phenomena is

required, particularly in quasi-elastic lepton-proton scattering, Compton scattering, antiproton-proton scattering, etc. The cleanest test of the PQCD prediction is to check for minimal attenuation in large momentum transfer lepton-proton scattering in nuclei since there are no complications from pinch singularities or resonance interference effects.

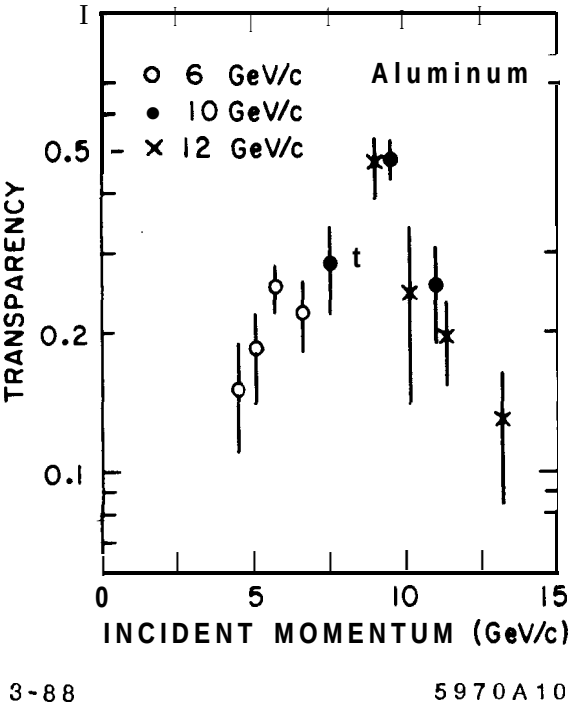

Figure 28. Measurements of the transparency ratio

$$T = \frac{Z_{eff}}{Z} = \frac{d\sigma}{dt}[pA \to p(A-1)]/\frac{d\sigma}{dt}[pA \to pp]$$

near 90" on Aluminum.[99] Conventional theory predicts that T should be small and roughly constant in energy. Perturbative QCD[14] predicts a monotonic rise to $T = 1$.

One can also understand the origin of color transparency as a consequence of the PQCD prediction that soft initial-state corrections to reactions such as $\bar{p}p \to \bar{\ell}\ell$ are suppressed at high lepton pair mass. This is a remarkable consequence of gauge theory and is quite contrary to normal treatments of initial interactions based on Glauber theory. This novel effect can be studied in quasielastic $\bar{p}A \to \bar{\ell}\ell\ (A-1)$ reaction. in which there are no extra hadrons produced and the produced leptons are coplanar with the beam. (The nucleus $(A-1)$ can be left excited). Since PQCD predicts the absence of initial-state elastic and inelastic interactions, the number of

such events should be strictly additive in the number Z of protons in the nucleus, every proton in the nucleus is equally available for short-distance annihilation. In traditional Glauber theory only the surface protons can participate because of the strong absorption of the $\bar{p}$ as it traverses the nucleus.

The above description is the ideal result for large s. QCD predicts that additivity is approached monotonically with increasing energy, corresponding to two effects: a) the effective transverse size of the $\bar{p}$ wavefunction is $b_\perp \sim 1/\sqrt{s}$, and b) the formation time for the $\bar{p}$ is sufficiently long, such that the Fock state stays small during transit of the nucleus.

The color transparency phenomena is also important to test in purely hadronic quasiexclusive antiproton-nuclear reactions. For large p_T one predicts

$$\frac{d\sigma}{dt\,dy}\,(\bar{p}A \to \pi^+\pi^- + (A-1)) \simeq \sum_{p\epsilon A} G_{p/A}(y)\,\frac{d\sigma}{dt}\,(\bar{p}p \to \pi^+\pi^-)\ ,$$

where $G_{p/A}(y)$ is the probability distribution to find the proton in the nucleus with light-cone momentum fraction y = $(p^0 + p^z)/(p^0_A + p^z_A)$, and

$$\frac{d\sigma}{dt}(\bar{p}p \to \pi^+\pi^-) \simeq \left(\frac{1}{p_T^2}\right)^8 f(\cos\theta_{\rm cm})\ .$$

The distribution $G_{p/A}(y)$ can also be measured in $eA \to ep(A-1)$ quasiexclusive reactions. A remarkable feature of the above prediction is that there are no corrections required from initial-state absorption of the $\bar{p}$ as it traverses the nucleus, nor final-state interactions of the outgoing pions. Again the basic point is that the only part of hadron wavefunctions which is involved in the large p_T reaction is $\psi_H(b_\perp \sim \mathcal{O}(1/p_T))$. i.e. the amplitude where all the valence quarks are at small relative impact parameter. These configurations correspond to small color singlet states which, because of color cancellations, have negligible hadronic interactions in the target. Measurements of these reactions thus test a fundamental feature of the Fock state description of large p_T exclusive reactions.

Another interesting feature which can be probed in such reactions is the behavior of $G_{p/A}$ (y) for y well away from the Fermi distribution peak at y $\sim m_N/M_A$. For y $\to$ 1 spectator counting rules[102] predict $G_{p/A}(y) \sim (1-y)^{2N_s-1} = (1-y)^{6A-7}$ where $N_s = 3(A-1)$ is the number of quark spectators required to "stop" (y; $\to$ 0) as y $\to$ 1. This simple formula has been quite successful in accounting for distributions measured in the forward fragmentation of nuclei at the BEVALAC.[28] Color transparency can also be studied by measuring quasiexclusive J/ψ production by anti-protons in a nuclear target $\bar{p}A \to J/\psi(A-1)$ where the nucleus is left in a

ground or excited state, but extra hadrons are not created (see Fig. 29). The cross section involves a convolution of the $\bar{p}p \rightarrow J/\psi$ subprocess cross section with the distribution $G_{p/A}(y)$ where y = $(p^0 + p^3)/(p_A^0 + p_A^3)$ is the boost-invariant light-cone fraction for protons in the nucleus. This distribution can be determined from quasiexclusive lepton-nucleon scattering $\ell A \rightarrow \ell p(A - 1)$.

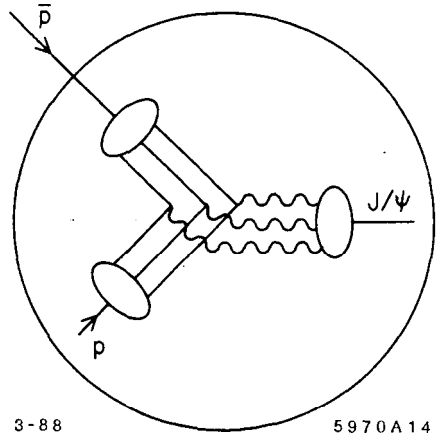

Figure 29. Schematic representation of quasielastic charmonium production in $\bar{p}A$ reactions.

In first approximation $\bar{p}p \rightarrow J/\psi$ involves $qqq + \overline{qqq}$ annihilation into three charmed quarks. The transverse momentum integrations are controlled by the charm mass scale and thus only the Fock state of the incident antiproton which contains three antiquarks at small impact separation can annihilate. Again it follows that this state has a relatively small color dipole moment, and thus it should have a longer than usual mean-free path in nuclear matter; *i.e.* color transparency. Unlike traditional expectations, QCD predicts that the $\bar{p}p$ annihilation into charmonium is not restricted to the front surface of the nucleus. The exact nuclear dependence depends on the formation time for the physical $\bar{p}$ to couple to the small $\overline{qqq}$ configuration, $\tau_F \propto E_p$. It may be possible to study the effect of finite formation time by varying the beam energy, E_p, and using the Fermi-motion of the nucleon to stay at the J/ψ resonance. Since the J/ψ is produced at nonrelativistic velocities in this low energy experiment, it is formed inside the nucleus. The A-dependence of the quasiexclusive reaction can thus be used to determine the J/$-nucleon cross section at low energies. For a normal hadronic reaction $\bar{p}A \rightarrow HX$, we expect $A_{\text{eff}} \sim A^{1/3}$, corresponding to absorption in the initial and final state. In the case of $\bar{p}A \rightarrow J/\psi$ X one expects A_{eff} much closer to A^1 if color transparency is fully effective and a(J/ψ N) is small.

11. Spin Correlations in Proton-Proton Scattering

One of the most serious challenges to quantum chromodynamics is the behavior of the spin-spin correlation asymmetry $A_{NN} = \frac{[d\sigma(\uparrow\uparrow) - d\sigma(\uparrow\downarrow)]}{[d\sigma(\uparrow\uparrow) + d\sigma(\uparrow\downarrow)]}$ measured in large momentum transfer pp elastic scattering (see Fig. 30). At p_{lab} = 11.75 GeV/c and $\theta_{cm} = \pi/2$, A_{NN} rises to $\simeq$ SO%, corresponding to four times more probability for protons to scatter with their incident spins both normal to the scattering plane and parallel, rather than normal and opposite.

The polarized cross section shows a striking energy and angular dependence not expected from the slowly-changing perturbative QCD predictions. However, the unpolarized data is in first approximation consistent with the fixed angle scaling law $s^{10} d\sigma/dt(pp \to pp) = f(\theta_{CM})$ expected from the perturbative analysis (see Fig. 9). The onset of new structure[104] at s $\simeq$ 23 GeV^2 is a sign of new degrees of freedom in the two-baryon system. In this section, I will discuss a possible explanation[101] for (1) the observed spin correlations, (2) the deviations from fixed-angle scaling laws, and (3) the anomalous energy dependence of absorptive corrections to quasielastic pp scattering in nuclear targets, in terms of a simple model based on two $J = L$ = S = 1 broad resonances (or threshold enhancements) interfering with a perturbative QCD quark-interchange background amplitude. The structures in the $pp \to pp$ amplitude may be associated with the onset of strange and charmed thresholds. The fact that the produced quark-and anti-quark have opposite parity* explains why the L = 1 channel is involved. If the charm threshold explanation is correct, large angle pp elastic scattering would have been virtually featureless for $p_{lab} \geq 5$ GeV/c, had it not been for the onset of heavy flavor production. As a further illustration of the threshold effect, one can see the effect in A_{NN} due to a narrow $^3F_3$ pp resonance at $\sqrt{s}$ = 2.17 GeV (p_{lab} = 1.26 GeV/c) associated with the $p\Delta$ threshold.

The perturbative QCD analysis[34] of exclusive amplitudes assumes that large momentum transfer exclusive scattering reactions are controlled by short distance quark-gluon subprocesses, and that corrections from quark masses and intrinsic transverse momenta can be ignored. The main predictions are fixed-angle scaling laws[41] (with small corrections due to evolution of the distribution amplitudes, the running coupling constant, and pinch singularities), hadron helicity conservation,[39] and the novel phenomenon, "color transparency."

As discussed in Section 9, a test of color transparency in large momentum transfer quasielastic pp scattering at $\theta_{cm} \simeq \pi/2$ has recently been carried out at BNL using several nuclear targets (C, Al, Pb).[99] The attenuation at p_{lab} = 10 GeV/c in the various nuclear targets was observed to be in fact much less than that predicted by traditional Glauber theory (see Fig. 28). This appears to support the

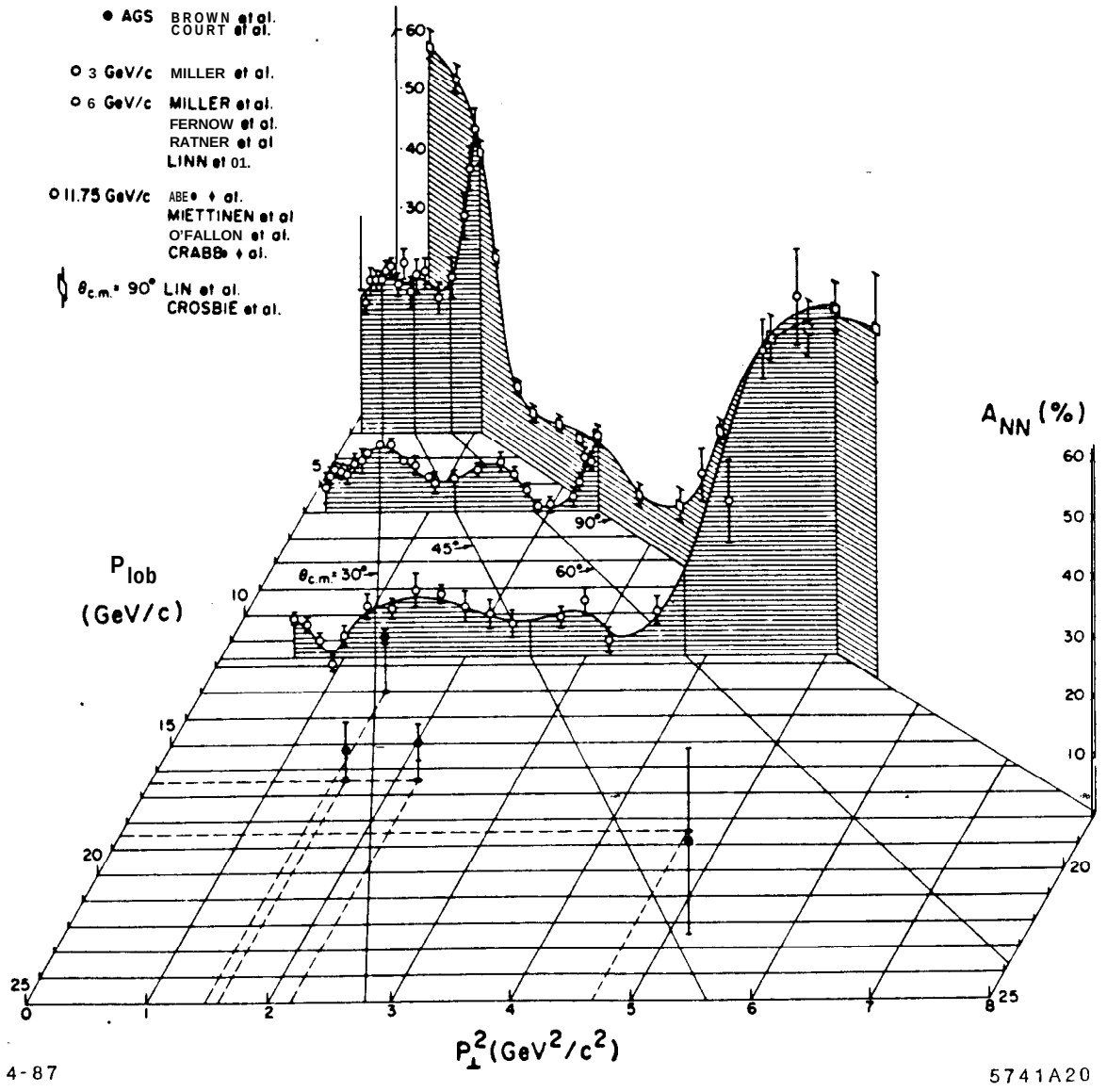

Figure 30. The spin-spin correlation A_{NN} for elastic **pp** scattering with beam and target protons polarized normal to the scattering plane.[103] A_{NN} = 60% implies that it is four times more probable for the protons to scatter with spins parallel rather than antiparallel.

color transparency prediction.

The expectation from perturbative QCD is that the transparency effect should become even more apparent as the momentum transfer rises. Nevertheless, at p_{lab} = 12 GeV/c, normal attenuation was observed. One can explain this surprising result if the scattering at p_{lab} = 12 GeV/c ($\sqrt{s}$ = 4.93 GeV), is dominated by an s-channel B=2 resonance (or resonance-like structure) with mass near 5 GeV,

since unlike a hard-scattering reaction, a resonance couples to the fully-interacting large-scale structure of the proton. If the resonance has spin S = 1, this can also explain the large spin correlation A_{NN} measured nearly at the same momentum, p_{lab} = 11.75 GeV/c. Conversely, in the momentum range p_{lab} = 5 to 10 GeV/c one predicts that the perturbative hard-scattering amplitude is dominant at large angles. The experimental observation of diminished attenuation at p_{lab} = 10 GeV/c thus provides support for the QCD description of exclusive reactions and color transparency.

What could cause a resonance at $\sqrt{s}$ = 5 GeV, more than 3 GeV beyond the pp threshold? There are a number of possibilities: (a) a multigluonic excitation such as $|qqqqqqggg\rangle$, (b) a "hidden color" color singlet $|qqqqqq\rangle$ excitation,[105] or (c) a "hidden flavor" $|qqqqqq\overline{Q}Q\rangle$ excitation, which is the most interesting possibility, since it naturally explains the spin-parity of the resonance or threshold enhancement, and it leads to many testable consequences.

As in QED, where final state interactions give large enhancement factors for attractive channels in which $Z\alpha/v_{rel}$ is large, one expects resonances or threshold enhancements in QCD in color-singlet channels at heavy quark production thresholds since all the produced quarks have similar velocities.[106] One thus can expect resonant behavior at M^* = 2.55 GeV and M^* = 5.08 GeV, corresponding to the threshold values for open strangeness: $pp \to \Lambda K^+ p$, and open charm: $pp \to \Lambda_c D^0 p$, respectively. In any case, the structure at 5 GeV is highly inelastic: its branching ratio to the proton-proton channel is $B^{pp} \simeq 1.5\%$.

A model for this phenomenon is given in Ref. 101. In order not to over complicate the phenomenology; the simplest Breit-Wigner parameterization of the resonances was used. There has not been an attempt to optimize the parameters of the model to obtain a best fit. It is possible that what is identified a single resonance is actually a cluster of resonances.

The background component of the model is the perturbative QCD amplitude. Although complete calculations are not yet available, many features of the QCD predictions are understood, including the approximate s^{-4} scaling of the $pp \to pp$ amplitude at fixed θ_{cm} and the dominance of those amplitudes that conserve hadron helicity.[39] Furthermore, recent data comparing different exclusive two-body scattering channels from BNL[42] show that quark interchange amplitudes[107] dominate quark annihilation or gluon exchange contributions. Assuming the usual symmetries, there are five independent pp helicity amplitudes: $\phi_1 = M(++, ++)$, $\phi_2 = M(--, ++)$, $\phi_3 = M(+-, +-)$, $\phi_4 = M(-+, +-)$, $\phi_5 = M(++, +-)$. The he-

licity amplitudes for quark interchange have a definite relationship:[51]

$$\phi_1(\mathrm{PQCD}) = 2\phi_3(\mathrm{PQCD}) = -2\phi_4(\mathrm{PQCD})$$
$$= 4\pi C F(t)F(u)\left[\frac{t-m_d^2}{u-m_d^2} + (u \leftrightarrow t)\right]e^{i\delta}$$

The hadron helicity non-conserving amplitudes, $\phi_2(\mathrm{PQCD})$ and $\phi_5(\mathrm{PQCD})$ are zero. This form is consistent with the nominal power-law dependence predicted by perturbative QCD and also gives a good representation of the angular distribution over a broad range of energies.[108] Here F(t) is the helicity conserving proton form factor, taken as the standard dipole form: F(t) = $(1 - t/m_d^2)^{-2}$, with m_d^2 = 0.71 GeV^2. As shown in Ref. 51, the P&CD-quark-interchange structure alone predicts $A_{NN} \simeq 1/3$, nearly independent of energy and angle.

Because of the rapid fixed-angle s^{-4} falloff of the perturbative QCD amplitude, even a very weakly-coupled resonance can have a sizeable effect at large momentum transfer. The large empirical values for A_{NN} suggest a resonant $pp \rightarrow pp$ amplitude with $J = L = S$ = 1 since this gives A_{NN} = 1 (in absence of background) and a smooth angular distribution. Because of the Pauli principle, an S = 1 di-proton resonances must have odd parity and thus odd orbital angular momentum. The the two non-zero helicity amplitudes for a J = L = S = 1 resonance can be parameterized in Breit-Wigner form:

$$\phi_3(\mathrm{resonance}) = 12\pi\frac{\sqrt{s}}{p_{\mathrm{cm}}}d^1_{1,1}(\theta_{\mathrm{cm}})\frac{\frac{1}{2}\Gamma^{pp}(s)}{M^* - E_{\mathrm{cm}} - \frac{i}{2}\Gamma} \quad ,$$

$$\phi_4(\mathrm{resonance}) = -12\pi\frac{\sqrt{s}}{p_{\mathrm{cm}}}d^1_{-1,1}(\theta_{\mathrm{cm}})\frac{\frac{1}{2}\Gamma^{pp}(s)}{M^* - E_{\mathrm{cm}} - \frac{i}{2}\Gamma} \quad .$$

(The ${}^3F_3$ resonance amplitudes have the same form with $d^3_{\pm 1\ 1}$ replacing $d^1_{\pm 1,1}$.) As in the case of a narrow resonance like the Z^0, the partial width into nucleon pairs is proportional to the square of the time-like proton form factor: $\Gamma^{pp}(s)/\Gamma = B^{pp}|F(s)|^2/|F(M^{*2})|^2$, corresponding to the formation of two protons at this invariant energy. The resonant amplitudes then die away by one inverse power of $(E_{\mathrm{cm}} - M^*)$ relative to the dominant PQCD amplitudes. (In this sense, they are higher twist contributions relative to the leading twist perturbative QCD amplitudes.) The model is thus very simple: each pp helicity amplitude ϕ_i is the coherent sum of PQCD plus resonance components: $\phi = \phi(\mathrm{PQCD}) + \Sigma\phi(\mathrm{resonance})$. Because of pinch singularities and higher-order corrections, the hard QCD amplitudes

are expected to have a nontrivial phase;[15] the model allows for a constant phase δ in ϕ(PQCD). Because of the absence of the ϕ_5 helicity-flip amplitude, the model predicts zero single spin asymmetry A_N. This is consistent with the large angle data at p_{lab} = 11.75 GeV/c.[109]

At low transverse momentum, $p_T \leq 1.5$ GeV, the power-law fall-off of ϕ(PQCD) in s disagrees with the more slowly falling large-angle data, and one has little guidance from basic theory. The main interest in this low-energy region is to illustrate the effects of resonances and threshold effects on A_{NN}. In order to keep the model tractable, one can extend the background quark interchange and the resonance amplitudes at low energies using the same forms as above but replacing the dipole form factor by a phenomenological form F(t) $\propto e^{-1/2\beta\sqrt{|t|}}$. A kinematic factor of $\sqrt{s}/2p_{\rm cm}$ is included in the background amplitude. The value β = 0.85 GeV^{-1} then gives a good fit to $d\sigma/dt$ at $\theta_{\rm cm} = \pi/2$ for $p_{lab} \leq 5.5$ GeV/c.[110] The normalizations are chosen to maintain continuity of the amplitudes.

The predictions of the model and comparison with experiment are shown in Figs. 31-36. The following parameters are chosen: C = 2.9 $\times 10^3$, δ = -1 for the normalization and phase of ϕ(PQCD). The mass, width and pp branching ratio for the three resonances are $M_d^* = 2.17$ GeV, Γ_d = 0.04 GeV, $B_d^{pp} = 1$; $M_s^* = 2.55$ GeV, Γ_s = 1.6 GeV, B_s^{pp} = 0.65; and $M_c^* = 5.08$ GeV, Γ_c = 1.0 GeV, B_c^{pp} = 0.0155, respectively. As shown in Figs. 31 and 32, the deviations from the simple scaling predicted by the PQCD amplitudes are readily accounted for by the resonance structures. The cusp which appears in Fig. 32 marks the change in regime below p_{lab} = 5.5 GeV/c where PQCD becomes inapplicable. It is interesting to note that in this energy region normal attenuation of quasielastic pp scattering is observed.[99] The angular distribution (normalized to the data at $\theta_{\rm cm} = \pi/2$) is predicted to broaden relative to the steeper perturbative QCD form, when the resonance dominates. As shown in Fig. 33 this is consistent with experiment, comparing data at p_{lab} = 7.1 and 12.1 GeV/c.

The most striking test of the model is its prediction for the spin correlation A_{NN} shown in Fig. 34. The rise of A_{NN} to $\simeq$ 60% at p_{lab} = 11.75 GeV/c is correctly reproduced by the high energy J=1 resonance interfering with ϕ(PQCD). The narrow peak which appears in the data of Fig. 34 corresponds to the onset of the $pp \rightarrow p\Delta(1232)$ channel which can be interpreted as a $uuuuddq\bar{q}$ resonant state. Because of spin-color statistics one expects in this case a higher orbital momentum state, such as a $pp\ ^3F_3$ resonance. The model is also consistent with the recent high-energy data point for A_{NN} at p_{lab} = 18.5 GeV/c and $p_T^2 = 4.7$ GeV^2 (see Fig. 35). The data show a dramatic decrease of A_{NN} to zero or negative values. This is explained in the model by the destructive interference effects above the resonance region. The same effect accounts for the depression of A_{NN} for $p_{lab} \approx 6$ GeV/c

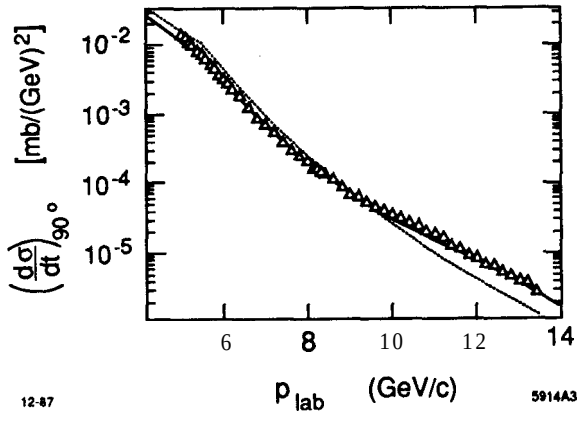

Figure 31. Prediction (solid curve) for $d\sigma/dt(pp \rightarrow pp)$ at $\theta_{cm} = \pi/2$ compared with the data of Akerlof **et** *al.*[110] The dotted line is the background PQCD prediction.

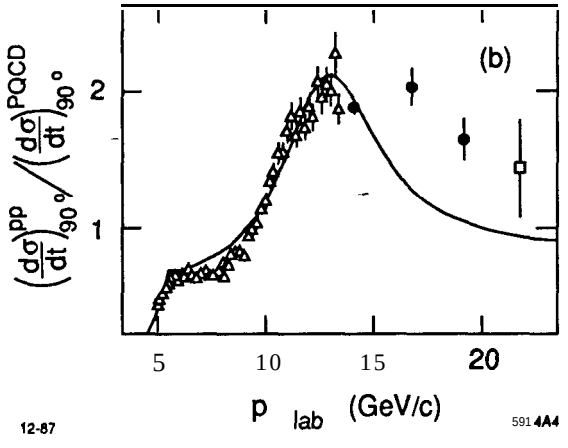

Figure 32. Ratio of $d\sigma/dt(pp \rightarrow pp)$ at θ_{cm} = x/2 to the PQCD prediction. The data[110] are from Akerlof **et** al. (open triangles), Allaby **et** al. (solid dots) and Cocconi et **al.** (open square). The cusp at $p_{lab} = 5.5$ GeV/c indicates the change of regime from PQCD.

shown in Fig. 34. The comparison of the angular dependence of A_{NN} with data at p_{lab} = 11.75 GeV/c is shown in Fig. 36. The agreement with the data[111] for the longitudinal spin correlation A_{LL} at the same p_{lab} is somewhat worse.

The simple model discussed here shows that many features can be naturally explained with only a few ingredients: a perturbative QCD background plus resonant amplitudes associated with rapid changes of the inelastic pp cross section. The model provides a good description of the s and t dependence of the differential cross section, including its "oscillatory" dependence[112] in s at fixed θ_{cm}, and the

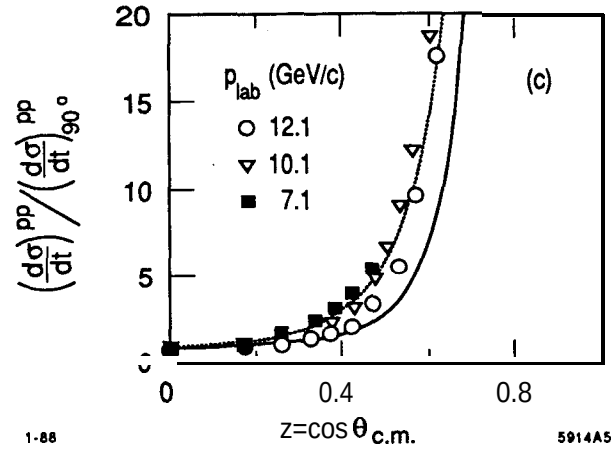

Figure 33. The $pp \rightarrow pp$ angular distribution normalized at $\theta_{\rm cm} = \pi/2$. The data are from the compilation given in Sivers **et al.,** Ref. 24. The solid and dotted lines are predictions for p_{lab} = 12.1 and 7.1 GeV/c, respectively, showing the broadening near resonance.

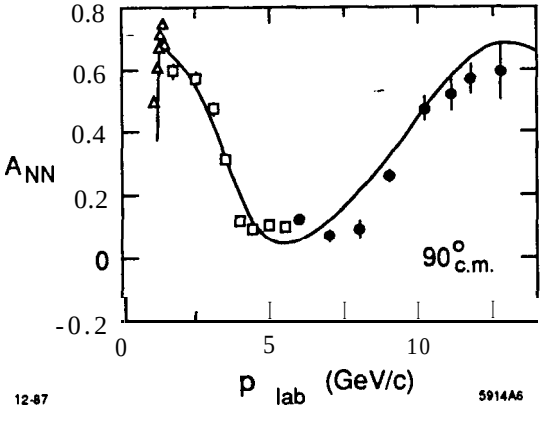

Figure 34. A_{NN} as a function of p_{lab} at $\theta_{cm} = \pi/2$. The data[110] are from Crosbie **et** al: (solid dots), Lin **et al.** (open squares) and Bhatia **et al.** (open triangles). The peak at $p_{lab} = 1.26$ GeV/c corresponds to the $p\Delta$ threshold. The data are well reproduced by the interference of the broad resonant structures at the strange (p_{lab} = 2.35 GeV/c) and charm (p_{lab} = 12.8 GeV/c) thresholds, interfering with a PQCD background. The value of A_{NN} from PQCD alone is 1/3.

broadening of the angular distribution near the resonances. Most important, it gives a consistent explanation for the striking behavior of both the spin-spin correlations and the anomalous energy dependence of the attenuation of quasielastic pp scattering in nuclei. It is predicted that color transparency should reappear at higher energies ($p_{lab} \geq 16$ GeV/c), and also at smaller angles ($\theta_{\rm cm} \approx 60°$) at

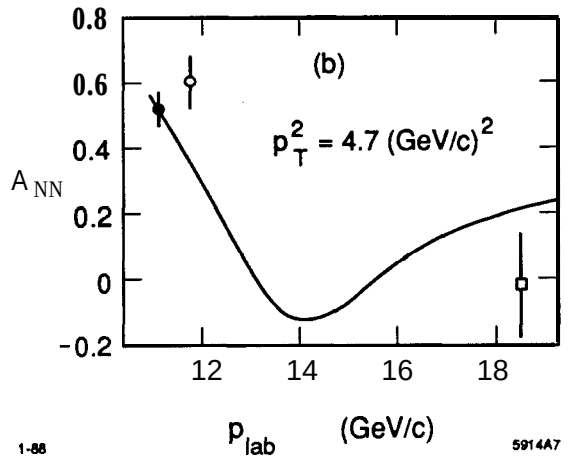

Figure 35. A_{NN} at fixed p_T^2 = (4.7 GeV/c)^2. The data point[110] at p_{lab} = 18.5 GeV/c is from Court *et al.*

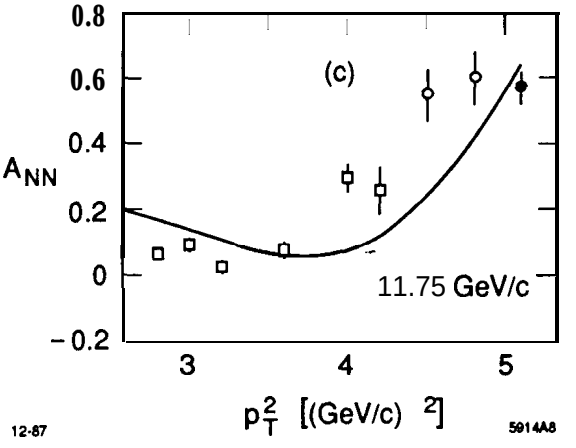

Figure 36. A_{NN} as a function of transverse momentum. The data[103] are from Crabb *et* al. (open circles) and O'Fallon *et* al. (open squares). Diffractive contributions should be included for $p_T^2 \leq 3$ GeV^2.

$p_{lab} = 12$ GeV/c where the perturbative QCD amplitude dominates. If the J=1 resonance structures in A_{NN} are indeed associated with heavy quark degrees of freedom, then the model predicts inelastic pp cross sections of the order of 1 mb and 1μb for the production of strange and charmed hadrons near their respective thresholds.[113] Thus a crucial test of the heavy quark hypothesis for explaining A_{NN}, rather than hidden color or gluonic excitations, is the observation of significant charm hadron production at $p_{lab} \geq 12$ GeV/c.

Recently Ralston and Pire[15] have proposed that the oscillations of the pp elas-

tic cross section and the apparent breakdown of color transparency are associated with the dominance of the Landshoff pinch contributions at $\sqrt{s} \sim 5\ GeV$. The oscillating behavior of $d\sigma/dt$ is due to the energy dependence of the relative phase between the pinch and hard-scattering contributions. They assume color transparency will disappear whenever the pinch contributions are dominant since such contributions could couple to wavefunctions of large transverse size. The large spin correlation in A_{NN} is not readily explained in the Ralston-Pire model. Furthermore, the recent analysis by Botts and Sterman[58] suggests that the pinch contributions should satisfy color transparency. In any event, more data and analysis are needed to discriminate between models.

Nuclear-Bound Quarkonia

The above analysis also has implications for the production of hidden charm near threshold in hadronic and nuclear collisions. For example, consider the reaction $dd \to \alpha(c\bar{c})$ where the charmonium state is produced nearly at rest. At the threshold for charm production, the incident nuclei will be stopped (in the center of mass frame) and will evidently fuse into a compound nucleus (the α) because of the strong attractive nuclear force. The charmonium state will be attracted to the nucleus by the QCD gluonic Van der Waals force. It is thus likely that a new type of nuclear bound state will be formed: charmonium bound to nuclear matter. Such a state should be observable at a distinct dd energy, and it will decay to unique signatures such as $dd \to \alpha\mu^+\mu^-$. The binding energy in the nucleus gives a precision measure of the charmonium's interactions with ordinary hadrons and nuclei; its decays will measure hadron-nucleus interactions and test color transparency starting from a unique initial state condition.

12. Discretized Light-Cone Quantization

Only a small fraction of strong interaction and nuclear physics can be addressed by perturbative QCD analyses. The solution to the mass and wavefunction of the proton requires a solution to the QCD bound-state problem. Even with the simplicity of the e^+e^- and $\gamma\gamma$ initial state, the full complexity of hadron dynamics is involved in understanding resonance production, exclusive channels near threshold, jet hadronization, the hadronic contribution to the photon structure function, and the total e^+e^- or $\gamma\gamma$ annihilation cross section. A primary question is whether we can ever hope to confront QCD directly in its nonperturbative domain. Lattice gauge theory and effective Lagrangian methods such as the Skyrme model offer some hope in understanding the low-lying hadron spectrum but dynamical computations relevant to $\gamma\gamma$ annihilation appear intractable. Considerable information[5] on the spectrum and the moments of hadron valence wavefunctions has been ob-

tained using the ITEP QCD sum rule method, but the region of applicability of this method to dynamical problems appears limited.

Recently a new method for analysing QCD in the nonperturbative domain has been developed: discretized light-cone quantization (DLCQ).[114] The method has the potential for providing detailed information on all the hadron's Fock light-cone components. DLCQ has been used to obtain the complete spectrum of neutral states in QED[9] and QCD[115] in one space and one time for any mass and coupling constant. The QED results agree with the Schwinger solution at infinite coupling. We will review the QCD[1+1] results below. Studies of QED in 3+1 dimensions are now underway.[116] Thus one can envision a nonperturbative method which in principle could allow a quantitative confrontation of QCD with the data even at low energies and momentum transfer.

The basic idea of DLCQ is as follows: QCD dynamics takes a rather simple form when quantized at equal light-cone "time" $\tau = t + z/c$. In light-cone gauge $A^+ = A^0 + A^z = 0$, the QCD light-cone Hamiltonian

$$H_{\rm QCD} = H_0 + gH_1 + g^2H_2$$

contains the usual S-point and 4-point interactions plus induced terms from instantaneous gluon exchange and instantaneous quark exchange diagrams. The perturbative vacuum is an eigenstate of $H_{\rm QCD}$ and serves as the lowest state in constructing a complete basis set of color singlet Fock states of H_0 in momentum space. Solving QCD is then equivalent to solving the eigenvalue problem:

$$H_{\rm QCD}|\Psi>= M^2|\Psi>$$

as a matrix equation on the free Fock basis. The set of eigenvalues $\{M^2\}$ represents the spectrum of the color-singlet states in QCD. The Fock projections of the eigenfunction corresponding to each hadron eigenvalue gives the quark and gluon Fock state wavefunctions $\psi_n(x_i, k_{\perp i}, \text{Xi})$ required to compute structure functions, distribution amplitudes, decay amplitudes, etc. For example, as shown by Drell and Yan,[36] the form-factor of a hadron can be computed at any momentum transfer Q from an overlap integral of the ψ_n summed over particle number n. The e^+e^- annihilation cross section into a given $J = 1$ hadronic channel can be computed directly from its $\psi_{q\bar{q}}$ Fock state wavefunction.

The light-cone momentum space Fock basis becomes discrete and amenable to computer representation if one chooses (anti-)periodic boundary conditions for the quark and gluon fields along the $z^- = z - ct$ and $z_\perp$ directions. In the case of renormalizable theories, a covariant ultraviolet cutoff A is introduced which limits

the maximum invariant mass of the particles in any Fock state. One thus obtains a finite matrix representation of $H_{\rm QCD}^{(\Lambda)}$ which has a straightforward continuum limit. The entire analysis is frame independent, and fermions present no special difficulties.

Since H_{LC}, P^+, $\vec{P}_\perp$, and the conserved charges all commute, H_{LC} is block diagonal. By choosing periodic (or anti-periodic) boundary conditions for the basis states along the negative light-cone $\psi(z^- = +L) = \pm\psi(z^- = -L)$, the Fock basis becomes restricted to finite dimensional representations. The eigenvalue problem thus reduces to the diagonalization of a finite Hermitian matrix. To see this, note that periodicity in z^- requires $P^+ = \frac{2\pi}{L}K$, $k_i^+ = \frac{2\pi}{L}\, n_i$, $\sum_{i=1}^{n} n_i = K$. The dimension of the representation corresponds to the number of partitions of the integer K as a sum of positive integers n. For a finite resolution K, the wavefunction is sampled at the discrete points

$$x_i = \frac{k_i^+}{P^+} = \frac{n_i}{K} = \left\{ \frac{1}{K}, \quad \frac{2}{K}, \quad \cdots \frac{K-1}{K} \right\} \quad .$$

The continuum limit is clearly $K \to \infty$.

One can easily show that P^- scales as L. One thus defines $P^- \equiv \frac{L}{2\pi}H$. The eigenstates with $P^2 = -M^2$ at fixed P^+ and $\vec{P}_\perp = 0$ thus satisfy $H_{LC}\,|\Psi\rangle = KH\,|\Psi\rangle = M^2\,|\Psi\rangle$, independent of L (which corresponds to a Lorentz boost factor).

The basis of the DLCQ method is thus conceptually simple: one quantizes the independent fields at equal light-cone time τ and requires them to be periodic or anti-periodic in light-cone space with period $2L$. The commuting operators, the light-cone momentum $P^+ = \frac{2\pi}{L}K$ and the light cone energy $P^- = \frac{L}{2\pi}\,H$ are constructed explicitly in a Fock space representation and diagonalized simultaneously. The eigenvalues give the physical spectrum: the invariant mass squared $M^2 = P^\nu P_\nu$. The eigenfunctions give the wavefunctions at equal τ and allow one to compute the current matrix elements, structure functions, and distribution amplitudes required for physical processes. All of these quantities are manifestly independent of L, since $M^2 = P^+P^- = HK$. Lorentz-invariance is violated by periodicity, but re-established at the end of the calculation by going to the continuum limit: $L \to \infty$, $K \to \infty$ with P^+ finite. In the case of gauge theory, the use of the light-cone gauge $A^+ = 0$ eliminates negative metric states in both Abelian and non-Abelian theories.

Since continuum as well as single hadron color singlet hadronic wavefunctions are obtained by the diagonalization of H_{LC}, one can also calculate scattering amplitudes as well as decay rates from overlap matrix elements of the interaction Hamiltonian for the weak or electromagnetic interactions. An important point is

that all higher Fock amplitudes including spectator gluons are kept in the light-cone quantization approach; such contributions cannot generally be neglected in decay amplitudes involving light quarks.

The simplest application of DLCQ to local gauge theory is QED in one-space and one-time dimensions. Since $A^+ = 0$ is a physical gauge there are no photon degrees of freedom. Explicit forms for the matrix representation of H_{QED} are given in Ref. 9.

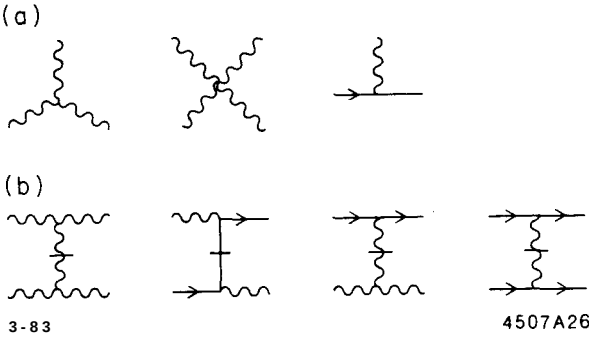

Figure 37. Diagrams which appear in the interaction Hamiltonian for QCD on the light cone. The propagators with horizontal bars represent "instantaneous" gluon and quark exchange which arise-from reduction of the dependent fields in $A^+ = 0$ gauge. (a) Basic interaction vertices in QCD. (b) "Instantaneous" contributions.

The basic interactions which occur in $H_{LC}(\mathrm{QCD})$ are illustrated in Fig. 37. Recently Hornbostel[115] has used DLCQ to obtain the complete color-singlet spectrum of QCD in one space and one time dimension for $N_C = 2, 3, 4$. The hadronic spectra are obtained as a function of quark mass and QCD coupling constant (see Fig. 38).

Where they are available, the spectra agree with results obtained earlier; in particular, the lowest meson mass in SU(2) agrees within errors with lattice Hamiltonian results.[117] The meson mass at $N_C = 4$ is close to the value obtained in the large N_C limit. The method also provides the first results for the baryon spectrum in a non-Abelian gauge theory. The lowest baryon mass is shown in Fig. 38 as a function of coupling constant. The ratio of meson to baryon mass as a function of N_C also agrees at strong coupling with results obtained by Frishman and Sonnenschein.[118] Precise values for the mass eigenvalue can be obtained by extrapolation to large K since the functional dependence in $1/K$ is understood.

As emphasized above, when the light-cone Hamiltonian is diagonalized for a finite resolution K, one gets a complete set of eigenvalues corresponding to the total dimension of the Fock state basis. A representative example of the spectrum

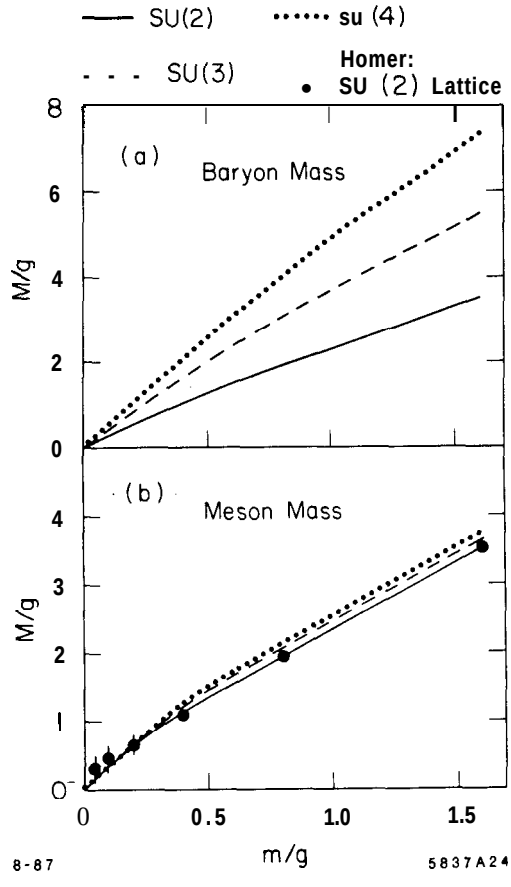

Figure 38. The baryon and meson spectrum in QCD [1+1] computed in DLCQ for $N_C = 2, 3, 4$ as a function of quark mass and coupling constant!“”

is shown in Fig. 39 for baryon states (B = 1) as a function of the dimensionless variable $\lambda = 1/(1+\pi m^2/g^2)$. Note that spectrum automatically includes continuum states with $B = 1$.

The structure functions for the lowest meson and baryon states in SU(3) at two different coupling strengths m/g = 1.6 and m/g = 0.1 are shown in Figs. 40 and 41. Higher Fock states have a very small probability; representative contributions to the baryon structure functions are shown in Figs. 42 and 43. For comparison, the valence wavefunction of a higher mass state which can be identified as a composite of meson pairs (analogous to a nucleus) is shown in Fig. 44. The interactions of the quarks in the pair state produce Fermi motion beyond x = 0.5. Although these results are for one time one space theory they do suggest that the sea quark distributions in physical hadrons may be highly structured.

In the case of gauge theory in 3+1 dimensions, one also takes the $k_\perp^i = (2\pi/L_\perp)n_\perp^i$ as discrete variables on a finite Cartesian basis. The theory is co-

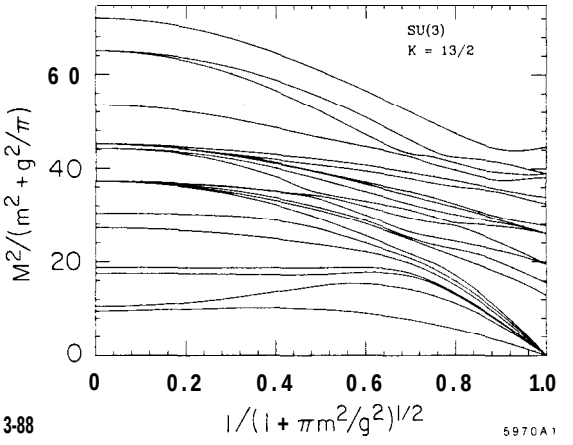

Figure 39. Representative baryon spectrum for QCD in one-space and one-time dimension.[115]

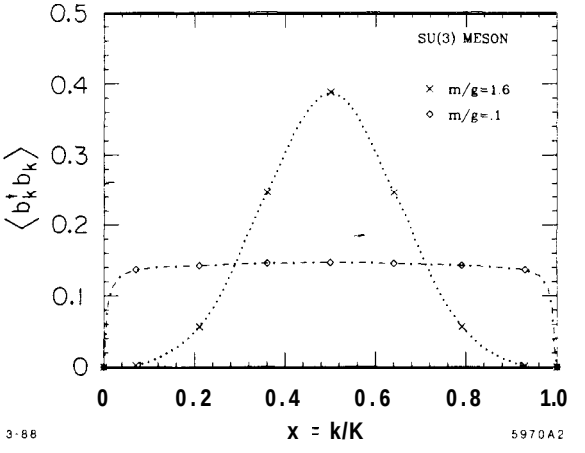

Figure 40. The meson quark momentum distribution in QCD[1+1] computed using DLCQ.[115]

variantly regulated if one restricts states by the condition

$$\sum_i \frac{k_{\perp i}^2 + m_i^2}{x_i} \leq \Lambda^2 \quad ,$$

where A is the ultraviolet cutoff. In effect, states with total light-cone kinetic energy beyond, Λ^2 are cut off. In a renormalizable theory physical quantities are independent of physics beyond the ultraviolet regulator; the only dependence on A appears in the coupling constant and mass parameters of the Hamiltonian, consistent with the renormalization group.[119] The resolution parameters need to be

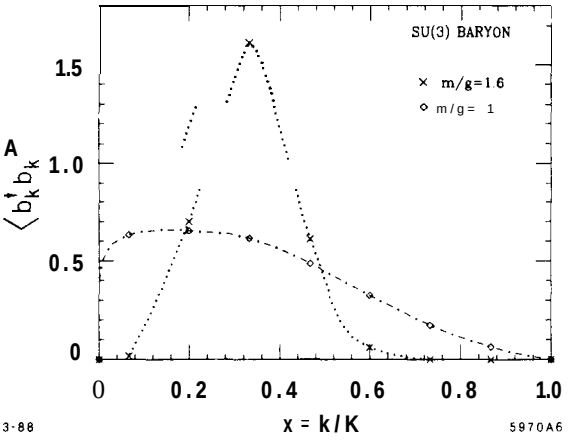

Figure 41. The baryon quark momentum distribution in QCD[1+1] computed using DLCQ. [115]

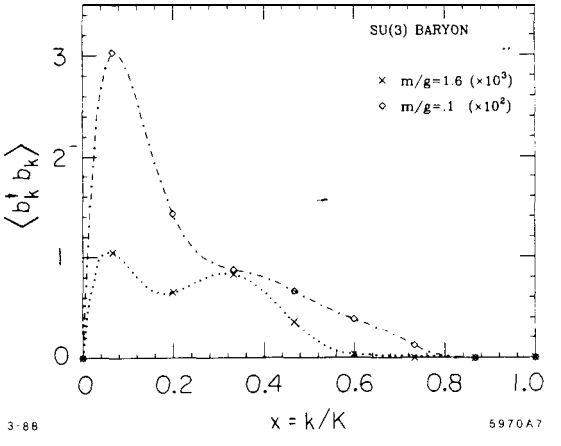

Figure 42. Contribution to the baryon quark momentum distribution from $qqq\bar{q}\bar{q}$ states for QCD[1+1].[115]

taken sufficiently large such that the theory is controlled by the continuum regulator A, rather than the discrete scales of the momentum space basis.

There are a number of important advantages of the DLCQ method which have emerged from this study of two-dimensional field theories:

1. The Fock space is denumerable and finite in particle number for any fixed resolution K. In the case of gauge theory in 3+1 dimensions, one expects that photon or gluon quanta with zero four-momentum decouple from neutral or color-singlet bound states, and thus need not be included in the Fock basis.
2. Because one is using a discrete momentum space representation, rather than

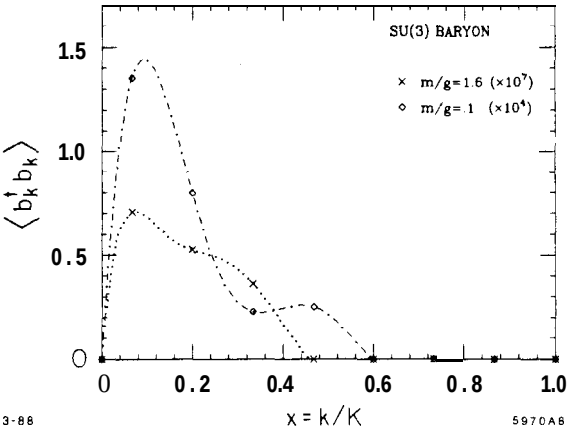

Figure 43. Contribution to the baryon quark momentum distribution from $qqq\overline{q}\overline{q}\overline{q}$ states for QCD[1+1].[115]

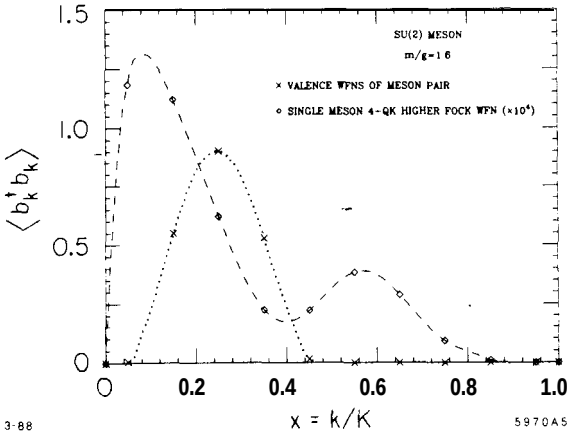

Figure 44. Comparison of the meson quark distributions in the $qq\overline{q}\overline{q}$ Fock sate with that of a continuum meson pair state. The structure in the former may be due to the fact that these four-particle wavefunctions are orthogonal.[115]

a space-time lattice, there are no special difficulties with fermions: e.g.no fermion doubling, fermion determinants, or necessity for a quenched approximation. Furthermore,-the discretized theory has basically the same ultraviolet structure as the continuum theory. It should be emphasized that unlike lattice calculations, there is no constraint or relationship between the physical size of the bound state and the length scale L.

3. The DLCQ method has the remarkable feature of generating the complete spectrum of the theory; bound states and continuum states alike. These can be separated by tracing their minimum Fock state content down to small

coupling constant since the continuum states have higher particle number content. In lattice gauge theory it appears intractable to obtain information on excited or scattering states or their correlations. The wavefunctions generated at equal light cone time have the immediate form required for relativistic scattering problems. In particular one can calculate the relativistic form factor from the matrix element of currents.

4. DLCQ is basically a relativistic many-body theory, including particle number creation and destruction, and is thus a basis for relativistic nuclear and atomic problems. In the nonrelativistic limit the theory is equivalent to the many- body Schrödinger theory.

Whether QCD can be solved using DLCQ — considering its large number of degrees of freedom is unclear, The studies for Abelian and non-Abelian gauge theory carried out so far in 1+1 dimensions give grounds for optimism.

Other Applications of Light-Cone Quantization

In the discretized light-cone quantization method, one can construct an explicit matrix representation of the QCD Hamiltonian on the light-cone momentum space Fock representation. The kinetic energy operator in this representation is diagonal. In principle one can diagonalize the total Hamiltonian on this representation to obtain not only the discrete and continuum eigenvalues, but also the corresponding light-cone wavefunctions required to compute intrinsic structure functions and distribution amplitudes. Since we are primarily interested in the lowest mass eigenstates of the hadron spectrum, we can use the variational method and simply minimize the expectation value of the light-cone Hamiltonian. This is currently being carried out by Tang[116] for the study of positronium at large α. The evaluation of the Fock state sum can be made highly efficient by using vectorized code and importance sampling algorithms such as Lepage's program *VEGAS*. On the other hand if the total Hamiltonian could be diagonalized, one could immediately construct the resolvent, and thus the $T-$ matrix for scattering problems. The fractional experimental resolution in center of mass energy squared $\delta s/s$ can be matched to the a corresponding resolution 1/K.

The light-cone Fock state representation can also be used advantageously in perturbation theory. For example, one can calculate any scattering amplitude in terms of the usual Lippman-Schwinger series:

$$T = H_I + H_I \frac{1}{P^- - H_0 + i\epsilon} H_I + \ldots.$$

Langnau and I are currently applying this method to the higher order calculation of the electron's anomalous magnetic moment in quantum electrodynamics. The

sum over intermediate Fock states is equivalent to summing all r-ordered diagrams and integrating over the transverse momentum and light-cone fractions x. Because of the restriction to positive x, diagrams corresponding to vacuum fluctuations or those containing backward-moving lines are eliminated. The amplitudes are regulated in the infrared and ultraviolet by cutting off the invariant mass. The ultraviolet regularization and renormalization of the perturbative contributions may be carried out by using the "alternating denominator method"[120] which yields an automatic construction of mass renormalization counter-terms.

The same method can also be used to compute perturbative contributions to the-annihilation ratio $R_{e^+e^-} = \sigma(e^+e^- \text{ -t } hadrons)/\sigma(e^+e^- \to \mu^+\mu^-)$ as well as the quark and gluon jet distribution. The results are obtained in the light-cone variables, x, $k_\perp$, λ, which are the natural covariant variables for this problem. Since there are no Fadeev-Popov or Gupta-Bleuler ghost fields in the light-cone gauge $A^+ = 0$, the calculations are explicitly unitary. It is hoped that one can in this way check the three-loop calculation of Gorishny, et al.[121] who found a surprisingly large value of 64.9 for the coefficient of $(\alpha_s/\pi)^3$ of $R_{e^+e^-}$ in the MS scheme.

13. Conclusions

In this colloquium I have emphasized several novel. features of quantum chromodynamics, features which lead to new insights into the structure of the hadrons and their interactions. Among the highlights:

1. The structure of the proton now appears both theoretically and experimentally to be surprisingly complex, very much at variance with intuition based on non-relativistic quark model. The most convenient covariant representation of the hadron in QCD is given by the light-cone Fock basis. According to QCD sum rules, the valence Fock state wavefunction of the proton turns out to be highly structured and asymmetric between the valence u and d quarks. Polarized deep inelastic structure function measurements by the SLAC-Yale and CERN-EMC collaborations show that the gluons and strange quarks have strong spin correlations with the proton spin. There is even the possibility of a small admixture of hidden charm in the nucleon wavefunction. I have also discussed the distinctions between intrinsic (bound state) versus extrinsic (collision-induced) contributions to the proton structure functions, and a new approach to understanding the non-additive shadowing and anti-shadowing features of the leading twist nuclear structure functions.
2. The perturbative QCD analysis of exclusive amplitudes has now become a highly-developed field, based on all-orders factorization theorems, evolution

equations, Sudakov-regulated pinch contributions, etc. The application to experiment has been highly successful; the recent confirmation by the TPC-$\gamma\gamma$ experiment of the PQCD predictions for the photon-q transition form factor is an important verification of the theory, as significant as Bjorken scaling in deep inelastic inclusive reactions. The recent observation at SLAC of reduced-amplitude scaling for large angle photo-disintegration provides a striking demonstration of the dominance of simple quark-gluon degrees of freedom in nuclear amplitudes at the few GeV scale. The observation at BNL of increasing color transparency of quasi-elastic pp scattering in nuclei has confirmed perhaps the most novel feature of perturbative QCD. The experimental results contradict the standard Glauber treatment of initial and final state interactions but support the PQCD prediction that -large-angle pp scattering involves only the small color-dipole moment configurations of the proton Fock state. The observation of color transparency rules against a description of large momentum exclusive amplitudes in terms of the convolution of soft hadronic wavefunctions. It is clearly essential that color transparency be tested in other channels, particularly, quasi-elastic $e - p$ scattering.

3. It should be emphasized that experimental and theoretical studies of exclusive amplitudes are necessary for the fundamental understanding of the structure of the hadronic wavefunctions. Exclusive amplitudes provide a testing ground for hadronization in the simplest, most controlled amplitudes. These tests are essential if we are ever able to understand coherence and coalescence phenomena in the hadronization of QCD jets. The calculation of weak decay matrix elements and the extraction of quark mixing parameters of electroweak theory also require a detailed understanding of hadronic wavefunctions.

4. I have described a new approach to the problem of solving QCD in the nonperturbative domain-discretized light-cone quantization. The application of the method to QCD in one-space and one-time has been very encouraging. The challenge now is to apply this method to obtain the mass spectrum and light-cone Fock wave functions of the hadrons in QCD[3+1]. A very interesting feature of the DLCQ results for QCD[1+1] are the oscillations which emerge in the higher Fock state contributions to the hadron structure functions. The DLCQ method also leads naturally to a perturbative method for computing $R_{e^+e^-}$ as well as coherent contributions to jet observables at the amplitude rather than probabilistic level.

5. One of the most important challenges to the PQCD analysis of exclusive reactions is the striking behavior observed in the spin-spin correlation A_{NN} in large-angle pp scattering at $E_{cm} \sim 5\ GeV$. As I have discussed in this lecture, this phenomena can be interpreted as due to a threshold enhance-

ment or resonance due to open charm production in the intermediate state. This explanation also naturally accounts for the observed diminishing of color transparency seen in the BNL experiment at the same kinematic domain. A corollary of this explanation is the prediction of new bound states of charmonium with nucleons or nuclei, just below the production threshold for open charm.

Quantum Chromodynamics has now emerged as a science in itself, unifying hadron and nuclear physics in terms of a common set of fundamental degrees of freedom. It is clear that we have only begun the study its novel perturbative and non-perturbative features.

ACKNOWLEDGEMENTS

Some of the work discussed in this lecture was based on collaboration with others, including: G. P. Lepage, J. F. Gunion, E. L. Berger, P. Hoyer, I. Schmidt, H. Lu, T. Huang, A. Langnau, G. Farrar, G. de Teramond, J. R. Hiller, K. Hornbostel, C. R. Ji, A. H. Mueller, H. C. Pauli, D. E. Soper, A. Tang and S. F. Tuan. I also wish to thank Ed Tang and his colleagues at the University of Minnesota for their outstanding hospitality.

REFERENCES

1. For general reviews of QCD see J. C. Collins and D. E. Soper, Ann. Rev. Nucl. Part. Sci., 37, 383 (1987); E. Reya, Phys. Rept. 69, 195 (1981); A.H. Mueller, Lectures on perturbative QCD given at the Theoretical Advanced Study Inst., New Haven, 1985; *Quarks and Gluons in Particle and Nuclei*, Proc. of the UCSB Institute for Theoretical Physics Workshop on Nuclear Chromodynamics, eds., S.J. Brodsky and E. Moniz (World Scientific, 1985). For a more detailed discussion of exclusive processes in QCD, see S. J. Brodsky and G. P. Lepage, SLAC-PUB-4947 (1989).
2. C.Klopfenstein *et al.*, CUSB 83-07 (1983).
3. K. Varvell *et* al., CERN/EP 87-46 (1987).
4. S.J. Brodsky, G.P. Lepage and P.B. Mackenzie, Phys. Rev. D28, 228 (1983). The problem of setting the scale of the argument of the running coupling constant is discussed in this paper.
5. V.L. Chernyak and A.R. Zhitnitskii, Phys. Rept. 112, 173 (1984). See also Xiao-Duang Xiang, Wang Xin-Nian, and Huang Tao, BIHEP-TH-84, 23 and 29 (1984).
6. S. Bethke, LBL-26958, (1989).
7. I.D. King and C.T. Sachrajda, SHEP-85/86-15 (1986), p. 36. .
8. G. Martinelli and C.T. Sachrajda, CERN-TH-4637/87 (1987). The results are based on the method of S. Gottlieb and A.S. Kronfeld, Phys. Rev. D33, 227 (1986); A.S. Kronfeld and D.M. Photiadis, Phys. Rev. D31, 2939 (1985).
9. T. Eller, H. C. Pauli and S. J. Brodsky, Phys. Rev. D35, 1493 (1987).
10. P.A.M. Dirac, Rev. Mod. Phys. 21, 392 (1949). Further references to light-cone quantization are given in ref. 9.
11. A. V. Crewe, Science 154,729 (1966).
12. S.J. Brodsky, J.F. Gunion and R.L. Jaffe Phys. Rev. D6, 2487 (1972).
13. P. Hoodbhoy and R.L. Jaffe, Phys. Rev. D35, 113 (1987); R.L. Jaffe, CTP #1315 (1985).
14. A. H. Mueller, Proc. XVII Recontre de Moriond (1982); S. J. Brodsky, Proc. XIII Int. Symp. on Multiparticle Dynamics, Volendam (1982). See also G. Bertsch, A. S. Goldhaber, and J. F. Gunion, Phys. Rev. Lett. 47, 297 (1981); G. R. Farrar, H. Liu, L. L. Frankfurt, M. J. Strikmann, Phys. Rev. Lett. 61, 686 (1988); A. H. Mueller, CU-TP-415, talk given at the DPF meeting, Stoors, Conn (1988), and CU-TP-412 talk given at the

Workshop on Nuclear and Particle Physics on the Light-Cone, Los Alamos, (1988); B. Pire and J. P. Ralston, ref. 15.

15. J. P. Ralston and B. Pire, Phys. Rev. Lett. 57, 2330 (1986); Phys. Lett. 117B, 233 (1982).

16. S.J. Brodsky, G.T. Bodwin and G.P. Lepage, in the Proc. of the Volendam Multipart. Dyn. Conf., 1982, p. 841; Proc. of the Banff Summer Inst., 1981, p. 513. This effect is related to the formation zone principle of L. Landau and I. Pomeranchuk, Dok. Akademii Nauk SSSR 92, 535,735 (1953).

17. G.T. Bodwin, Phys. Rev. D31, 2616 (1985); G.T. Bodwin, S.J. Brodsky and G.P. Lepage, ANL-HEP-CP-85-32-mc (1985), presented at 20th Rencontre de Moriond, Les Arcs, France, March 10-17, 1985.

18. A. Sommerfeld, *Atombau and Spektallinen* (Vieweg, Braunschweig, 1939).

19. G. T. Bodwin, S. J. Brodsky, and G. P. Lepage, Phys. Rev. D39, 3287 (1989).

20. S. J. Brodsky and Hung Lu, in preparation.

21. See e.g. S. J. Brodsky, J. Ellis and M. Karliner, Phys. Lett. 206B, 309 (1988).

22. Further discussion will appear in S. J. Brodsky and I. Schmidt, to be published. For a corresponding example in atomic physics see M. L. Goldberger and F. E. Low, Phys. Rev. 176, 1778 (1968).

23. J.F. Gunion, P. Nason and R. Blankenbecler, Phys. Rev. D29, 2491 (1984); Phys. Lett. 117B, 353 (1982).

24. J.F. Gunion, S. J. Brodsky and R. Blankenbecler, Phys. Rev. D8, 287 (1973); Phys. Lett. 39B, 649 (1972); D. Sivers, S. J. Brodsky and R. Blankenbecler, Phys. Reports 23C, 1 (1976). Extensive references to fixed angle scattering are given in this review.

25. E.L. Berger and S.J. Brodsky, Phys. Rev. D24, 2428 (1981).

26. E.L. Berger and F. Coester, ANL-HEP-PR-87-13 (1987).

27. J.J. Aubert et al., Phys. Lett. 123B, 275 (1983); For a recent review see E.L. Berger and F. Coester, ANL-HEP-PR-87-13 (to be published in Ann. Rev. of Nucl. Part. Sci.).

28. I.A. Schmidt and R. Blankenbecler, Phys. Rev. D15, 3321 (1977).

29. S.J. Brodsky and G.R. Farrar, Phys. Rev. Lett. 31, 1153 (1973); Phys. Rev. D11, 1309 (1975).

30. S.J. Brodsky and B.T. Chertok, Phys. Rev. Lett. 37, 269 (1976); Phys. Rev. D114, 3003 (1976).

31. S.J. Brodsky and G.P. Lepage, Phys. Rev. D24, 1808 (1981). The next to leading order evaluation of T_H for these processes is given by B. Nezic, Ph.D. Thesis, Cornell Univ. (1985).

32. S. J. Brodsky, J. F. Gunion and D. E. Soper, Phys. Rev. D36, 2710 (1987).

33. S. J. Brodsky, G. Kopp, and P. Zerwas Phys. Rev. Lett. 58, 443 (1987).

34. General QCD analyses of exclusive processes are given in Ref. 38, S. J. Brodsky and G. P. Lepage, SLAC-PUB-2294, presented at the Workshop on Current Topics in High Energy Physics, Cal Tech (Feb. 1979), S. J. Brodsky, in the Proc. of the La Jolla Inst. Summer Workshop on QCD, La Jolla (1978), A. V. Efremov and A. V. Radyushkin, Phys. Lett. B94, 245 (1980), V. L. Chernyak, V. G. Serbo, and A. R. Zhitnitskii, Yad. Fiz. 31, 1069 (1980), S. J. Brodsky, Y. Frishman, G. P. Lepage, and C. Sachrajda, Phys. Lett. 91B, 239 (1980), and A. Duncan and A. H. Mueller, Phys. Rev. D21, 1636 (1980).

35. J. Ashman *et al.*, Phys. Lett. 206B, 384 (1988).

36. S. D. Drell and T. M. Yan, Phys. Rev. Lett. 24, 181 (1970).

37. S. J. Brodsky, SLAC-PUB-4342 and in the *Proceedings of the VIIIth Nuclear and Particle Physics Summer School*, Launceston, Australia, 1987.

38. G. P. Lepage and S. J. Brodsky, Phys. Rev. D22, 2157 (1980); Phys. Lett. 87B, 359 (1979); Phys. Rev. Lett. 43, 545, 1625(E) (1979).

39. S. J. Brodsky and G. P. Lepage, Phys. Rev. D24, 2848 (1981).

40. Arguments for the conservation of baryon chirality in large-momentum transfer processes have been given by B. L. Ioffe, Phys. Lett. 63B, 425 (1976). For some processes this rule leads to predictions which differ from the QCD results given here. The QCD helicity conservation rule also differs from the electroproduction helicity rules given in 0. Nachtmann, Nucl. Phys. B115, 61 (1976).

41. See Ref. 29 and also V. A. Matveev, R. M. Muradyan and A. V. Tavkheldize, Lett. Nuovo Cimento 7, 719 (1973).

42. G. C. Blazey *et al.*, Phys. Rev. Lett. 55, 1820 (1985); G. C. Blazey, Ph.D. Thesis, University of Minnesota (1987); B. R. Baller, Ph.D. Thesis, University of Minnesota (1987); D. S. Barton, *et al.*, J. de Phys. 46, C2, Supp. 2 (1985). For a review, see D. Sivers, Ref. 24.

43. V. D. Burkert, CEBAF-PR-87-006.

44. M. Peskin, Phys. Lett. 88B, 128 (1979); A. Duncan and A. H. Mueller, Phys. Lett. 90B, 159 (1980); Phys. Rev. D21, 1636 (1980).

45. M. D. Mestayer, SLAC-Report 214 (1978) F. Martin, *et al.*, Phys. Rev. Lett. 38, 1320 (1977); W. P. Schultz, *et al.*, Phys. Rev. Lett. 38, 259 (1977); R. G. Arnold, *et al.*, Phys. Rev. Lett. 40, 1429 (1978); SLAC-PUB-2373 (1979); B. T. Chertok, Phys. Lett. 41, 1155 (1978); D. Day, *et al.*, Phys. Rev. Lett. 43, 1143 (1979). summaries of the data for nucleon and nuclear form factors at large Q^2 are given in B. T. Chertok, in Progress in Particle and Nuclear Physics, Proceeding of the International School of Nuclear Physics, 5th Course, Erice (1978), and Proceedings of the XVI Rencontre de Moriond, Les Arcs, Savoie, France, 1981.

46. S. J. Brodsky, Y. Frishman, G. P. Lepage and C. Sachrajda, Phys. Lett. 91B, 239 (1980).

47. R. G. Arnold *et al.*, Phys. Rev. Lett. $7, 174 (1986).

48. R. L. Anderson *et* al., Phys. Rev. Lett. 30, 627 (1973).

49. A. W. Hendry, Phys. Rev. D10, 2300 (1974).

50. G. R. Court *et al.*, UM-HE-86-03, April 1986, 14 pp.

51. S. J. Brodsky, C. E. Carlson and H. J. Lipkin, Phys. Rev. D20, 2278 (1979); G. R. Farrar, S. Gottlieb, D. Sivers and G. Thomas, Phys. Rev. D20, 202 (1979).

52. G. R. Farrar, RU-85-46, 1986.

53. S. J. Brodsky, C. E. Carlson and H. J. Lipkin, Ref. 51; H. J. Lipkin, (private communication).

54. A.H. Mueller, Phys. Rept. 73, 237 (1981). See also S. S. Kanwal, Phys. Lett. 142B, 294 (1984).

55. S. Gupta, Phys. Rev. D24, 1169 (1981).

56. P. H. Damgaard, Nucl. Phys. B211, 435,(1983).

57. G. R. Farrar, G. Sterman, and H. Zhang, Rutgers Preprint 89-07 (1989).

58. J. Botts, G. Sterman ITP-SB-89-7,8,44 (1989).

59. V. L. Chernyak, A. A. Ogloblin and I. R. Zhitnitsky, Novosibirsk preprints INP 87–135,136, and references therein. See also Xiao-Duang Xiang, Wang Xin-Nian, and Huang Tao, BIHEP-TH-84, 23 and 29, 1984, and M. J. Lavelle, ICTP-84-85-12; Nucl. Phys. B260, 323 (1985).

60. I. D. King and C. T. Sachrajda, Nucl. Phys. B279, 785 (1987). .

61. G. P. Lepage, S. J. Brodsky, Tao Huang and P. B. Mackenzie, published in the *Proceedings of the Banff Summer Institute*, 1981.

62. M. Gari and N. Stefanis, Phys. Lett. B175, 462 (1986), M. Gari and N. Stefanis, Phys. Lett. 187B, 401 (1987).

63. C-R Ji, A. F. Sill and R. M. Lombard-Nelsen, Phys. Rev. D36, 165 (1987).

64. Z. Dziembowski and L. Mankiewicz, Phys. Rev. Lett. 58, 2175 (1987); Z. Dziembowski, Phys. Rev. D37, 768, 778, 2030 (1988)

65. See also G. R. Farrar, presented to the Workshop on Quantum Chromodynamics at Santa Barbara, 1988.

66. N. Isgur and C.H. Llewellyn Smith, Phys. Rev. Lett. 52, 1080 (1984). G. P. Korchemskii, A. V. Radyushkin, Sov. J. Nucl. Phys. 45, 910 (1987) and references therein.

67. S. Gottlieb and A. S. Kronfeld, Ref. 8; CLNS-85/646, June 1985.

68. G. Martinelli and C. T. Sachrajda, Phys. Lett. 190B, 151, 196B, 184, (1987); Phys. Lett. B217, 319, (1989).

69. G. W. Atkinson, J. Sucher, and K. Tsokos, Phys. Lett. 137B, 407 (1984); G. R. Farrar, E. Maina, and F. Neri, Nucl. Phys. B259, 702 (1985) Err.-ibid. B263, 746 (1986).; E. Maina, Rutgers Ph.D. Thesis (1985); J. F. Gunion, D. Millers, and K. Sparks, Phys. Rev. D33, 689 (1986); P. H. Damgaard, Ref. 56; B. Nezic, Ph.D. Thesis, Cornell University (1985); D. Millers and J. F. Gunion, Phys. Rev. D34, 2657 (1986).

70. Z. Dziembowski, G. R. Farrar, H. Zhang, and L. Mankiewicz, contribution to the 12th Int. Conf. on Few Body Problems in Physics, Vancouver, 1989.

71. Z. Dziembowski and J. Franklin contribution to the 12th Int. Conf. on Few Body Problems in Physics, Vancouver, 1989.

72. C. Carlson and F. Gross, Phys. Rev. Lett. 53, 127 (1984); Phys. Rev. D36 2060 (1987).

73. 0. C. Jacob and L. S. Kisslinger, Phys. Rev. Lett. 56, 225 (1986).

74. The connection of the parton model to QCD is discussed in G. Altarelli, Phys. Rep. 81, No. 1, 1982.

75. V. N. Gribov and L. V. Lipatov, Sov. Jour. Nucl Phys. 15, 438, 675 (1972).

76. R. P. Feynman, Photon-Hadron Interactions, (W. A. Benjamin, Reading, Mass. 1972).

77. P. V. Landshoff, J. C. Polkinghorne Phys. Rev. D10, 891 (1974).

78. B. R. Baller, et al., Phys. Rev. Lett. 60, 1118 (1988).

79. For general discussions of $\gamma\gamma$ annihilation in $e^+e^- \to e^+e^-X$ reactions, see S. J. Brodsky, T. Kinoshita, and H. Terazawa, Phys. Rev. Lett. 25, 972 (1970), Phys. Rev. D4, 1532 (1971), V. E. Balakin, V. M. Budnev, and I. F. Ginzburg, JETP Lett. 11, 388 (1970), N. Arteaga-Romero, A. Jaccarini, and P. Kessler, Phys. Rev. D3, 1569 (1971), R. W. Brown and

I. J. Muzinich, Phys. Rev. D4, 1496 (1971), and C. E. Carlson and W.-K. Tung, Phys. Rev. D4, 2873 (1971). Reviews and further references are given in H. Kolanoski and P. M. Zerwas, DESY 87-175 (1987), H. Kolanoski, *Two-Photon Physics in e^+e^- Storage Rings,* Springer-Verlag (1984), and Ch. Berger and W. Wagner, Phys. Rep. 136 (1987); J. H. Field, University of Paris Preprint LPNHE 84-04 (1984).

80. G. Köpp, T. F. Walsh, and P. Zerwas, Nucl. Phys. B70, 461 (1974). F. M. Renard, Proc. of the Vth International Workshop on $\gamma\gamma$ Interactions, and Nuovo Cim. 80, 1 (1984). Backgrounds to the C = +, J = 1 signal can occur from tagged $e^+e^- \to e^+e^-X$ events which produce C = − resonances.

81. H. Aihara *et* al., Phys. Rev. Lett. 57, 51, 404 (1986). Mark II data for combined charged meson pair production are also in good agreement with the PQCD predictions. See J. Boyer *et al.*, Phys. Rev. Lett. 56, 207 (1986).

82. H. Suura, T. F. Walsh, and B. L. Young, Lett. Nuovo Cimento 4, 505 (1972). See also M. K. Chase, Nucl. Phys. B167, 125 (1980).

83. J. Boyer *et* al., Ref. 81; TPC/Two Gamma Collaboration (H. Aihara *et al.*), Phys. Rev. Lett. 57, 404 (1986).

84. M. Benyayoun and V. L. Chernyak, College de France preprint LPC 89 10 (1989).

85. B. Nizic Phys. Rev. D35, 80 (1987)

86. G. R. Farrar RU-88-47, Invited talk given at Workshop on Particle and Nuclear Physics on the Light Cone, Los Alamos, New Mexico, 1988; G. R. Farrar, H. Zhang, A. A. Globlin and I. R. Zhitnitsky, Nucl. Phys. B311, 585 (1989); G. R. Farrar, E. Maina, and F. Neri, Phys. Rev. Lett. 53, 28 and, 742 (1984).

87. M. A. Shupe, et al., Phys. Rev. D19, 1921 (1979).

88. A simple method for estimating hadron pair production cross sections near threshold in $\gamma\gamma$ collisions is given in Ref. 33.

89. See Ref. 31. The next-to-leading order evaluation of T_H for these processes is given by B. Nezic, Ph.D. Thesis, Cornell University (1985).

90. See Ref. 30 and S. J. Brodsky and J. R. Hiller, Phys. Rev. C28, 475 (1983).

91. C. R. Ji and S. J. Brodsky, Phys. Rev. D34, 1460 (1986); D33, 1951, 1406, 2653, (1986). For a review of multi-quark evolution, see S. J. Brodsky, C.-R. Ji, SLAC-PUB-3747, (1985).

92. The data are compiled in Brodsky and Hiller, Ref. 90.

93. J. Napolitano *et al.*, ANL preprint PHY-5265-ME-88 (1988).

94. T. S.-H. Lee, ANL preprint (1988).

95. H. Myers *et* al., Phys. Rev. 121, 630 (1961); R. Ching and C. Schaerf, Phys. Rev. 141, 1320 (1966); P. Dougan *et al.*, Z. Phys. A 276, 55 (1976).

96. T. Fujita, MPI-Heidelberg preprint, 1989.

97. S. J. Brodsky, C.-R. Ji, G. P. Lepage, Phys. Rev. Lett. 51, 83 (1983).

98. L.A. Kondratyuk and M. G. Sapozhnikov, Dubna preprint E4-88-808.

99. A. S. Carroll, *et* al., Phys. Rev. Lett. 61, 1698 (1988).

100. G. R. Court *et al.*, Phys. Rev. Lett. 57, 507 (1986).

101. S. J. Brodsky and G. de Teramond, Phys. Rev. Lett. 60, 1924 (1988).

102. R. Blankenbecler and S. J. Brodsky, Phys. Rev. D10, 2973 (1974).

103. See Ref. 100; T. S. Bhatia *et al.*, Phys. Rev. Lett. 49, 1135 (1982); E. A. Crosbie *et al.*, Phys. Rev. D23, 600 (1981); A. Lin *et* al., Phys. Lett. 74B, 273 (1978); D. G. Crabb *et al.*, Phys. Rev. Lett. 41, 1257 (1978); J. R. O'Fallon *et al.*, Phys. Rev. Lett. 39, 733 (1977); For a review, see A. D. Krisch, UM-HE-86-39 (1987).

104. For other attempts to explain the spin correlation data, see C. Avilez, G. Cocho and M. Moreno, Phys. Rev. D24, 634 (1981); G. R. Farrar, Phys. Rev. Lett. 56, 1643 (1986), Err-ibid. 56, 2771 (1986); H. J. Lipkin, Nature 324, 14 (1986); S. M. Troshin and N. E. Tyurin, JETP Lett. 44, 149 (1986) [Pisma Zh. Eksp. Teor. Fiz. 44, 117 (1986)]; G. Preparata and J. Soffer, Phys. Lett. 180B, 281 (1986); S. V. Goloskokov, S. P. Kuleshov and 0. V. Seljugin, *Proceedings of the VII International Symposium on High Energy* Spin *Physics*, Protvino (1986); C. Bourrely and J. Soffer, Phys. Rev. D35, 145 (1987).

105. There are five different combinations of six quarks which yield a color singlet B=2 state. It is expected that these QCD degrees of freedom should be expressed as B=2 resonances. See, e.g. S. J. Brodsky and C. R. Ji, Ref. 91.

106. For other examples of threshold enhancements in QCD, see S. J. Brodsky, J. F. Gunion and D. E. Soper, Ref. 32 and also Ref. 88. Resonances are often associated with the onset of a new threshold. For a discussion, see D. Bugg, Presented at the IV LEAR Workshop, Villars-Sur-Ollon, Switzerland, September 6-13, 1987.

107. J. F. Gunion, R. Blankenbecler and S. J. Brodsky, Phys. Rev. D6, 2652 (1972).

108. With the above normalization, the unpolarized *pp* elastic cross section is $d\sigma/dt = \Sigma_{i=1,2,...5} \mid \phi_i^2 \mid /(128\pi s p_{cm}^2)$.

109. At low momentum transfers one expects the presence of both helicity-conserving and helicity non-conserving pomeron amplitudes. It is possible that the data for A_N at p_{lab} = 11.75 GeV/c can be understood over the full angular range in these terms. The large value of $A_N = 24 \pm 8\%$ at p_{lab} = 28 GeV/c and p_T^2 = 6.5 GeV^2 remains an open problem. See P. R. Cameron *et al.,* Phys. Rev. D32, 3070 (1985).

110. K. Abe *et al.,* Phys. Rev. D12, 1 (1975), and references therein. The high energy data for $d\sigma/dt$ at θ_{cm} = n/2 are from C. W. Akerlof *et al.,* Phys. Rev. 159, 1138 (1967); G. Cocconi *et al.,* Phys. Rev. Lett. 11, 499 (1963); J. V. Allaby *et al.,* Phys. Lett. 23, 389 (1966).

111. I. P. Auer *et al.,* Phys. Rev. Lett. 52, 808 (1984). Comparison with the low energy data for A_{LL} at $\theta_{cm} = \pi/2$ suggests that the resonant amplitude below p_{lab} = 5.5 GeV/c has more structure than the single resonance form adopted here. See I. P. Auer *et al.,* Phys. Rev. Lett. 48, 1150 (1982).

112. See Ref. 49 and N. Jahren and J. Hiller, University of Minnesota preprint, 1987.

113. The neutral strange inclusive pp cross section measured at p_{lab} = 5.5 GeV/c is 0.45 $\pm$ 0.04 mb; see G. Alexander *et al.,* Phys. Rev. 154, 1284 (1967).

114. H. C. Pauli and S. J. Brodsky, Phys. Rev. D32, 1993, 2001 (1985) and Ref. 9.

115. K. Hornbostel, SLAC-0333, Dec 1988; K. Hornbostel, S. J. Brodsky, and H. C. Pauli, SLAC-PUB-4678, Talk presented to Workshop on Relativistic Many Body Physics, Columbus, Ohio, June, 1988.

116. S. J. Brodsky, H. C. Pauli, and A. Tang, in preparation.

117. C. J. Burden and C. J. Hamer, Phys. Rev. D37, 479 (1988), and references therein.

118. Y. Frishman and J. Sonnenschein, Nucl. Phys. B294, 801 (1987), and Nucl. Phys. B301, 346 (1988).

119. For a discussion of renormalization in light-cone perturbation theory, see Ref. 120 and also Ref. 38.

120. S. J. Brodsky, R. Suaya, and R. Roskies, Phys. Rev. D8, 4574 (1973).

121. S. G. Gorishny, A. L. Kataev, and S. A. Larin, Phys. Lett. B212, 238 (1988).